T.C.

ALTINBASUNIVERSITY
Institute of Graduate Studies
Electrical and Computer Engineering

A STUDY OF DEEP NEURAL NETWORK CONTROLLER BASED POWER QUALITY IMPROVEMENT OF HYBRID PV/WIND SYSTEMS BY USING SMART INVERTER

Adel AB-BELKHIR

Doctor of Philosophy

Supervisor

Prof.OğuzBAYAT

Istanbul, 2021

A STUDY OF DEEP NEURAL NETWORK CONTROLLER BASED POWER QUALITY IMPROVEMENT OF HYBRID PV/WIND SYSTEMS BY USING SMART INVERTER

by

Adel Ab-BelKhir

Electrical and Computer Engineering

Submitted to the Institute of Graduate Studies

in partial fulfillment of the requirements for the degree of

Doctor of Philosophy

ALTINBAŞ UNIVERSITY

2021

The thesis titled "A STUDY OF DEEP NEURAL NETWORK CONTROLLER BASED POWER QUALİTY IMPROVEMENT OF HYBRİD PV/WİND SYSTEMS BY USİNG SMART INVERTER" prepared and presented by "Adel Ab-Belkhair" was accepted as a Doctor of Philosophy Thesis inElectrical and Computer Engineering.

____

Prof. Dr. OğuzBAYAT

Supervisor

Thesis Defense Jury Members:

Prof.Dr. Oğuz BAYAT	School of Engineering and Natural Sciences, Altinbas University	___________________
Prof.Dr.Osman Nuri UÇAN.	School of Engineering and Natural Sciences, Altinbas University	___________________
Prof.Dr Hasan Huseyın BALIK..	School of Engineering and Natural Sciences, Yıldız Teknik University	___________________
Asst. Prof.Dr.Çağatay AYDIN	School of Engineering and Natural Sciences, Altinbas University	___________________
Asst. Prof.Dr. Adil Deniz DURU	School of Engineering and Natural Sciences, Marmara University	___________________

I certify that this thesis satisfies all the requirements as a thesis for the degree of Doctor of Philosophy.

Approval Date of Institute of Graduate Studies:
____/____/____

I hereby declare that all information in this document has been obtained and presented in accordance with academic rules and ethical conduct. I also declare that, as required by these rules and conduct, I have fully cited and referenced all material and results that are not original to this work.

Adel Ab-BelKhair

[Signature]

ACKNOWLEDGEMENTS

I would like to thanks to my great supervisor Professor Dr. Oğuz BAYATfor helping me in preparing the thesis. This thesis is wholeheartedlydedicated to my beloved father, who has been my source of inspiration.To my wife, who has been through so much with me and has helped me achieve this goal, eventually for my mother's soul

ABSTRACT

A STUDY OF DEEP NEURAL NETWORK CONTROLLER BASED POWER QUALITY IMPROVEMENT OF HYBRID PV/WIND SYSTEMS BY USING SMART INVERTER

Ab-BelKhair, Adel

Ph.D., Electrical and Computer Engineering,Altınbaş University,

Supervisor: Professor Dr. Oğuz BAYAT

Date: 18.02.2021

Pages: 97

Nowadays, the world is witnessing uncontrollable changes, such as global warming and climate change because of excessive fossil fuel utilization for transportation and power generation; therefore, the developed world is mainly concentrating on alternative resource development; for which, they have taken major research and development initiatives. Generally, certain alternative power generation sources, including wind, solar, and hydropower are not detrimental to nature. For this reason, solar and wind power have been declared as useful alternative energy resources, and besides, they are abundant. This thesis shows the investigation of the performances of wind energy systems and photovoltaic cells when weather conditions keep on changing. The findings of this research provide the basis for developing an advanced intelligent control system to maximize power generation. For renewable energy sources, the MPPT controller is essential because weather conditions are mostly unpredictable. This thesis has been written with a major objective to suggest a new algorithm, which is based on deep neural network (DNN), and to apply it for maximum power point tracking (MPPT). MATLAB was used to simulate this project for wind-based power generation systems and photovoltaic (PV) cells. An advanced DNN controller was developed for reducing the THD value and improving the output power quality of a microgrid-integrated hybrid wind/PV power generation system. The performance of the proposed system was tested and analyzed in several possible operating conditions using MATLAB to assure its functionality. In the end, we also analyzed the results of simulations using the IEEE 1547 standard.

Keywords: Artificial Intelligence, Deep Neural Network, PV, Wind Power, MPPT, Microgrid

TABLE OF CONTENTS

Pages

ABSTRACT .... **vii**

TABLE OF CONTENTS .... **ix**

LIST OF FIGURES .... **xii**

LIST OF ABBREVIATIONS .... **xvi**

1. INTRODUCTION **1**

1.1 OBJECTIVES 5

1.2 PROBLEM STATEMENT 5

1.3 MOTIVATION BEHIND THE THESIS 5

1.5 OBJECTIVE OF THE THESIS 6

1.6 THESIS ORGANIZATION 6

2. PHOTOVOLTAIC SYSTEM **8**

2.1 BACKGROUND 8

2.2 PV PANELS 9

2.3 BATTERY AND BIODIRECTIONAL CONVERTER 12

2.3.1 BATTERY MODEL 12

2.3.2 Bidirectional Converter 15

2.4 INVERTER AND LC FILTER 17

2.4.1 VSC Inverter 17

2.4.2 LC Filter 18

2.5 PV CONTROLLER 20

2.5.1 MPPT Module 20

2.5.2 Reference Power Output 22

2.6 BATTERY CONTROLLER 23

2.7 INVERTER CONTROLLER......24
2.7.1 VSC Controller......26
3.1 WIND POWER FUNDAMENTALS......26
3.2 MATHEMATICAL FORMULATION OF WIND TURBINE......31
3.3 MATHEMATICAL MODELLING OF PV......34
3.4 WIND TURBINE MODEL......36
3.5 DEEP NEURAL NETWORK MODELLING AND DNN BASED MPPT FOR PV......38
4. EXPERIMENTAL RESULTS......40
4.1 MAXIMUM POWER POINT TRACKING ALGORITHM......40
4.2 DISCUSSION......62
5. CONCLUSION AND FUTURE WORK......69
5.1 CONCLUSION......69
5.2 FUTURE WORK......70
REFERENCES......71
APPENDIX......86

LIST OF TABLES

Pages

Table 4. 1: DNN data of MPPT controller 42

Table 4. 2: DNN data of an MPPT controller for a wind system 53

Table 4. 3: DNN data of the grid system controller...60

Table 4. 4: comparative Analyses of THD values, Grid, Wind and PV 62

LIST OF FIGURES

Pages

Figure 1. 1: Block diagram of the proposed microgrid system and its controller 4

Figure 2. 1: Equivalent model of PV cell 10

Figure 2. 2: Structure diagram of PV array 11

Figure 2. 3: Schematic diagram of battery 12

Figure 2. 4: Typical discharge curve of battery 14

Figure 2. 5: Schematic diagram of bidirectional converter 16

Figure 2. 6: Schematic diagram of inverter 17

Figure 2. 7: Schematic diagram of PV MPPT control 20

Figure 2. 8: PV panel MPPT curves 21

Figure 2. 9: Schematic diagram of PV reference power control 22

Figure 2. 10: Schematic diagram of battery charge/discharge control 23

Figure 2. 11: Schematic diagram of inverter control 24

Figure 2. 12: Schematic diagram of inverter VQ control 27

Figure 3. 1: Feedforward deep neural network (single neuron model) 39

Figure 4. 1: Proposed DNN-based MPPT algorithm 41

Figure 4. 2: Simulation model of DNN controller-based MPPT algorithm for the PV system 41

Figure 4. 3: a) Flow chart DNN Model for PV-MPPT system, b) DNN Model for PV-MPPT system...43

Figure 4. 4: DNN-PV MPPT controller showing best validation performance 40

Figure 4. 5: DNN-PV MPPT controller error histogram 40

Figure 4. 6: DNN-PV MPPT controller training data...41

Figure 4. 7: DNN-PV MPPT controller showing best regression 41

Figure 4. 8: Simulation results of DNN-PV MPPT power with respect to irradiance and temperature 42

Figure 4. 9: Simulation results of DNN-PV MPPT boost converter voltage and current with respect to irradiance and temperature 43

Figure 4. 10: Proposed DNN-based MPPT algorithm (wind energy system)..............................49

Figure 4. 11: Simulation model of DNN controller-based MPPT algorithm (wind energy system) 49

Figure 4. 12: a) Flow Chart DNN model of a wind-based MPPT System, b: DNN model of a wind-based MPPT System 50

Figure 4. 13: Best validation performance of a DNN-Wind MPPT controller 51

Figure 4. 14: Histogram of the DNN-Wind MPPT controller..52

Figure 4. 15: Training data of the DNN-Wind MPPT controller 52

Figure 4. 16: Training and validation of a DNN-Wind MPPT controller...................................53

Figure 4. 17: Simulation results of DNN-Wind MPPT power (for different wind speeds) 54

Figure 4. 18: Simulation results for DNN-Wind MPPT converter voltage and current (for different wind speeds) 54

Figure 4. 19: Comparative analysis with and without Wind MPPT power (for different wind speeds) 50

Figure 4. 20: Proposed simulation model of the DNN controller-based microgrid integrated with a hybrid PV / wind energy system 51

Figure 4. 21: DNN controller-based voltage source controller for smart inverters......................51

Figure 4. 22: DNN based current regulator for smart inverter 52

Figure 4. 23: a) DNN model of a current regulator for smart inverters, b) Flow chart DNN model of a current regulator for smart inverters...53

Figure 4. 24: Histogram of DNN-current regulator error...59

Figure 4. 25: DNN-current regulator's best validation performance..59

Figure 4. 26: Training data for the DNN-current regulator..60

Figure 4. 27: Test, training, and validation of a DNN-current regulator 60

Figure 4. 28: Real power consumed by the load...63

Figure 4. 29: Reactive power consumed by the laod 63

Figure 4. 30: Total power generated by the hybrid PV / wind energy system 63

Figure 4. 31: Current waveform and microgrid voltage..64

Figure 4. 32: Grid-power supplied to the load...64

Figure 4. 33: THD values of PV system voltage 65

Figure 4. 34: THD values of PV system current..60

Figure 4. 35: THD values of wind voltage 60

Figure 4. 36: THD values of wind current 61

Figure 4. 37: THD values of Microgrid load current 61

Figure 4. 38: THD values of Microgrid load voltage 62

LIST OF ABBREVIATIONS

RE	Renewable energy
PV	Photovoltaic
WP	Wind Power
MG	Microgrid
OPF	Optimal Power Flow
RESs	Renewable Energy Sources
MPPT	Maximum Power Point Tracking
DNN	Depp Neural Network
PV-EC	photovoltaic electrochemical device
THD	Total Harmonic Distortion
MPC	model predictive control
BESS	battery energy storage systems

1. INTRODUCTION

The Last ten years have witnessed a rise in global warming, which became a serious issue with intimidating consequences for life our planet. Experts, for the first time in history, seriously focused on variable fuel prices and dangerous environmental issues, which emerged as consequences of fuel consumption, and led them to renewable/alternative energy for power generation. Wind power (WP) and PV-based electric power generation are now obvious resources because they are abundant and besides, they are harmless [1][2]. The main power grid can be connected to the RE sources, and the development of microgrids (MGs) and smart grids have provided substantial technological impetus to the whole concept of renewable energy. New technologies and possibilities, such as distributive power networks, hi-tech active transmission, advanced controllers, self-healing technologies, and flexible loads can beused witha microgrid [3][4][5]. Fast-growing RES is used with WT and PV reproductive technologies, which reduce the overall project cost. Moreover, wind turbines and solar PVs are popular and they have beenextensively adopted. In a previous study [1], it is mentioned that electrical energy from RES (WT andPV)is low-cost, which can decrease the generation cost of electricity. The WT and PV properties, sizes, and characteristics determine the cost factors, which help producers understand theimpact of the mentioned technologies on monetary factors, including electricity loss, energy fees, and other first-rate indicators.

Nowadays, hybrid renewable power generation technologies are popular because they can sustainably generate electricity, and also because they can use multiplerenewable energy sources. Currently, solar and wind resources have potential but solar energy has gained more significance because of cost reduction per unit of electricity[6][7][8]. Hybrid systemsgenerally have certain issues, such as integration problems, stability issues, irregular operations, difficult-to-manage operations, highly-variable power generation stochastic operations. They have some challenging situations, including variable voltage, load discrepancy, low quality of power, reliability issues, poor load following, and frequency deviation [9][10][11]. A hybrid system has a high power flow (HPF), which is controlled in a power system with the help of a control system. Moreover,the mathematical formulation also helps to handlelarge, static, linear, and non-linear problems, including complex linear transformation issues. Many PV system tunings and WT integration with the power system increase the OPF complexity because it has transient power characteristics. To define and resolve the OPF at WT and PV, a typical framework is as follows: (a) there should bea context and significance of the issue; (b) WT and PV outputs should be estimated based on reliable solar radiation and wind speed statistics; (c) goal functions should be chosen; (d) adaptive control,dependable diversity, andtechnical issues should be outlined, and (e) method for resolving the OPF problem should be mentioned. During recent years, many researchers have attempted and successfully addressed the OPF issue by focusing on a few functions [12][13].Novel and innovativetechnologies and concepts are still required for increasing the penetration of the RE resources in a power grid for handling the issues.

Hybrid power system optimization is another major research issue pertaining to the smart grid framework, keeping in view the design of the model predictive control (MPC). It can maximize renewable energy use through a strategy, for example, using PV, wind turbine, battery storage, and minimization of the utility grid used for industrial electricity requirements. Grid-connected applicationsand renewable energy resources (RERs) are used in different contexts[14][15][16][17][18] for developing the idea of integrating PV energy storage systems in commercial buildings. In conjunction with other technologies, the microgrid environment results in energy coordination, which creates power flow stability, and it means balance between power generation and consumption. A survey of the available literature on renewable energy in global energy scenarios mainly includes battery energy storage systems (BESS) and solar photovoltaic (PV) devices. The predictive regulator controls the power flow within the tie-lines despite frequency deviations in a microgrid. It results in the maintenance of power balance between active power demands of a system and the generation of total active power.

The frequency controls and active power are significant tasksformaking any electrical network assure a sufficient supply of electricity with reliability for the convenience of the customers [14]. Frequency stability in each area is assured by adjusting the generator's active outputs to a certain value and controlling variations in the tie-line active power flow. Theyare major tasks for network operators.For actualpower cost calculations,this kind of system design is implemented after integrating it with renewable powerto meet the consumers' demands right according to their requirements[17].The author has clearly addressed different contexts, in which, renewable energy resources (RERs) and grid-connected applications are utilized[15]. The concept ofintegrating PV energy storage has been used for commercial buildings. Some generally used RERs, including the wind and solar RERs,are differently designed keeping in view the geographic locations and seasonal variations, which act as a guiding principle to design energy storage systemsfor providing a platform for optimal RER usage[16].

A novel deep neural network algorithm has been presented in this thesis to solve power systemproblems when it is integrated with PVs and wind-based generators, asFigure 1.1 indicates. The main contributions in this context include the following:

1. The PV/wind energy uses DNN, for which, we designed an MPPT controller and modeled it for analyzing its performance in different weathers.

2. A wind/PV energy system was also designed and modeled using a smart inverter tointegrate the hybrid system with a microgrid.
3. A DNN-based voltage source controller was designed to synchronize a microgrid tothe already mentionedhybrid energy system.
4. It was found that a smart inverter, which is based on DNN, improves the power stability andquality and decreases harmonics.

.

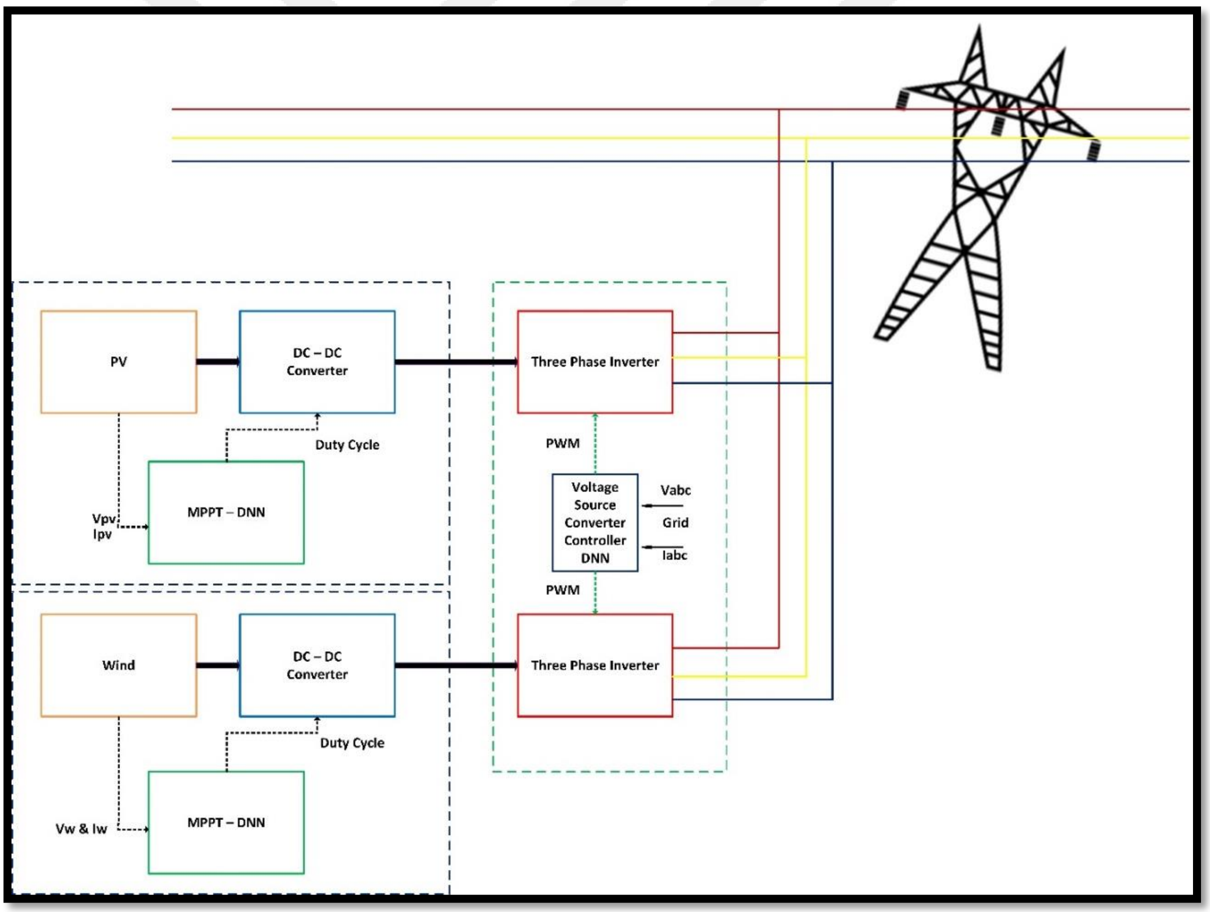

Figure1.1: Block diagram of the proposed microgrid system and its controller

The remaining parts of thethesisare organized as follows: An MPPT algorithm based on DNN has been given in Section II, and that is used for PV systems. Section II includes an analysis ofthealgorithm performance in differentpossible weather conditions. The same algorithm (for wind-based energy systems)has been given in Section III, and its performance has been analyzed under different wind speeds. Moreover, theexplanation of the obtained results is also given in this section. Section IV illustrates our DNN-based microgrid and the way it is integrated intothe wind-PV hybrid power generation system. Section V models a smart inverter controller, which is based on DNN,and includes its performance evaluation. Section VI shows simulation results, and after that, the conclusions are listed.

1.1 OBJECTIVES

This thesis has been prepared with the main objective to develop an effective hybrid system that performs despite weather issues.

1.2 PROBLEM STATEMENT

In PV and wind-based hybrid systems, a turbine controls the output, which is a problem because sometimes, the controller is unable to obtain high power. This thesis primarily solved this issue with the help of a DNN-based MPPT algorithm, and we have simulated it in MATLAB for both PV and FC.

1.3 MOTIVATION BEHIND THE THESIS

In today's energy-deficient world, power demand is soaring with every passing day partly due to population growth and partly because of industrialization. Traditional power plants are unable to meet the growing consumer needs because of increasing environmental issues; so, finding and utilizing alternates to conventional power generation is essential to meet the consumers' demands. Now, in many developed as well as developing countries, most governments are attempting to generate massive amounts of electricity through renewable energy resources, which are abundant and nature-friendly, including solar, wind, fuel cells, and water. Power generation through renewable energy resources mainly depends on the rich access to the resources. Renewable energy resources are available for the most part of the day; however, they keep on fluctuating.

1.4AIM OF THESIS

This thesis is based on research, which involves the application of the latest DNN controller to improve the quality of the output power, which has been generated through a hybrid combination of wind-based and PV generation systems. We developed and simulated this system to analyze its performance in different conditions. All the mentioned steps led to improve a control strategy to alleviate the instability issue from the distribution system as well as broaden the stable operational region for the system. A unified control strategy has been adapted for the DER systems to enable it for islanded and grid-connected operations. These issues are barriers that limit the penetration of PV distributed generations (PVDGs) into the power system.

1.5 OBJECTIVE OF THE THESIS

Maintaining the microgrid current and voltage with little or no oscillation is the most significant objective of this thesis. To achieve it, we will find the Total Harmonic Distortion (THD) values fora wind turbine, PV, current profile, and distributed grid voltage.

1.6 THESIS ORGANIZATION

We have organized this thesis as follows: Chapter 2 reviews various methodologies for PVs. Chapter 3 describes the wind turbine. Chapter 4 depicts the implementation of the selected methodology and illustrates the results and analyses of the outcomes. Deep Neural Network-basedMPPT algorithm is shown in Section 4 and the same section analyzes theproposed algorithm's performanceindifferent weathers/climatic conditions. Chapter 5 discusses the conclusion and future scope for research.

2. PHOTOVOLTAIC SYSTEM

2.1 BACKGROUND

A considerable amount of research on PV generation, battery charge/discharge control, and VSC has been done in the past several decades.

Firstly, some papers' models are based on the AC bus[19][20][21][22].These models can easily achieve the differentlytargeted voltage levels in the same microgrid, but this solution will increase the fluctuations in the battery output voltage. At the same time, some papers[23][24][25][26][27][28][29][30] are based on the use ofa DC bus. AC and DC buses can beused in the same model[31] that will improve the application range and improve the accessibility of the equipment, but it is likely to increase the system complexity.

Secondly, the energy source of a microgrid can be different. PV-based generation was the main choice for previous researches [32][33][34][35], but with the development of the grid system, wind power became a highly acceptable renewable energy source for the microgrid [36][37]; however, one-time investment of wind-based power generation is too high.

Thirdly, there are many choices for the energy storage system: hydrogen storage, battery [38][39][40][41], supercapacitor and a proton-exchange membrane fuel cell. Most authors have chosen battery as the first choice for energy storage based on their cost considerations.

From the view of structural design, some papers [42][43][44]show the overall structure of a PV-based microgrid. On the point of PV generation, some researchers useda PV series, which increases the PV module's output voltage, but it affects the system stability.

During different stages of electric cardevelopment, some researchers used PV generation and battery in the electrical car[45], so this design will be beneficial to decrease the greenhouse gases; however, it increases the cost.

Authors chiefly used a bidirectional converter[46]for controlling charge/discharge, and the battery power, but the control methods maybe different. Some papers used the PQ control method for power flow control by changing the duty cycle. In their work, the battery wasdirectly connected with the PV generatorbecause sometimes, PV cannot work in the MPPT mode, and reduces the life of the battery since the output current of PV generation is sometimes too high for thebattery.

As far as the selection of inverter is concerned, many papers[47][48]used 3-phase DC/AC inverters. They belong to a traditional kind of inverters, which consist of six transistors, and they can bi-directionally transmit the energy. Some authors[49][50] used voltage source inverters, which can easily control the DC bus voltage. The researchers[51][52]used a four-transistor full-bridge inverter that reduces the cost. Some other authors also mentioned flyback and boost converters in their papers[53][54][55].

2.2 PV PANELS

Nowadays, power generation through solar energy takes place through thefollowing methods: concentrated thermal power generation, photochemistry, and photovoltaic devices. The Photovoltaic effect forms the basis fora solar photovoltaic generation. Solar irradiation is directly transformed into electricity using PV panels. Itsbenefits includelong life, no emission, and easy application. Sometimes, its efficiency increases and becomes 24.7%. This has made PV generation a widely-used process.Figure 2.1 is the circuit diagram (equivalent model) of a single photovoltaic cell.

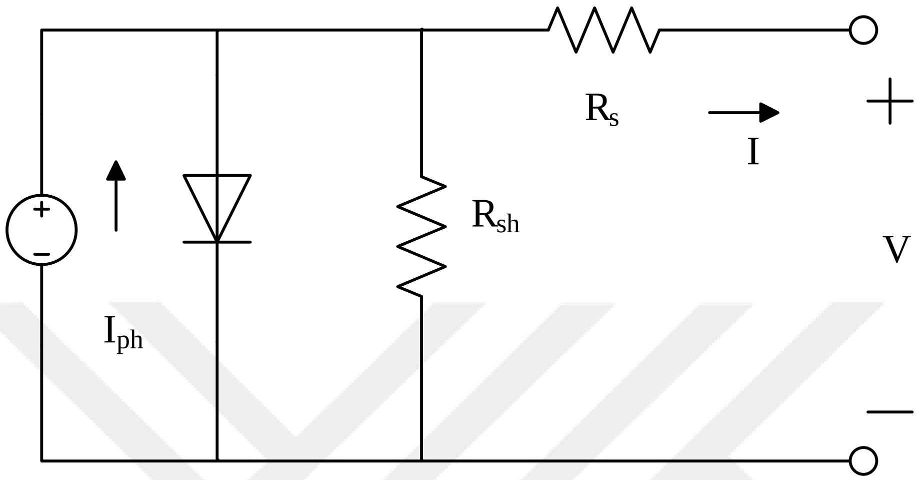

Figure2.1: Equivalent model of PV cell

The PV panel has the following mathematical model:

$$I = I_{ph} - I_{os}\left\{exp\left[\frac{qV_{oc}}{AKT}\right] - 1\right\} - \frac{V_{oc}}{R_{sh}} \quad (2.1)$$

In this case:

I: Output current of a PV cell (A)

G: Sunlight intensity (W/m^2)

T: PV battery working temperature (K)

q: elementary charge

I_{os}: Reverse saturation current of a diode *k*: Boltzmann's constant

Iph: Output current of a photo-generated current source

K_I: Temperature coefficient for short-circuit current, whichis equal to0.10017 (A/˚C)

V: Output voltage of a PV cell (V)

I_{or}: Saturation current of a diode at the reference temperature

Figure 2.2shows the structuralarray diagram:

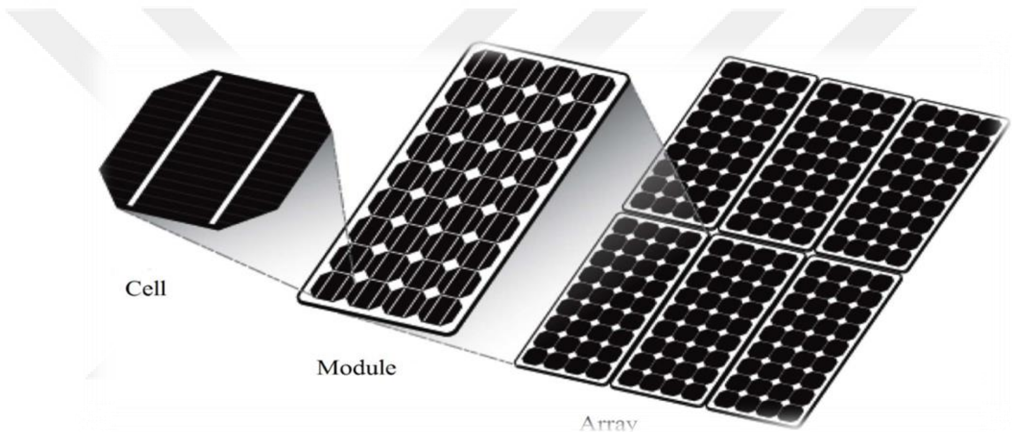

Figure2.2: Structure diagram of PV array

According to the figure, the module is constituted by some cells and the PV array is constituted by some modules. Bothvoltage and current outputs are determined usingPV cells' arrangement. Suppose that a series has *n* (number of cells) with m (parallel number of cells). Moreover,in this case, the output cell voltage is$V_{cell}$and the current isI_{cell}. The output power of a module is:

$$Pmodule = Vmodule*Imodule = nVcell*mIcell \quad (2.2)$$

2.3 BATTERY AND BIDIRECTIONAL CONVERTER

2.3.1 BATTERY MODEL

A microgrid needs energy storage, which should be able to reject the fluctuations that affect power quality. Secondly, the storage provides a short-term power supply. Besides, there is no inertial device such as a large synchronous generator in the microgrid. The storage is vital for maintaining stable microgrid operations. Table 2.1 shows key parameters of some common types of energy storage.

Table2.1: Comparison of different storage devices

Energy storage devices	**Super capacitor**	**Lead-acid battery**	**Flywheel energy storage**
Energy Density /($Wh*kg^{-1}$)	2˜5	30˜200	5˜50
Power Density /($W*kg^{-1}$)	7000˜18000	100˜700	180˜1800
Service Life/(year)	30	8	30
Efficiency/(%)	95	92	90
Safety	high	high	low
Average Annual Price /($\$/kWh$)	110	18	80

Batteries filled with lead-acid are used for microgridsbecause of their annual costs, prices, and energy density.

We have applied a mathematical model to describe the state of charge (SOC). Figure 2.3shows a discharging battery through a flow diagram.

The applied model is just like Shepherd's model [56].

Equation 2.3 shows the expression for the battery:

$$V_{batt} = E_{0-}k \times Q/(Q - i_t) \times i_t + A \times xpe(-B \times i_t)(2.3)$$

In this expression

R=internal resistance (Ω)

E_0= constant voltage for a battery (V)

K=polarization resistance (Ω)

B=exponential zone time constant inverse $(Ah)^{-1}$

A=exponential zone amplitude (V)

V_{batt}=battery voltage (V)

$it = ^{R}idt$=actual battery charge (Ah)

Q=battery capacity (Ah)

i=battery current (A)

i^*=filtered current (A)

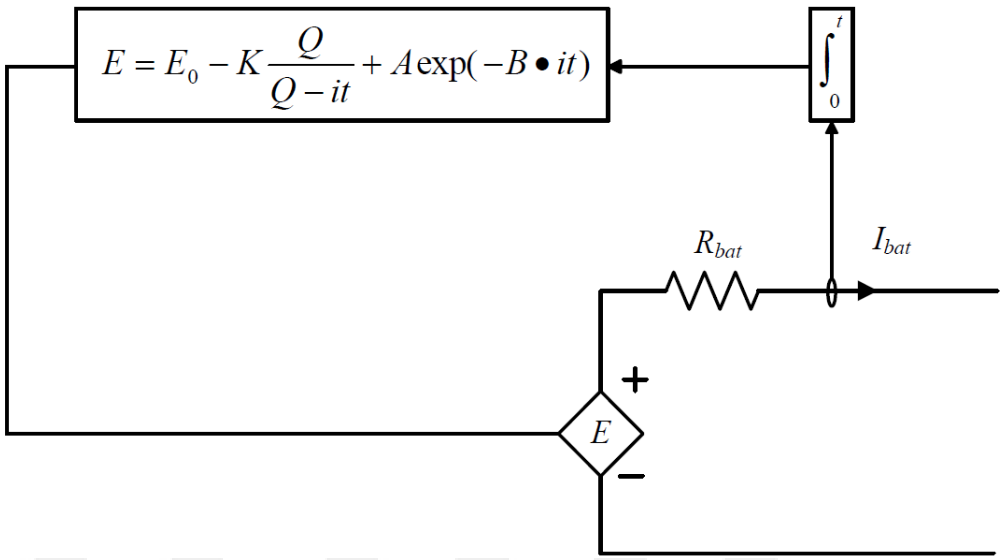

Figure2.3: Schematic diagram of battery

The typical discharge curve of the battery is shown in figure 2.4.

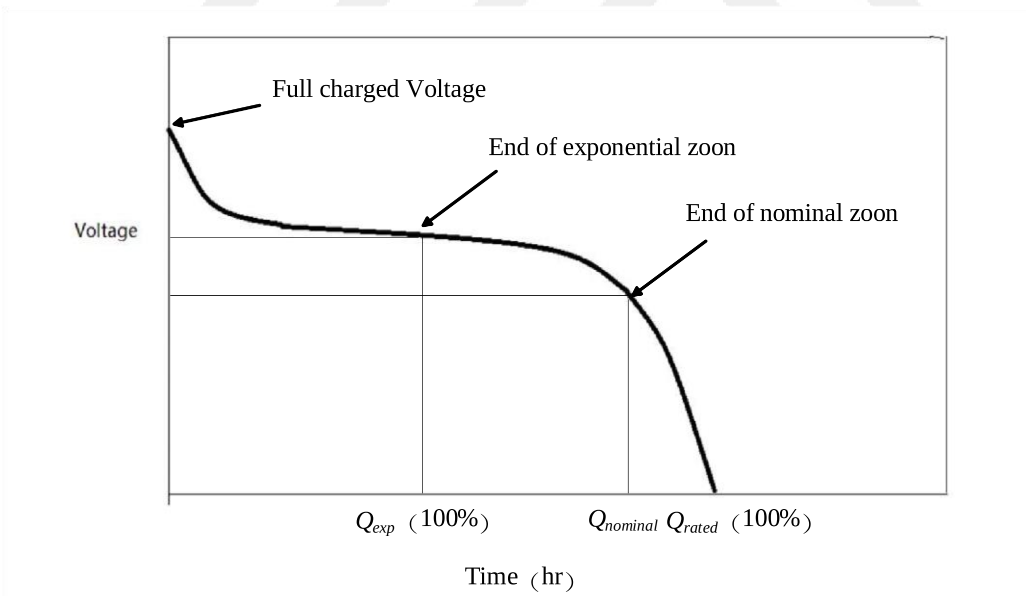

Figure2.4: Typical discharge curve of battery

Substituting SOC to "*it*," which is the time integral of the current, the discharging battery equation can be represented as given in Equation 2.4.

$$E = E_0 = K * \frac{1}{SOC} + Aexp(= BQ(1 = SOC))(2.4)$$

The more the battery is charged, the larger the polarization resistance will be. Thus, the battery voltage is high when a battery is almost fully charged. It can be expressedin the following equation:

$Pol. Resistance = K \frac{Q}{it}$(2.5)

For a fully charged battery, the polarization resistance approximately equals infinity, but the experimental result shows that the value of polarization resistance will be changed by 10% of the battery's total capacity; so, Equation 2.5 will take the following form:

$$Pol. Resistance = K \frac{Q}{it=0/0.1Q}(2.6)$$

The output voltage in the charge model:

$$E_{xp}^{\cdot}(t) = B*|i(t)|*(-Exp\,(t) + Au\,(t)) \qquad (2.7)$$

While

$i(t)$ = charging current (A) and both $u(t)$ and $E_{xp}(t)$= exponential zone voltage (V)areequal to 1 when the battery works in the charge mode.

In this thesis, we supposed that when SOC exceeds 95%, the battery has a full charge but if it is 20% or less, the battery cannot provide energy to the outer circuit.

2.3.2 Bidirectional Converter

In a microgrid, a bidirectional converter is often usedfor connectingthe battery and the grid. The battery output voltage is normally less than the voltage in a DC bus; therefore, welinked thebattery to the DC bus using a boost converter. A buck converter was also used for linkingthe battery with the DC bus. Figure 2.5 is the diagram of a bi-directional converter.

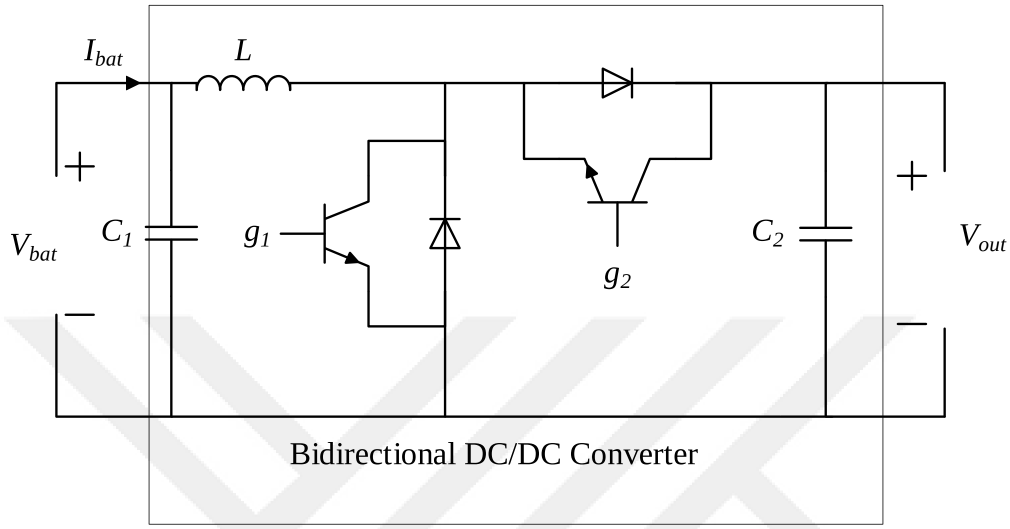

Figure2.5: Schematic diagram of bidirectional converter

In case of gate S_2 has 0 signal while the signal at gate S_1 is 1; so, the bi-directional converter will be in a boost mode, in which, power transmits to a DC bus while battery operation will take place in the discharge mode. In case the signal at gate S_2 is 1 but gate S_1 has 0signals, thebi-directional converter operation will be in buck mode, through which, power transmission takes place to the battery and the battery is likely to operate in a charged mode.

2.4 INVERTER AND LC FILTER

2.4.1 VSC Inverter

A VSC inverter performs voltage regulationin the DC bus with the help of a controller.

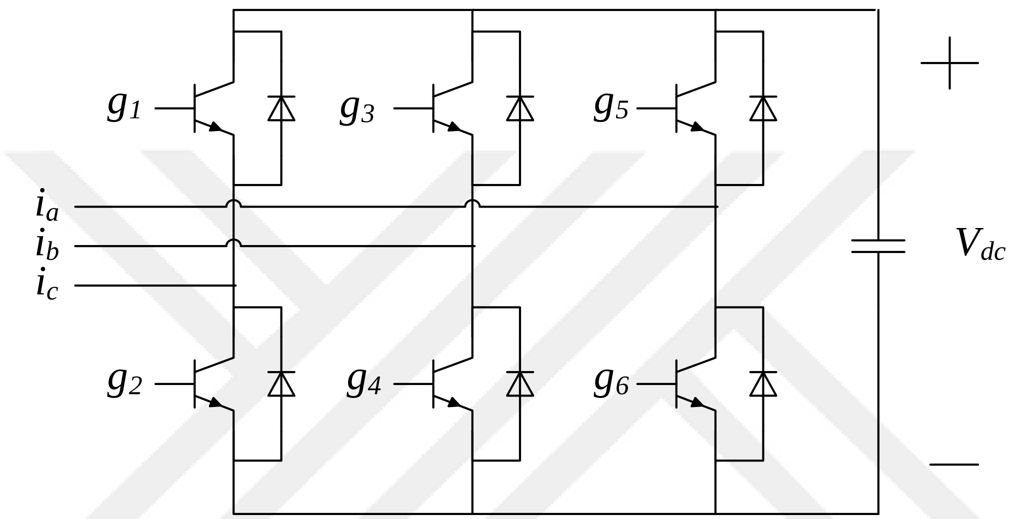

Figure2.6: Schematic diagram of inverter

The figure given above indicates the VSC, which includes six Insulated-Gate Bipolar Transistors (IGBTs), g_1 and g_2 can't work at the same time, whileg_3,g_4, g_5,and g_6 are the same. By controlling the six gates, it can control two of the variables of the system: active power, reactive power, DC bus voltage. It uses a QV control because it has the following benefits:

1. The system can get a stable DC bus voltage, so it will be easier to add DCload toa DC microsystem without any DC-DC converter, so it will reduce the cost and it will be more convenient to expand the system.

2. Increase the reliability of the DC microgrid: When there is a critical loadin the DC microgrid, and it uses a VQ control strategy to control the inverter. When the load changes in a

short time, the grid uses the VQ control strategy, which will get more power from the large grid much faster as compared to the grid using the PQ control strategy. Since the grid using PQ control strategy should measure the power changed in the microgrid, which changes the $P_{fer}$to adjust the power provided to the microgrid.

2.4.2 LC Filter

The power electronic devices are controlled using Sinusoidal Pulse Width Modulation (SPWM) system. This system has an inverter of the same type. That will generate a higher-order harmonic at the switching frequency, so the filter should be used to filter out the interference of the higher-order harmonics. This system is equipped with an LC low-pass filter, which eliminates higher-order harmonics in the range closer to the switching frequency.

2.4.2.1 Selection of the Filter Inductor

Under the same switching frequency, the smaller inductor will increase the-steadystate accuracy of the output voltage, but it will cause a relatively large ripple in the output current.This ripple will lead to greater system noise and electromagnetic interference. On the other hand,if the inductor is designed too large, even though that will contribute to a better output current, it will affect the steady-state voltageoutput. Following requirements should be considered when designing the inductor:

(1) The inductor’s output current should track the reference current;

(2) The waveform of the output voltage should meet the requirements of the unrealindex;

(3) The value of the inductor should reduce the effect of the output voltage accuracy;

(4) Under the premise of filter effectiveness and speed of response, the inductor should be large enough for inhibiting the circulating current.

From the previous papers [57][58], we can get the following:

$$\frac{5u_{dc}}{16f_sI_a} \le L \le \sqrt{u_{dc}^2} = 220^2/(I_{a\omega}(2.8)$$

Where

I_α: rated value of grid current;f_s: Switching Frequency;u_{dc}: voltage of DC bus;ω: angular frequency

So the range of L can be judged from the inequality, then it can use this value of the inductor to decide the value of the capacitor.

2.4.2.2 Selection of the Filter Capacitor

If a large capacity is used in the system, it will be better for the stability of the load voltage, but it will increase the reactive current in the capacitor. And, the current in the inductor and switch will increase, which will lead tolower efficiency. Furthermore, a smaller capacitor needs a larger inductor, but a large inductor will increase the voltage drop in the inductor.

The LC low-pass filter is composed of an inductor and a capacitor. In case, the resonant frequency is lower as compared to the higher-order harmonic frequency, and higher-order harmonic frequency will attenuate at a steady rate of 40dB/sec, so the designed resonant frequency is usually ten times to twenty times larger than the base frequency. According to this design idea, a small capacitor should be used, so we decided to choose a multiple of 20, which formed the following equation:

$$C = \frac{1}{L(2\pi f_1 \times 20)} \quad (2.9)$$

Where, f_1, the base frequency with opposite values for inductor and capacitor will decrease the effect of the interference from the higher harmonic frequency to the simulation result.

2.5 PV CONTROLLER

Between the PV panels and DC bus, a DC-DC converter is added to assure maximum output of the PV panels. To set the output voltage for the PV panels, a controller is needed that is equal to the DC/DC converter's input voltage, which is always equal to V_{pv-max}. The schematic diagram of PV MPPT control is shown in Figure 2.7.

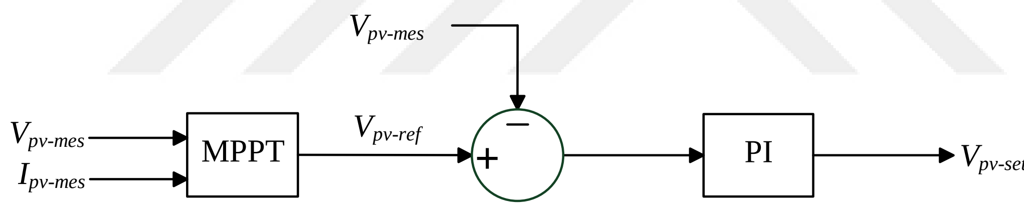

Figure2.7: Schematic diagram of PV MPPT control

2.5.1 MPPT Module

This controller has a key point in the Maximum Power Point Tracking (MPPT) module. In Figure 2.8, the PV module's output characteristic curve has been presented:

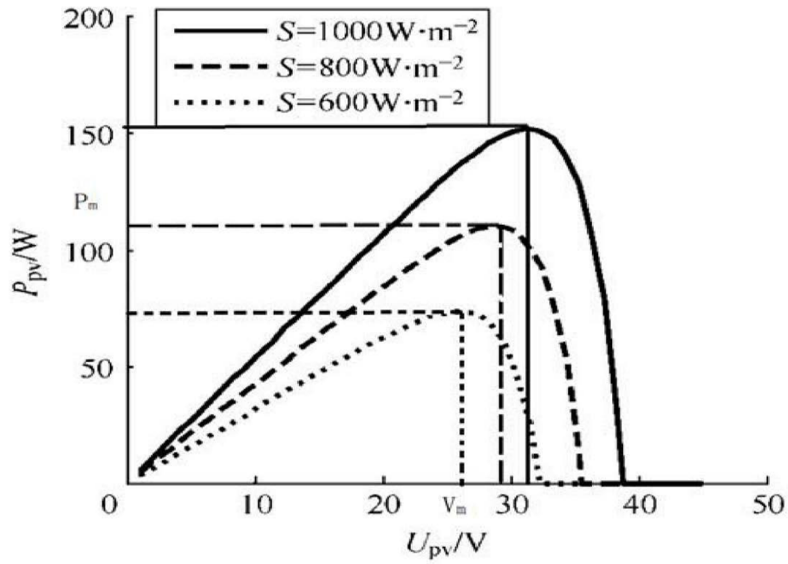

Figure2. 8: PV panel MPPT curves

It is obvious in Figure 2.8 that only when the working voltage equals V_m, PV generation works at the maximum-output power mode; so, the PV generation should track V_m, which means that PV generation works in the MPPT mode; so, the key point in the design of the controller in the PV generation is the MPPT.

From Figure 2.8, it is clear that the three curves have the same temperature while the sunlight irradiation is different for each one of them, and the output power changes when theoutput voltage is different; so,we should find a control algorithm to make the U_{pv-max} get the MPP.

Generally, there are two theories about the MPPT control algorithm: Perturb and Observe algorithm andIncremental Conductance algorithm. The first method shows that the MPPT controller will change voltage with the array's small value and measures the power. When power output increases, the controller continues adjusting the voltage in that direction until the output power no longer increases. This method is easy to understand.From the curve in Figure 2.8, we can observe that in the two directions of the point of maximum power, the slope is eitherpositive or negative; so, this method is easy to implement; however, since the controller needs to change the voltage all the time, this method will affect the stability of the output power.

The second method is based on the Incremental Conductance algorithm, which compares the array conductance(*I/V)* with the incremental conductance($\Delta I/\Delta V$), when both of them are the same, and the output voltage should be maximum. Using this method will eliminate the output power oscillations, but the controller using this approach will need more calculations, and excessive calculations will increase the cost of the system.

2.5.2 Reference Power Output

When the system works in another mode, PV generation should generate the given power, so there is a need for another controller for output power control. In Figure 2.9, PV reference power control has been shown through a schematic diagram.

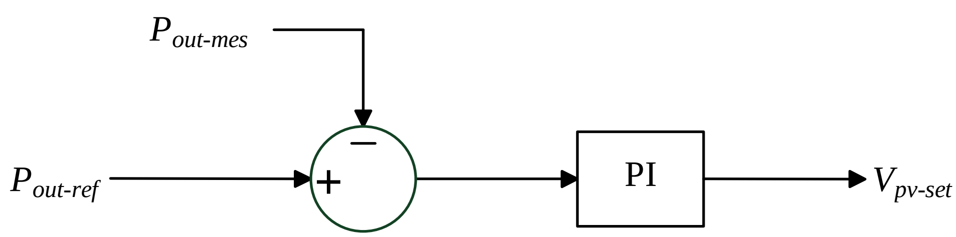

Figure2.9: Schematic diagram of PV reference power control

In the system, when the battery is fully charged, the microgirdconstantly supplies power to the grid. If that constant power value is lower as compared to the PV's MPP value; in that situation, reducing the output power of the PV generation is required; so, a controller (shown in Figure 2.9) is used to increase the operability of the system.

2.6 BATTERY CONTROLLER

In this system, to increase the stability of this microsystem, a battery is added, and a controller of the battery should be used for operating the battery in either charge or discharge mode.

From Figure 2.10, it is obvious thatfirst, the controller needs to judge whether the battery should work in charge or discharge mode. Let us suppose that the battery works in the discharge mode; so,$P_{batt}>0$, and if $P_{batt}<0$, it means that the battery works in charge mode. The next thing the controller needs to do is controlling the two gates in a bi-directional converter to manage the power flow. Usually, the battery voltage level is lower as compared to the DC bus; therefore, the system needs a battery-to-DC Bus and DC bus-to-battery boost converter.

DC bus boost converter.

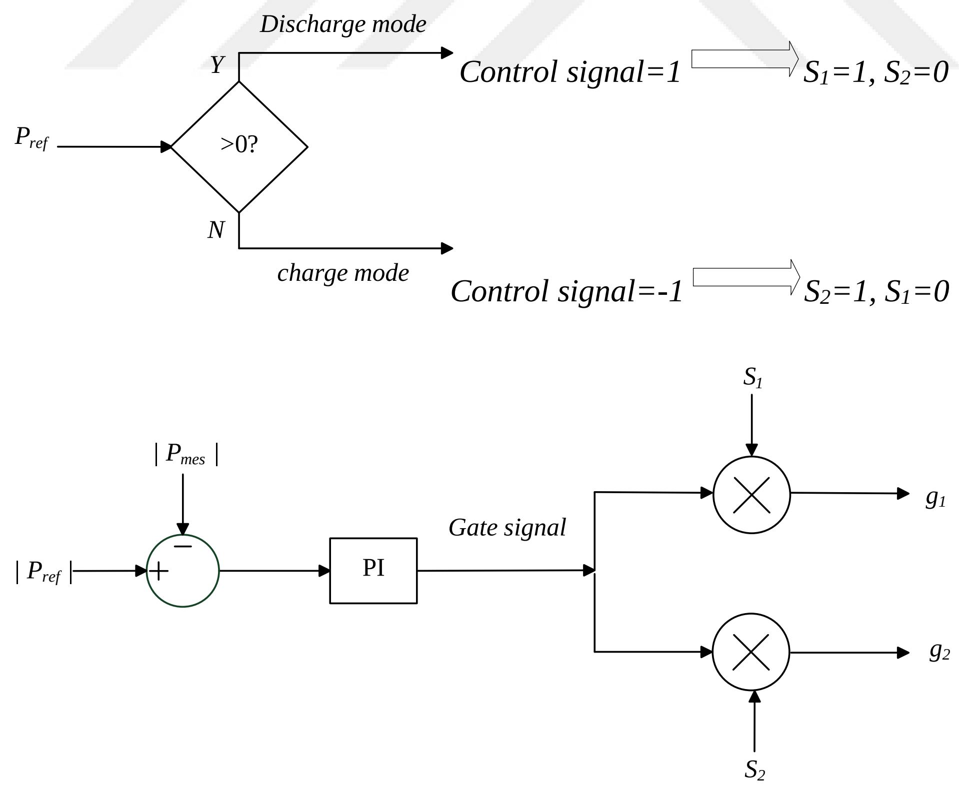

Figure2.10: Schematic diagram of battery charge/discharge control

2.7 INVERTER CONTROLLER

Throughthe inverter, the DC microgrid connects with the main grid, so the controller design affects the overall system’s operation. Figure 2.11 is the schematic diagram of the inverter control:

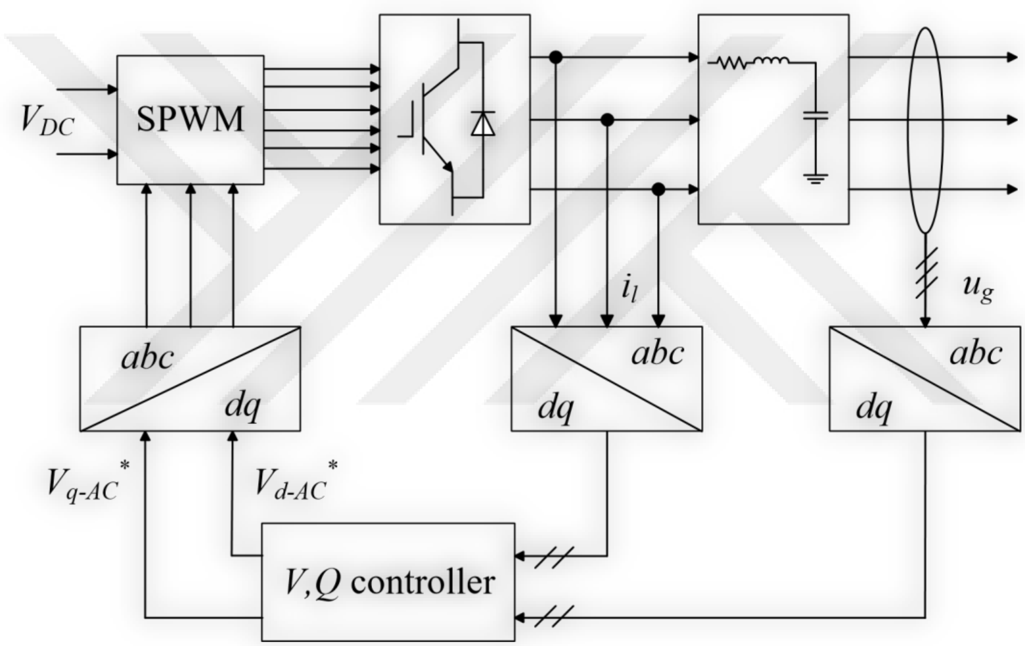

Figure2.11: Schematic diagram of inverter control

From the circuit, the inductor current i_l and capacitor voltage u_g are state variables. In order to calculate more easily, it can use the coordinate transformation method to transform the variable from a three-phase static coordinate to a synchronous dq coordinate, which is also called Park Transform.The following equation is the Park Transform equation:

$$C_{3S}/_{2r} = \sqrt{2/3}\begin{bmatrix} cos\,\theta_1 & cos\,\theta_1 - 120^{\circ} & cos\,\theta_1 + 120^{\circ} \\ = sin\,\theta_1 & -sin\,\theta_1 - 120^{\circ} & -sin\,\theta_1 + 120^{\circ} \end{bmatrix} \quad (2.10)$$

The inverter output voltage isu_g, its amplitude is U_m; so, the inverter output voltage will be:

$$\begin{bmatrix} u_{ga} \\ u_{gb} \\ u_{gc} \end{bmatrix} = \begin{bmatrix} U_m cos * \omega t \\ U_m cos * (\omega t = 120^{\circ}) \\ U_m cos * (\omega t + 120^{\circ}) \end{bmatrix} \quad (2.11)$$

Applying Park Transform on u_g, because the synchronous dq coordinate is based on grid-based frequency, which means $\theta_1 = \omega t$, so:

$$\begin{bmatrix} u_{gd} \\ u_{gq} \end{bmatrix} = C_{3s}/2r = \sqrt{2}/3 \begin{bmatrix} U_m \\ 0 \end{bmatrix} \quad (2.12)$$

From Equation 2.12, Park Transform achieved the transformation from AC to DC while u_{gd}= 0. Similarly, implementing the Park Transform to the inverter output current $i_g$can get the current in the synchronous dq coordinate, which is $i_{gd}$and i_{gq}; so, the inverter's output power, which is synchronous with the dq coordinate, can be expressed as:

$$\begin{cases} P = u_{gd} i_{gd} + u_{gq} i_{gq} \\ Q = u_{qq} i_{qq} - u_{gd} i_{gd} \end{cases} \quad (2.13)$$

Since the system has a DC bus, u_{gd}=0, so Equation 2.13 can be expressed as:

$$\begin{cases} P = u_{gd} i_{gd} \\ Q - u_{gd} i_{gd} \end{cases} (2.14)$$

From Equation 2.14, there is a conclusion that in the synchronous dq coordinate, the current in the *q*-axis determines reactive power while the current in the *d*-axis determines the active power.

2.7.1 VSC Controller

This thesis shows that a DC bus voltage should be regulated, and the DC microgrid's load is resistive; so,it should control the reactive power, which becomes zero when transformed by the inverter, so we used QV control in this thesis.

In this part, the inverter's output current and the filter's output voltage are measured, then we applied the Park Transform to obtain the current and voltage values. In this case,through *d*-axis and *q*-axis, a controller gets the voltage and current, respectively. Thus the voltage in a DC bus is measured. From Equation 2.13, we can find the relationship between reactive power Q and I_q,

$$I_q = \frac{I_q V_q + Q}{V_d} (2.15)$$

Thus, we can get the following control schematic diagram (Figure 2.12 given below):

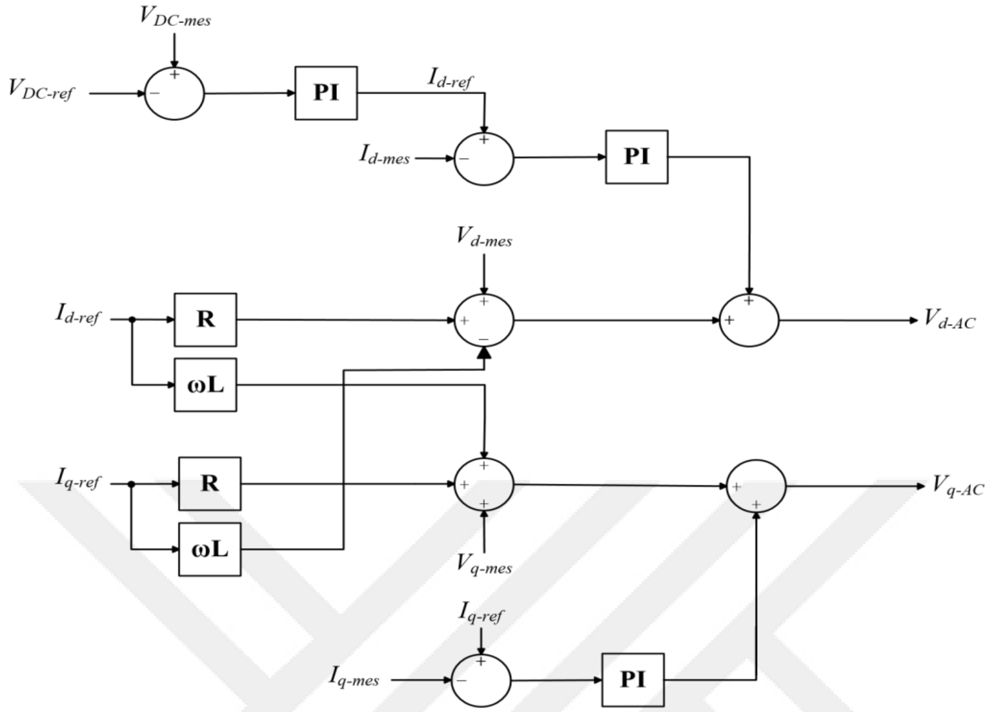

Figure2.12: Schematic diagram of inverter VQ control

Since the value of the capacitor in the filter is too small, the capacitor in the filter can be neglected. Using this controller, regulating the voltage of a DC bus to a given value is possible. According to a previous study[59], there are some limiting factors regarding the DC bus voltage:

$$V_{DC} \geq ACL - 1/m(2.16)$$

Here, m is the duty cycle of the inverter, which often uses 0.8 in this condition

3. WIND TURBINE STRUCTURE

If we look at the wind turbine structure, it has a rotor, which is mounted on a nacelle. It also has a tower, which has at least two blades. They are mechanically linked with an electric generator. Transformation of slow wind turbine rotation speed into a higher speed takes place through the gearbox in the mechanical assembly. The electric generator's shaft rotates and generates electricity while the control system maintains the output. Two types of wind turbine designs are available, and they are classified based on their rotational axis: Horizontal Axis Wind Turbine (HAWT) and Vertical Axis Wind Turbine (VAWT). The later turbine is sometimes termed as Darrieus rotor, which is named after Darrieus, who invented it [6]. HAWTs collect most of the wind energy during the day and their blades are adjusted when there is any wind storm. The wind turbine operations are either at a variable or a constant speed. When a constant-speed turbine is used, the angular speed of the rotor remains constant despite variations in the wind. This mode has an advantage: It does not require costly power electronics, including converters and inverters. It has a disadvantage: The rotor speed is constrained, which does not allow a turbine to operate at full efficiency in strong wind. This is why a constant-speed turbine generates lesser energy when there is a low wind speed in comparison with turbines that have variable wind speeds and a specific rotor speed. The wind speed and rotor speed are proportional even when it is lower as compared to the rated wind speed [1]. A wind turbine's output power/torque of a wind turbine is determined and influenced by many factors, including rotor blade tilt, turbine speed, shape and size of a turbine, rotor blade pitch angle, rotor geometry (irrespective of HAWT or VAWT type of turbine), wind speed, and area of the turbine. There is a relation between different variables and the output power, which helpsto constituting the wind turbine's mathematical model, and that is necessary to be developed for understanding wind turbine behaviors in its operational region, and besides, it helps to control the wind turbine's operational performance. In this paper, a specific model of a wind turbine is suggested, which meets our objectives.

In this section, we have presented the methodology used in this thesis in detail.

3.1 WIND POWER FUNDAMENTALS

Researchers and scientists have focused on wind power control, generation, and integration, and now, it has become a very popular power generation option[60]. Generally, researchers believe that wind power is the second most significant source to generate power[61]; therefore, research is continued on maximizing its potential, grid-integration, andpowerpoint tracking. Since it has significant uses, like charging wind-powered electric vehicles (EVs), and wind-powered battery charging besideother uses. Researchers are proposing and presenting maximum power tracking algorithms, and they are making changes in the matching design of a battery charging controller and real-time EV charging control. The cost of wind turbines is normally exorbitant, and the wind has numerous uncountable issues and stochastic nature; therefore, researchers are yet not been able to apply the presented algorithms in all kinds of weather conditions[62]. Forhandling this issue, an emulator is developed for a wind turbine foranalyzing the already developed algorithms. Emulators emulate the three parts of a wind turbine, including parking, pitch angle control, and maximum power point tracking [63]. After developing the wind turbine emulator, it was tested using two modes: Model simulation and real-time model testing.

The existing literature on wind turbine emulatorsincludesthe following efforts: A separately-excited DC motor was added for realizing the properties of a wind turbine [64]. For implementing the proportionally-integral control logic of an excited DC motor-based wind turbine emulator, a digital signal processor was used. Research shows [65] that the emulation of wind turbine characteristicswas performedusing a commercial DC motor drive. AdSPACE hardware board was used in this emulator for implementing the wind turbine's reference model, which was equipped with a PI control. Another publication presents PI-controlled wind turbine emulator [66]. In research, a simple gain-scheduled PI controller has been used, whichhas certain characteristics, which resembled the real-time wind turbinecharacteristics. They used a DC motor in their research work for emulating characteristics of a wind turbine [67]. Bothwind velocity and motor speed determine the reference model's output. A supervisory control was used with the help of a personal computer for implementing the emulator control. The efficiency of emulation was almost 88%. In another work[68], armature voltage and field controls were used to control a DC motor to note down the required wind turbine characteristics. Using armature voltage control, a PI control algorithm was implemented as a proportional control action for field flux control. The reference command is generated through a wind turbine reference model using wind velocity and motor speed. The researchers reported 90% emulation efficiency.

Research[69] was conducted on real-time wind turbine characteristics, which were emulated when the researchers used a separately-excited DC motor. For mathematical modeling of the wind turbine, an analog circuit concept was used. Using constrained optimization, PI control for the wind turbine emulator was optimized, and the emulator was realized when the researchers used a separately-excited DC motor[70]. The reference command was generated through a wind turbine reference model based on different parameters, including wind velocity,motor speed, and pitch angle. When amotor generates torque, it is controlled with the help of a PI control. The researcher reported 91% emulation efficiency in this case. Another work [71] shows that aPI-controlled DC motor can emulate the properties of a wind turbine. The reference torque was generated in a wind turbine with the help of wind velocity, pitch angle, and motor speed.

Theresearchers used a DS 1104 hardware control board for implementingPI control and a reference model of the wind turbine.

Another research [72]studied the open-loop DC motor control, which resembled the real-time characteristics of wind turbines, and to emulate them, field flux control and open-loop armature voltage control of a wind turbine were used. The DC motor voltage was controlledusing power resistors, which resulted in further power losses, and degraded the overall system efficiency. In a research work [73], the researchers simulated a wind turbine based on a DC motor with its associate control in MATLAB. Based on pitch angle, wind speed, and DC motor speed, the reference wind turbine model generated the required current signal. For keeping the DC motor torque in check and emulating the wind turbine properties, a PI control has been used. In a previous research paper[74], the researchers presented a fuzzy-based proportional derivative controlled wind turbine emulator. Fuzzy logic control was used to control both DC motor speed and torque. A conventional PI control was compared to a fuzzy logic controller, which showed that the system's emulation efficiency with fuzzy logic control was almost 92%. In another study[75], a permanent-magnet DC motor-based emulator for a wind turbine was used. They studied the hardware realization and simulation of a wind turbine. They suggested a PI torque-control scheme using a chopper-controlled four-quadrant DC motorand emulated some wind turbine characteristics[76]. They used Lab View software for implementing the wind turbine emulator control usinga microcontroller hardware control board. Using the PI control algorithm, the researchers implemented speed and current controls. The system's emulation efficiency was almost 91%. Research[77] on open-loop FPGA control DC motor shows that the model resembled certain wind turbine characteristics. For a DC-DC converter-fed motor,they used a wind velocity-based PWM pulse.For an FPGA control board, a wind turbine reference model program was used. Moreover, for standalone applications, a wind turbine emulator was developed[78].

Wind, solar, and other renewable resources are effective for pollution; more specifically, wind power is transformable into useful energy because of rapid wind-based power generation technologies, including wind turbines, which harness the wind’s kinetic energy for generating electricity.It is a fact that wind power is a viable alternative to polluting fossil fuels, and besides, no greenhouse gas is emitted; therefore,a significant difference can be observedin terms of the environment. After several wind power advancements, the cost to generate wind power reduced as compared to other renewable options; however, researches on wind turbine research should continue to make it an even more viable energy source [79][80].

Wind turbines use too many types of variable speed generators. According to numerous studies, Permanent Magnetic Synchronous Generators (PMSGs) have certain reportedbenefits as compared to other generators. PMSGs have slow rotation speeds and they work without needing any gearbox. PMSGs have their own benefits, such as low maintenance needs and high efficiency [81][82][83][84].

A Wind turbine is normally fitted with fixed frequency induction generators but the generated power is not enhanced for all wind conditions. Wind technologies need continuous development to improve the wind power generation system’s performance; however, its inverter unit has efficiency issues. A novel controller is used to enhance and improve efficiency and reliability. This controller consists of MPPT that will be integratedinto PWM and a back-to-back space vector.The rotor speed will also be measured and the rotor speed will be comparedto the optimum rotor speed. Both the inverter and the pitch angle controller gained improvementbecause of the performance regulation. Wind speed was combined to change different parameters, such as aerodynamic turbine torque [85][86][87][88].

The model of the entire wind power generation system includesgenerator-side and grid-side control techniques and it has a synchronous generator,which improvesthe system performance, and that is evident from different studies. This type of control mechanismand model system includesdifferent models for pitch angle control, PMSG wind turbine,generator-side inverter control, and grid-side inverter control.

It is evident from various studies on the wind turbine system, which includessome control functions for grid-side, generator-side, and a physical permanent magnet synchronous generator, and that increasesthe system's efficiency. The control strategies and the mentioned system havemodels for pitch angle control, grid-side inverter control, PMSG wind turbine, and generator-side inverter control. The grid-side and generator-side inverter controllers have pulse width modulationto make Maximum PowerPoint Tracking (MPPT) perform and decouple active as well as some reactive power controls by supplying the changing current to the x and y-axis of their inverters. To improve the control strategy, the researchers useda traditional PI controller. They integrated a pitch angle controller, and grid-side as well as generator-side inverters. To simulate as well as validate the performance, they used MATLAB Simulink. The effects of the integrated PMSG wind turbine would be clarified by the results(when autonomous controllers are used)[89].

3.2 MATHEMATICAL FORMULATION OF WIND TURBINE

The kinetic energy (E) of an object under constant acceleration “a” has velocity v and mass m while work is done W displaces the object from stationary position to distance s applying a force F, while E = W = Fs is given. Newton’s second law of motion states:

$$F = ma \qquad (3.1)$$

The kinetic energy will be:

$$F = mas \qquad (3.2)$$

Solid motion kinematics are shown by $V^2 \equiv u^2 + 2as$ whereas u stands for the objects’ initial velocity. It means $= \frac{V^2-u^2}{2s}$. We assume that the object’s initial velocity is zero, so $a = \frac{V^2}{2s}$. Using Equation 2, we get:

$$E = \frac{1}{2} mV^2 \qquad (3.3)$$

This formulation of kinetic energy formulation is fact-based that every solid object’s mass is constant but in case of wind (moving air) is a gas, so its velocity and density are variable; therefore, it does not have a constant mass. Reccab et al. [5] formulated a law of kinetic energy taking 2 3 as a factor instead of 1 2. This paper assumes that the air density does not considerably vary when there is any change in either temperature or altitude. Equation 3 shows the kinetic energy law. Kinetic energy (joules) of air has a mass m, and it moves with V_w (velocity of wind), and Equation 3 can be used to compute it. The wind power P represents the rate of change in kinetic energy, so:

$$p = \frac{dE}{dt} \equiv \frac{1}{2}\frac{dm}{dt} v_W^2 (3.4)$$

Here $\frac{dm}{dt}\rho AV_w$ shows the mass flow rate $\frac{dm}{dt}$ and A represents the wind flow area while ρ shows the density of air. Using this information, Equation 4 will be:

$$P = \frac{1}{2}\rho A v_W^3 (3.5)$$

The rotor blades extract the actual mechanical power Pw (watts), which represents the upstream-downstream wind power difference [1], which is given below:

$$P_w = \frac{1}{2}\rho A v_w (v_u^2 - v_d^2)(3.6)$$

Here $v_u$represents the upstream velocity of wind (m/s) on the rotor blades' entrance point while $v_d$vd represents a downstream velocity of wind (m/s), which exists at the exit point of a rotor blade. In the later parts of this thesis, we will see that both velocities combine and create a specific speed ratio on the blade-tip. The mass flow rate was used to obtain the following equation:

$$\rho A v_w = \frac{\rho A(v_u + v_d)}{2}(3.7)$$

Here, v_w is the average of the entry and exit velocities of the turbine rotor blades. Using this expression, Equation 6 will be $P_w = \frac{1}{2}\rho A v_w (v_u^2 - v_d^2)(\frac{v_u + v_d}{2})$ and that can be simplified as given below:

$$P = \frac{1}{2}\rho A v_u^3 C_P (3.8)$$

The C_P expression is given in Equation 8, which is a part of the upstream wind power used by the rotor blades. C_P is also termed as Betz limit because German physicist Albert Betz presented it in 1919. It is also called rotor efficiency and the rotor's power coefficient, which is not static but varies with changing the wind turbine's tip speed ratio. Here $\boldsymbol{\lambda}$ represents the downstream-upstream wind speed ratio:

$$\lambda = \frac{v_d}{v_u} \quad (3.9)$$

Or

$$\lambda = \frac{blade\ tip\ speed}{wind\ speed} \quad (3.10)$$

λrepresents the wind turbine tip speed ratio. The per second blade tip speed can be computed using the turbine's rotational speed and the blade length:

$$blade\ tip\ speed = \frac{angular\ speed\ of\ turbine(\omega) \times R}{wind\ speed} \quad (3.11)$$

Here, ω is measured in radian per second and R stands for the turbine radius.

In a complete system, other factors, which impede complete energy conversion, include bearings, gearbox, number of blades, and blade shape. Just 10–30% of the wind power actually converts into usable power. Here ρ is the air density with another flow input quantity. And, the function of air pressure and the temperature is denoted by ρ. Here, an increase in ρ increases air pressure but the air temperature reduces. It is according to the equation of the state:

$$P = \rho RT \qquad (3.12)$$

Here, R represents gas constant. Pressure and temperature decrease when elevation is increased. This proves that the site location is important because, as mentioned earlier, elevation substantially affects power generation because the air density is different.

3.3 MATHEMATICAL MODELLING OF PV

PV cellsarea current source, which performs in parallel in the equivalent circuit with a diode. When a real equivalent circuit model is used, it incorporates additional series and parallel resistors. It must be noted that there will be no power generation when there is no sunlight, PV cell performs likea p-n junction diode. The actual current from the current source (PV cell) will depend on sunlight, which falls on a PV cell (Photocurrent).

ThePV cell's mathematical model has been presented in this section. The output of the PV cell depends on a drop in voltage across the p-n junction (diode).

$$V = \left(\frac{NKT}{Q}\right) ln \frac{I_L - I_o}{I_o} + 1 \qquad (3.13)$$

In this case:

IL shows the light-generated current (Iph (A))

N shows diode ideality constant

V represents open circuit voltage

K represents Boltzmann constant (1.381x 10-23JK-1)

Io stands for the saturation diode current (A)

T is temperature (Kelvin)

Q shows electron charge (1.602 x 10-19 Coulombs)

Current generated through light:

$$I_L = \left(\frac{G}{G_{ref}}\right) * (I_{L\,ref} + \propto_{Isc} \left(T_C - T_{C\,ref}\right)) \qquad \text{(3.14)}$$

Here

Gref impliesradiation under standard conditions - 1000 W/m2

G represents radiation (W/m2)

Tc implies temperature in the present condition.

ILref is the Photo-electric reference current in standard condition at 0.15A

IL stands forlight generated current/radiation

αISC represents the short circuit current's temperature co-efficient when A/K=0.0065AK-1

TCrefshows module temperature in standard conditions- 298.0K

The reverse saturation current will be as follows:

$$Io = I_{or} \left(\frac{T_c}{T_{ref}}\right)^3 e^{\frac{(Q*Eg)}{(K*N)*\left[\left(\frac{1}{Tcref}\right)-\left(\frac{1}{Tc}\right)\right]}} \qquad \text{(3.15)}$$

$$I_{or} = \frac{I_{scn}}{e^{\left(\frac{V_{ocn}}{N*V_{tn}}\right)}} \qquad \text{(3.16)}$$

In this case:

I_{or}denotes the saturation current

Io denotes the reverse saturated current

Short circuit current: Ish = IL

Egstands for the silicon band gap (1.10eV)

N shows the ideality factor (1.50)

The cell generates the greatest amount of current, which is produced during short-circuit: Volts = 0.00V.

$$I_{sh} = (I_L - I_o) * \left(e^{\frac{eV}{KT}} - 1\right) A \qquad (3.17)$$

3.4 WIND TURBINE MODEL

Wind turbines are modeled to deliver peak output at 15m/sec wind speed. Initial wind turbine speed is associated with cut-in wind speed(almost 5m/s). The maximum power output has been delivered by the generator when the rated wind speed was 10-17m/s. The increase in wind velocities between 17 and 30m/s brings the rotor at a risk of damage and this speed is termed as cutout wind speed. Pitch control and stall control are power control methods for the wind turbine.

The wind power output can be calculated using the expression given in Equation 3.18

$$P_w = 0.5 \rho C_p A v_{\omega}^3 \qquad (3.18)$$

Where ρ denotes air density, P_w denotes captured wind power, v_ω denotes speed of the wind, Cp denotes the power coefficient, and R is the radius ofthe rotor blade. The relation between a power coefficient and a pitch angle of the blade is given in expressions3.19, 3.20, and 3.21.

$$C_p(\lambda,\beta)=C_1(\frac{C_2}{\lambda_i}-C_3\beta-C_4)e^{\frac{-C_5}{\lambda_i}}+c_6\lambda \qquad (3.19)$$

$$\lambda=\frac{\omega_t R}{v} \qquad (3.20)$$

$$\frac{1}{\lambda_i}=\frac{1}{\lambda+0.08\beta}-\frac{0.35}{\beta^3+1} \qquad (3.21)$$

In this equation, ω_r is turbine speed in radians per second. The peak value of the power coefficient is obtained when β is 0^0 while the tip speed ratio is 8.10 and the optimal power coefficient value is 0.48. The Betz limit for the highest C_p is 59.3%

The mechanical torque is obtained as follows:

$$T_m=\frac{P_m}{\omega_r} \qquad (3.22)$$

Considering a single rotating mass model for the drive train, the torque equation can be written as Equation 3.23.

$$J\frac{d\omega}{dt}=T_m-T_{em}-K.\omega \qquad (3.23)$$

Here T_{em}, K and J represent electrical torque, viscous friction, and total inertia constant, respectively.

The torque developed in terms of electrical parameters, which are represented by Equation 3.24:

$$T_e = \frac{3}{2}\frac{P}{2}\left(i_{qs}i_{dr} - i_{ds}i_{qr}\right) \quad (3.24)$$

3.5 DEEP NEURAL NETWORK MODELLING AND DNN BASED MPPT FOR PV

Since ANN has a feed-forward topology,it is alsotermed asa feed-forward artificial neural network, and it has just a single condition: The input-output information flow should have a single direction and no back-loops, as Figure 3.1 shows.The number of layers is not limited, and the same is true forthe number of connections between individual artificial neurons and types of transfer function, which are used in individual artificial neurons[18]. A single perceptron is actually the simplest feed-forward ANN, which can learn separable linear problems. For analytical description, asimple multi-layered feed-forward ANN is given below:

$$n1 = F1(w1x1 + b1) \quad (3.25)$$

$$n2 = F2(w2x2 + b2) \quad (3.26)$$

$$n3 = F3(w3x3 + b3)(3.25) \quad (3.27)$$

$$n4 = F4(w4x4 + b4) \quad (3.28)$$

$$m1 = F4(q1n1 + q2n2 + b4)(3.29)$$

$$m2 = F5(q3n3 + q4n4 + b5) \quad (3.30)$$

$$Y = F6(r1m1 + r2m2 + b6) \quad (3.31)$$

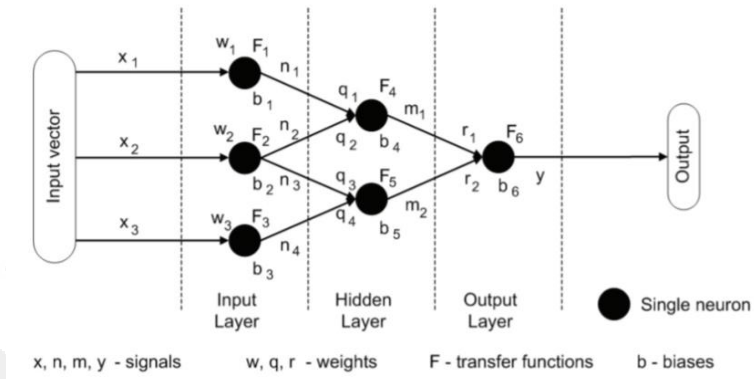

Figure3.1: Feed-forward deep neural network (single neuron model)

4. EXPERIMENTAL RESULTS

4.1 MAXIMUM POWER POINT TRACKING ALGORITHM

Itmaximizes power generation when a renewable energy resource is usedin variable weather and changing temperature. During the past 10 years,several researchers attempted to put forward a new MPPT algorithm applying different controllers, includingincremental conductance, P&O,Fuzzy, PSO,ANN,and ANFIS controllers, and feedback voltage and current[91][92][93]. This thesis is based on a DNN controller for developingthe MPPT algorithm, which is required for PVtechnology. A DNN learning algorithm consists of 66,000 items in the data for developingan MPPT algorithm (Figure 4.1). Our proposed system needed a simulation model for testing; so, it was simulated using MATLAB (Figure 4.2). A 20kW PV array is used in the proposed simulation model in addition toa boost converter to step up the voltage. A flowchart has been shown (Figure 4.3a) to demonstrate the DNN controller processes while Figure 4.3b shows the DNN layer, which has 1,000 hidden neurons,two input neurons and, an output neuron. For training the MPPT network with the help of data, this DNN layer has been used, which has an input (in the form of PV current and voltage) while theoutput is a converter's duty cycle.

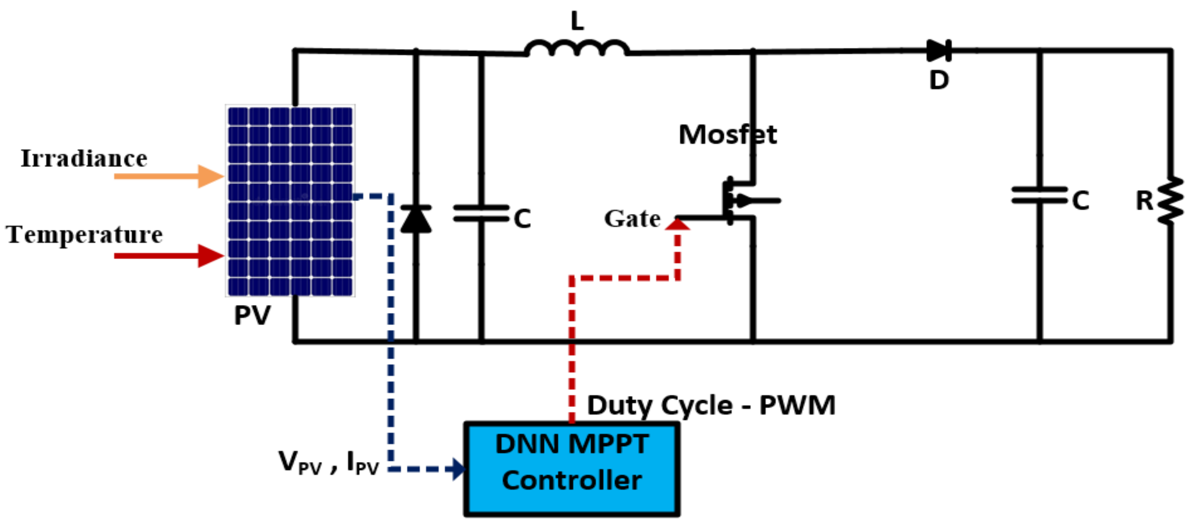

Figure4.1: Proposed DNN-based MPPT algorithm

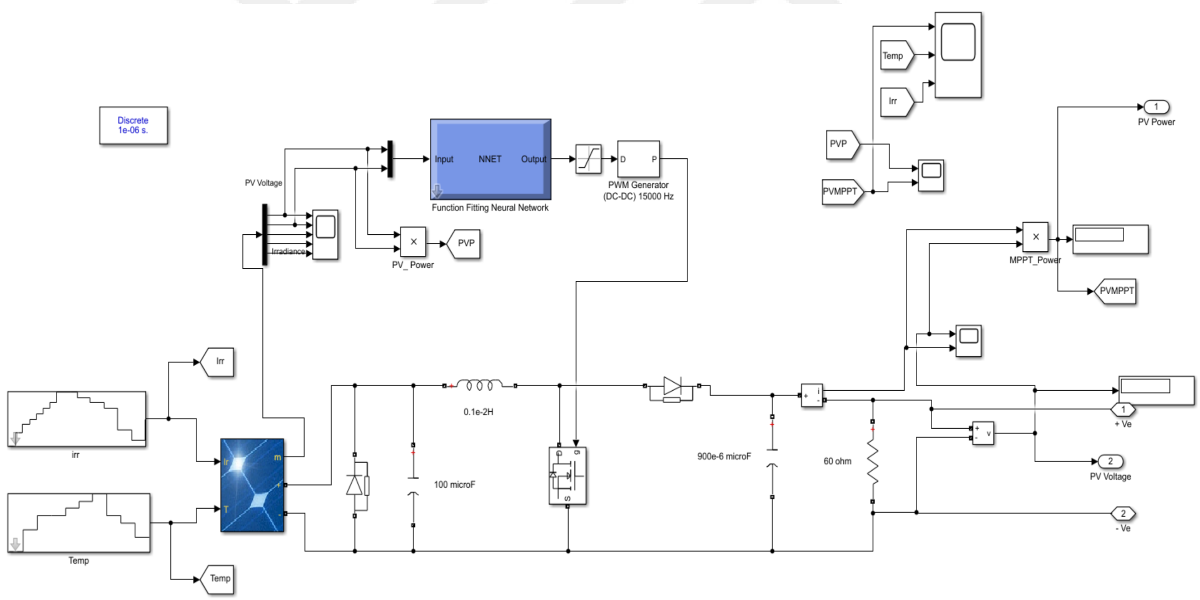

Figure4.2: Simulation model of DNN controller-based MPPT algorithm for the PV system

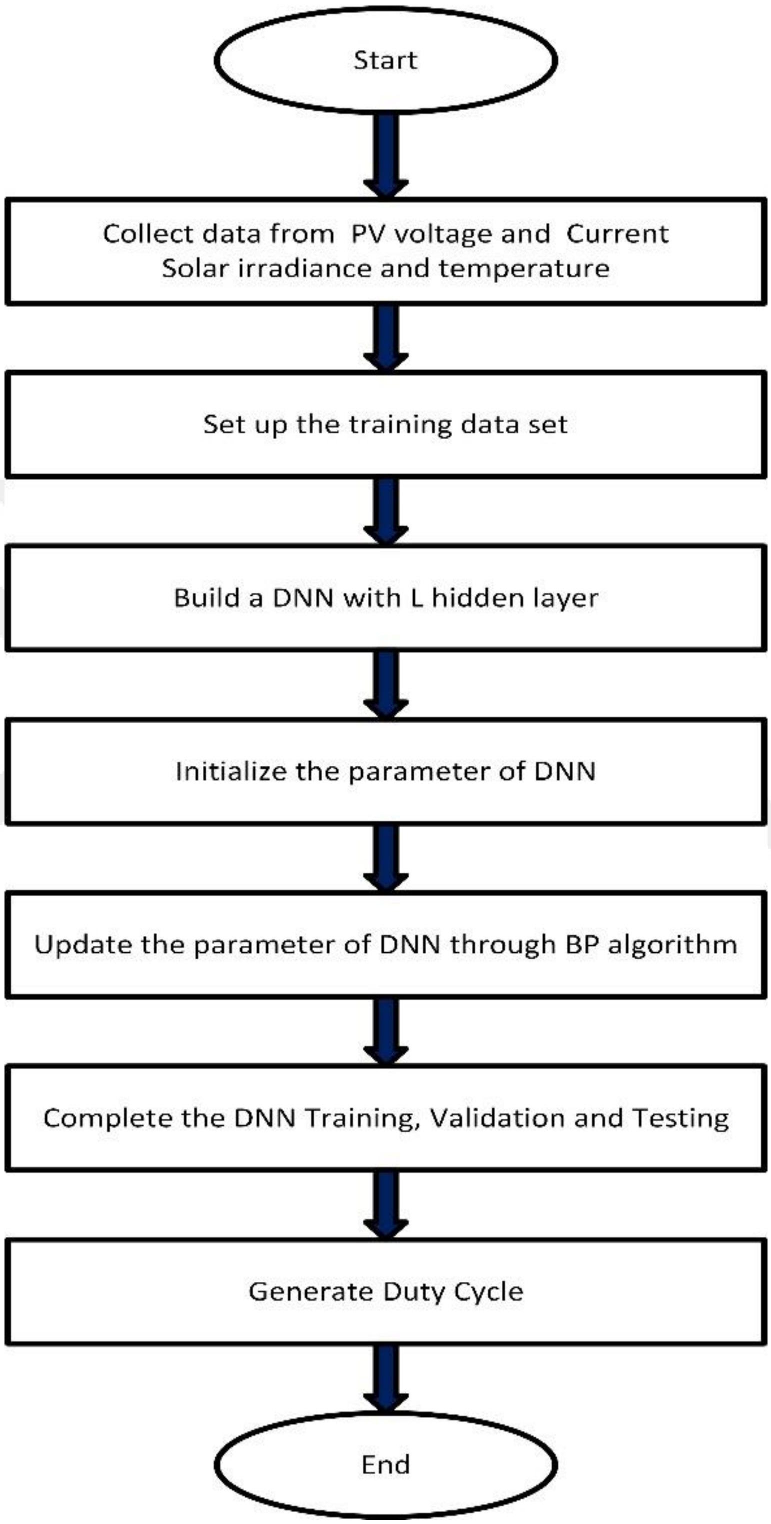
Start
Collect data from PV voltage and Current
Solar irradiance and temperature
Set up the training data set
Build a DNN with L hidden layer
Initialize the parameter of DNN
Update the parameter of DNN through BP algorithm
Complete the DNN Training, Validation and Testing
Generate Duty Cycle
End

(a)

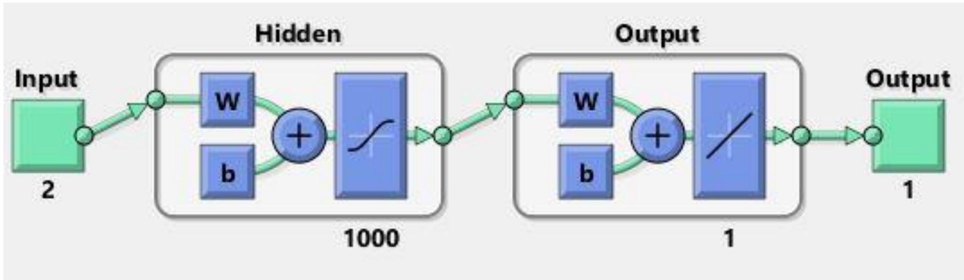

(b)

Figure4.3: a) Flow chart DNN Model for PV-MPPT system, b) DNN Model for PV-MPPT system

Using the above system, A DNN controller has been trained and Figure 4.4 shows its best validation performance. Figure 4.5 shows a histogram for a proposed DNN controller error.Optimum numbers of hidden layers and units are dependent on the network architecturecomplexity, number of I/O units, levels of noise in a sample data set, number of training samples, and training algorithm.

When thedata samples are too few or when the data is not so noisy, generally, there is no need for a hidden layer. To obtain accurate training and prediction, a linear/generalized linear model can be sufficient[3]. The nodes are affected by a hidden neuron, and such nodes are linked with the output. The neural network stability is analyzed by the existence of an error. The higher error means theworst stability while the minimal error means better stability. Over-fitting is caused by unnecessary hidden neurons, and the neural networks tend to overestimate the complication of the target issue.Figure 4.6 presents our DNN-trained network gradient and the validation check. Finally, after developing the algorithm, its best regression was used for testing, training, validating, and the overall performance evaluation of the data, which have been presented in Figure 4.7. Table 4.1 shows the overall DNN data.

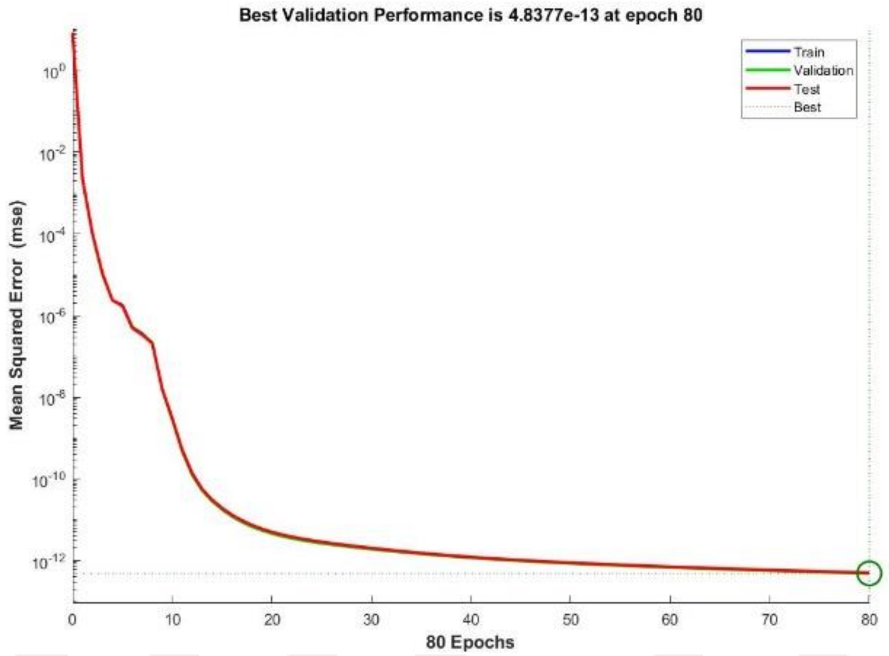

Figure4.4: DNN-PV MPPT controller showing best validation performance

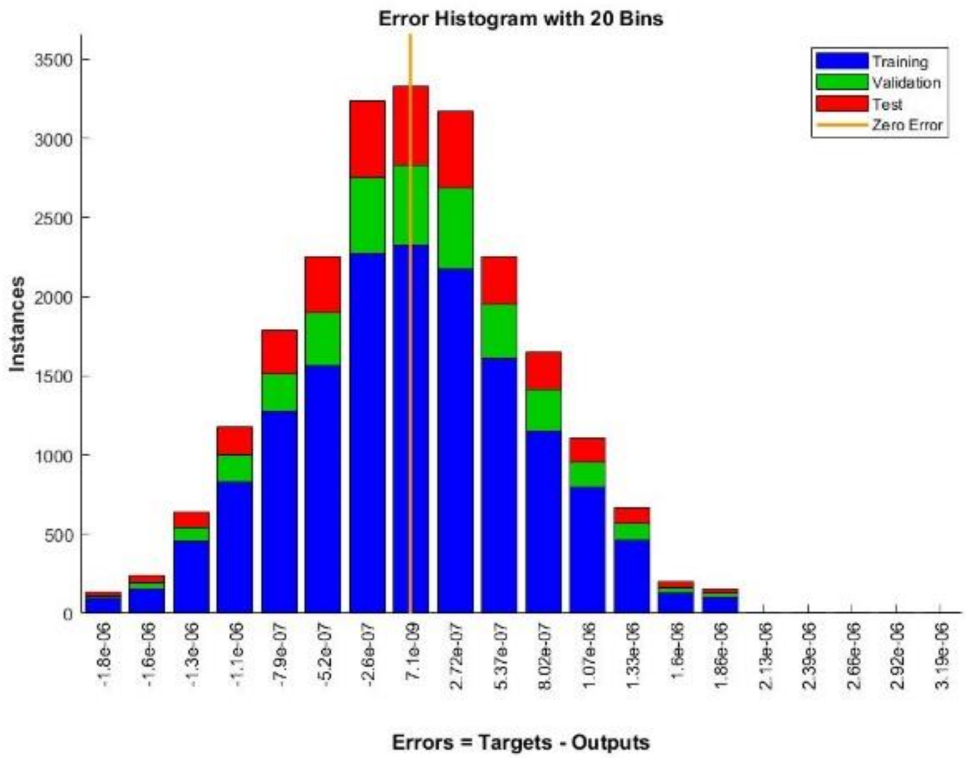

Figure4.5: DNN-PV MPPT controller error histogram

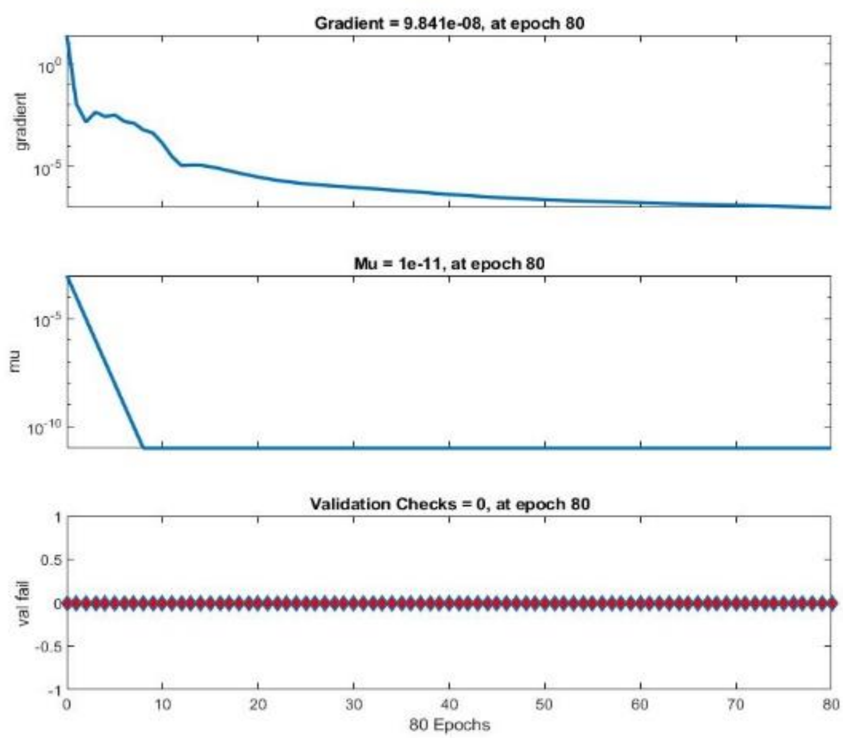

Figure4.6: DNN-PV MPPT controller training data

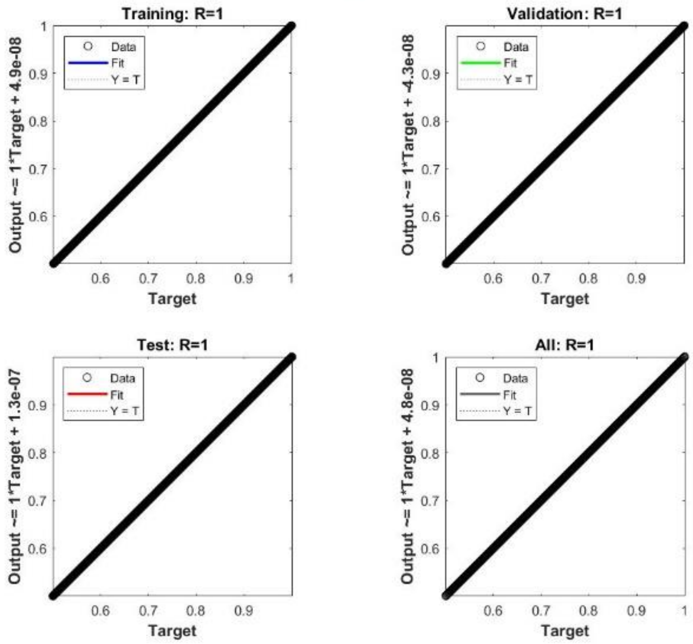

Figure4.7: Best regression of DNN-PV MPPT controller

Table4.1: DNN data of an MPPT controller

DNN – Wind MPPT	Values
Best Validation	4.8377e-13
Mu	1e-11
Gradient	9.841e-11
Training	1
Validation	1
Test	1
Overall regression	1

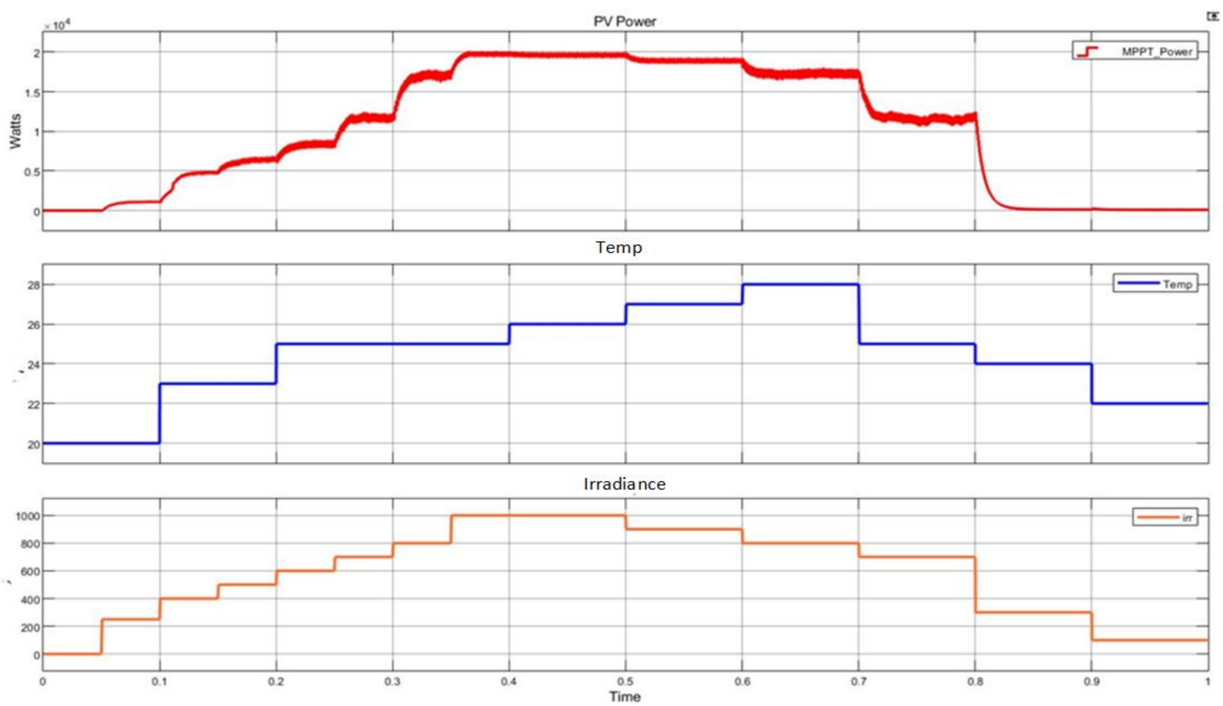

Figure4.8: Simulation results of DNN-PV MPPT power in terms of temperature and irradiance

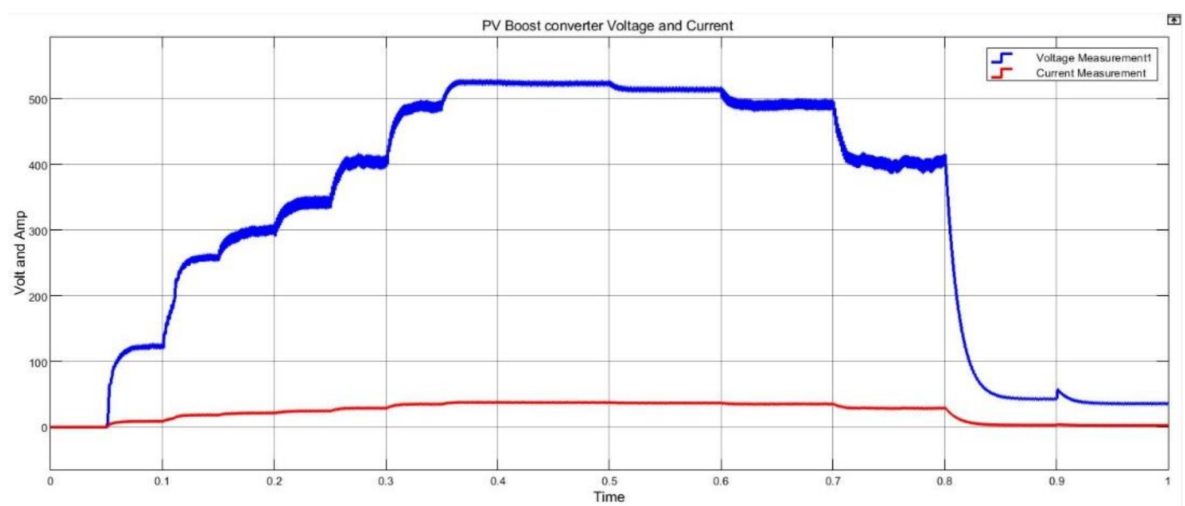

Figure4.9: Simulation results of DNN-PV MPPT boost converter voltage and current with respect to irradiance and temperature

We proposed the DNN-based MPPT algorithm and developed it, after which, it was applied to a 20kW PV system, and simulated inMATLAB. We analyzed the outcomes under different weather situations. The PV output power with various irradiance values andtemperatures is shown in Figure 4.8. Figure 4.9 shows the output voltage and the boost converter’s current waveform.

I. Deep Neural Network-based MPPT for Wind Power Systems

It was usedfor developingthe MPPT algorithm, which was developed for a wind power system (Figure 4.10). Approximately, 66,000 data items have been used in this DNN learning algorithm, which provided training for developing the algorithm[12]. The MPPT-based system was simulated in MATLAB (see Figure 4.11). For simulation, we used a30kW wind energy system and a boost converter to step up the voltage [94]. Figure 4.12b is a flowchart that describes the DNN layer and the controller. The mentioned layer has 1000 hidden-layer neurons,a couple of input neurons, and a single output neuron. MPPT network traininguses the input data (wind current and voltage), this DNN layer has been used while the converter’s duty cycle shows the output data.

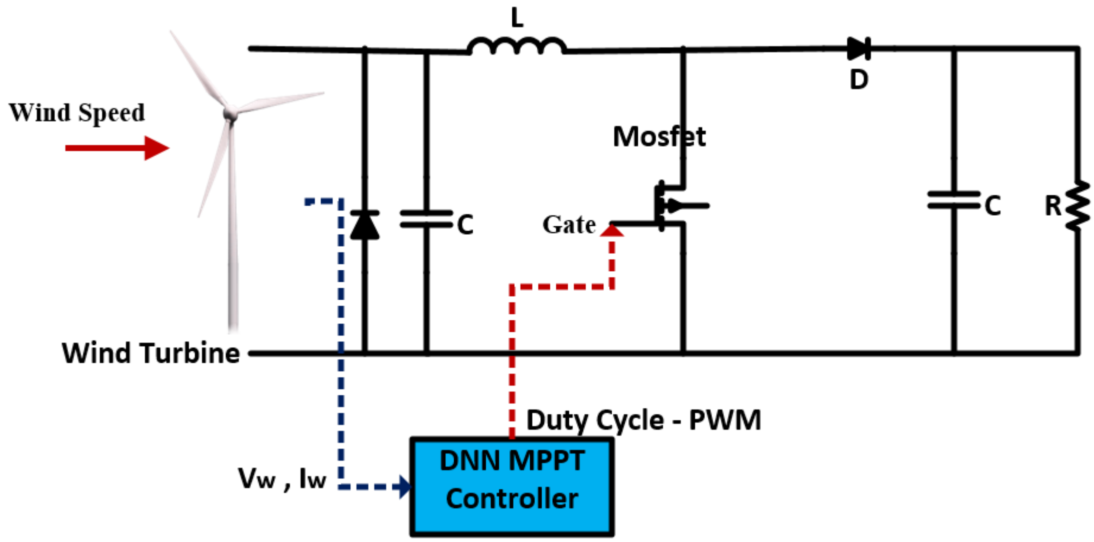

Figure4.10: Proposed DNN-based MPPT algorithm (wind energy system)

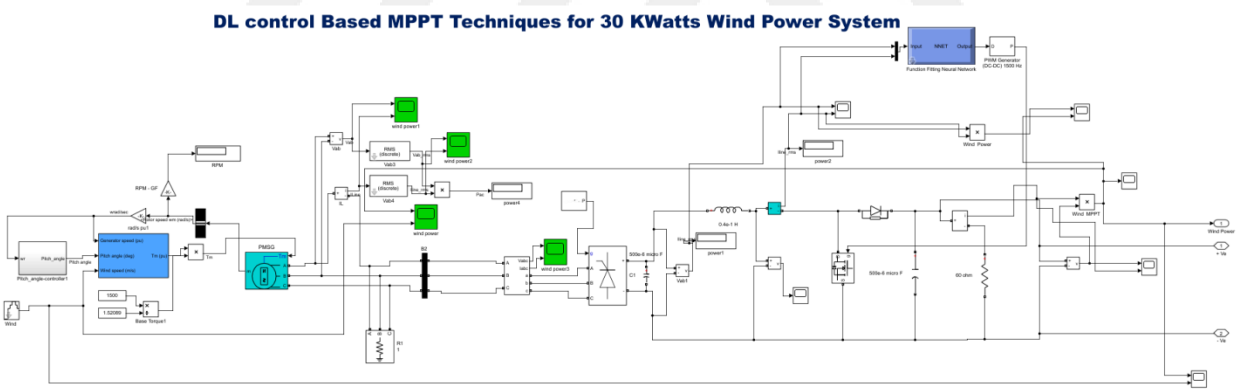

Figure4.11: Simulation model of DNN controller-based MPPT algorithm (wind energy system)

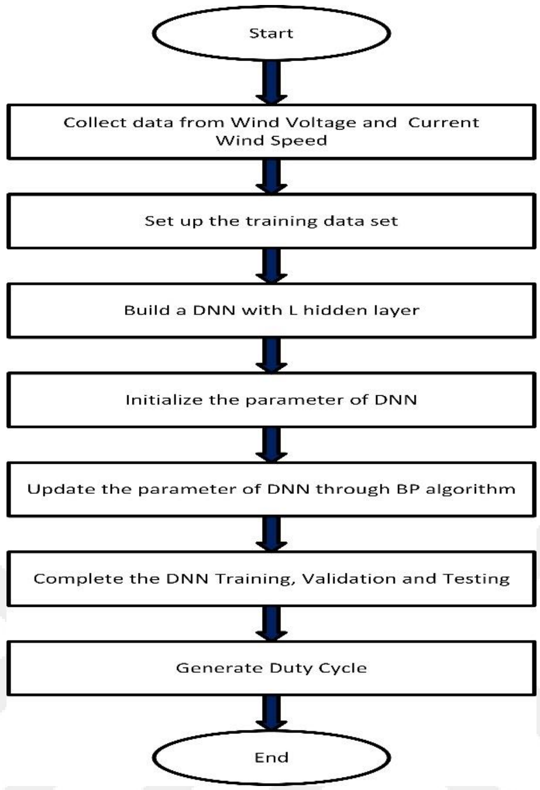

(a)

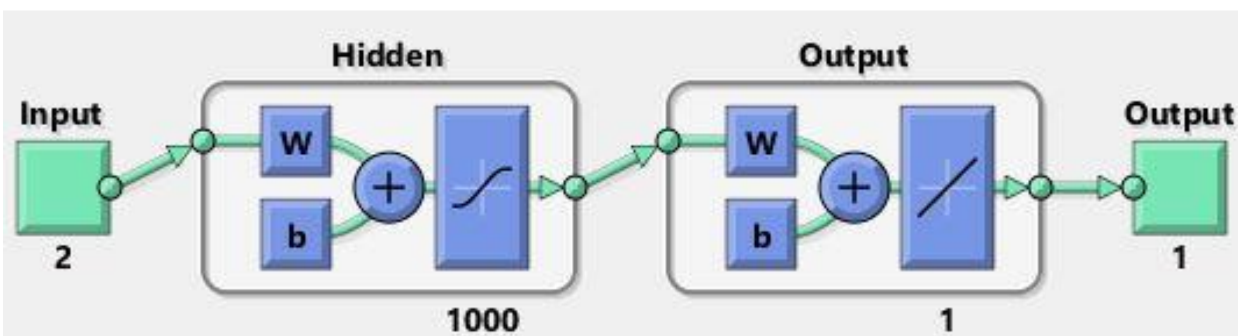

(b)

Figure4.12: a) Flow Chart of a wind-based MPPT System's DNN model; b) DNN model of a wind-based MPPT System

The mentioned system has shown the best validation when a DNN controller was trained, as Figure 4.13 shows while Figure 4.14 demonstrates the DNN controller error (target-to-output) as well as its histogram data. Figure 4.15, on the other hand, shows the validation check. Figure 4.16 shows the proposed algorithm andthevalue of best regression for testing, validation,training, and performance data. Here, the duty cycle is predicted through regression, which shows the duty cycle as an output variable, and a function of two inputs (wind current andvoltage). Table 4.2 shows the overall DNN data.

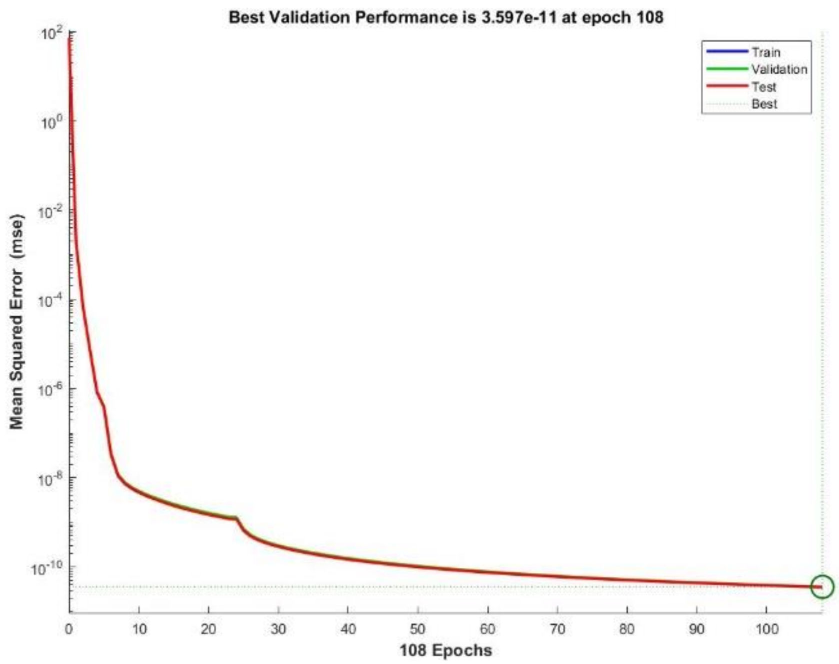

Figure4.13: DNN-Wind MPPT controllershowing best validation performance

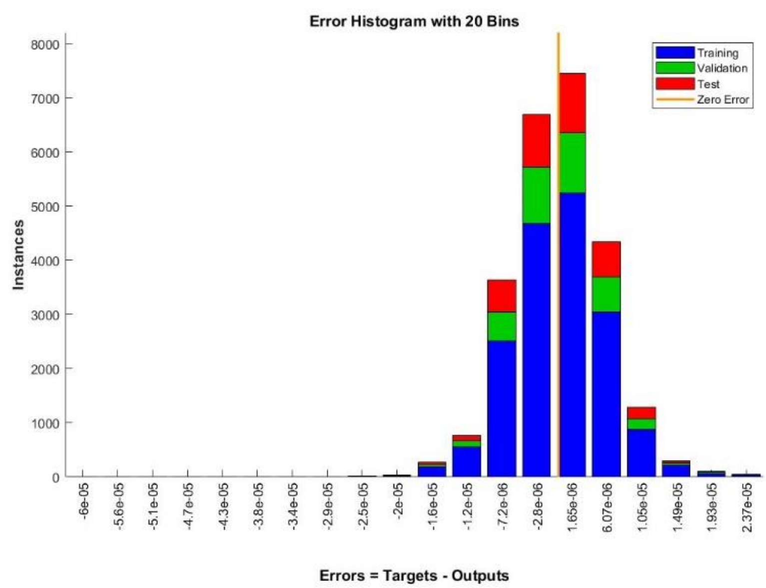

Figure4.14: DNN-Wind MPPT controller histogram

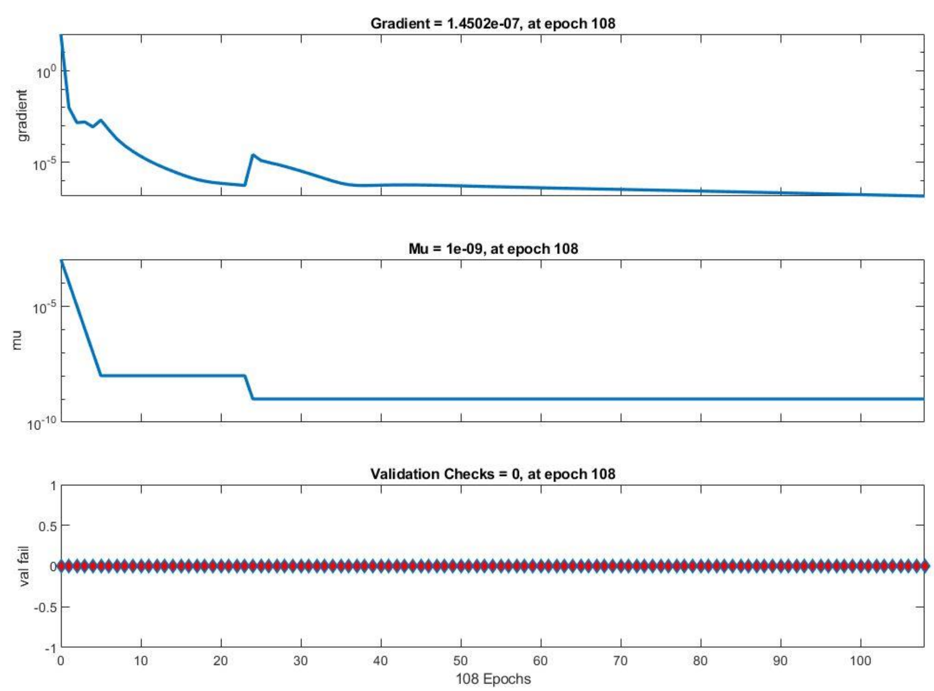

Figure4.15: DNN-Wind MPPT controller - training data

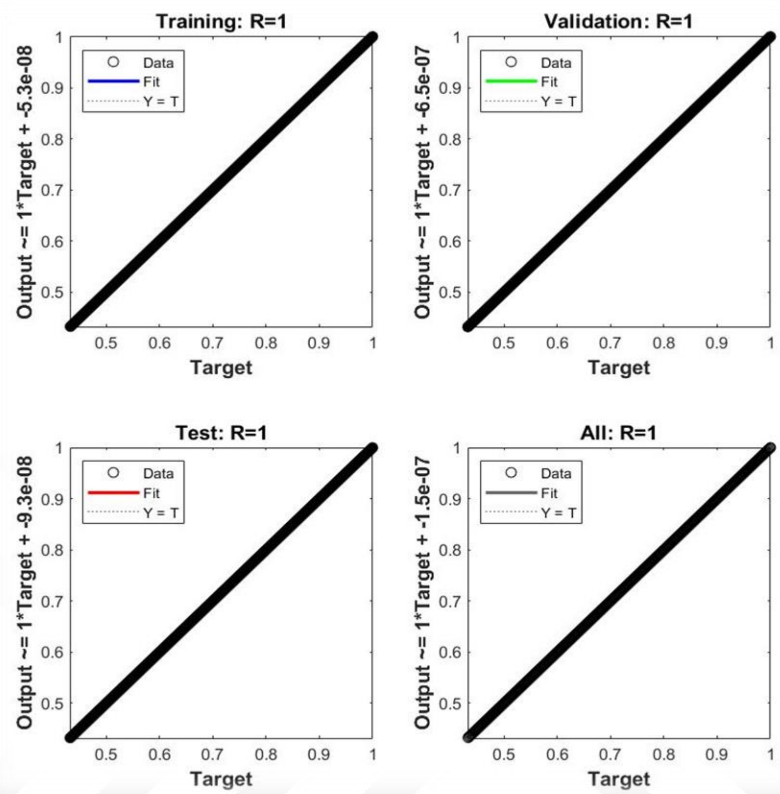

Figure4.16: DNN-Wind MPPT controller training and validation

Table4. 2: DNN data of an MPPT controller (wind system)

DNN – Wind MPPT	**Values**
Best Validation	3.597e-11
Mu	1e-9
Gradient	1.4502e-7
Training	1
Validation	1
Test	1

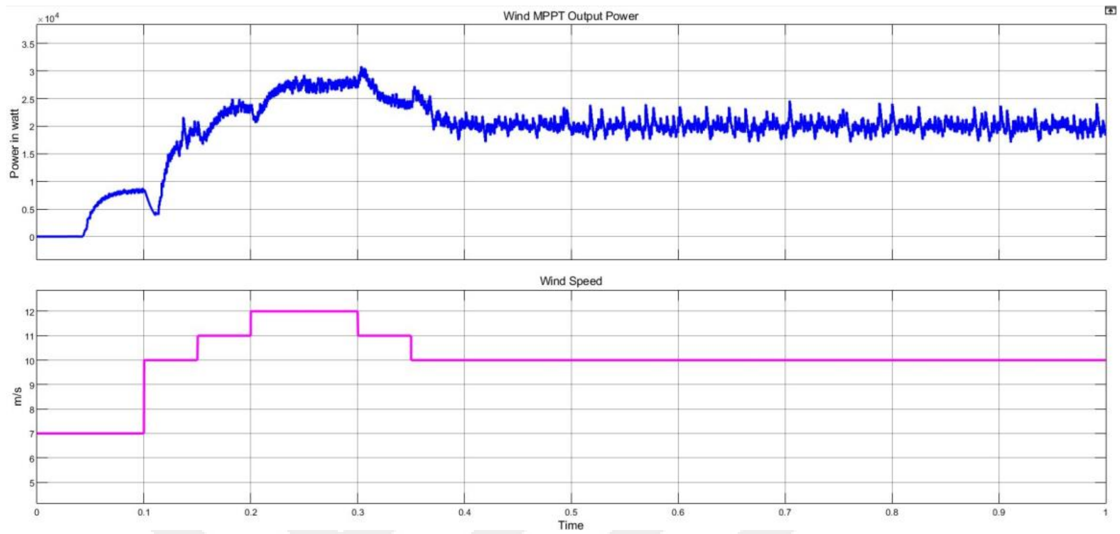

Figure4.17: DNN-Wind MPPT power Simulation results (different wind speeds)

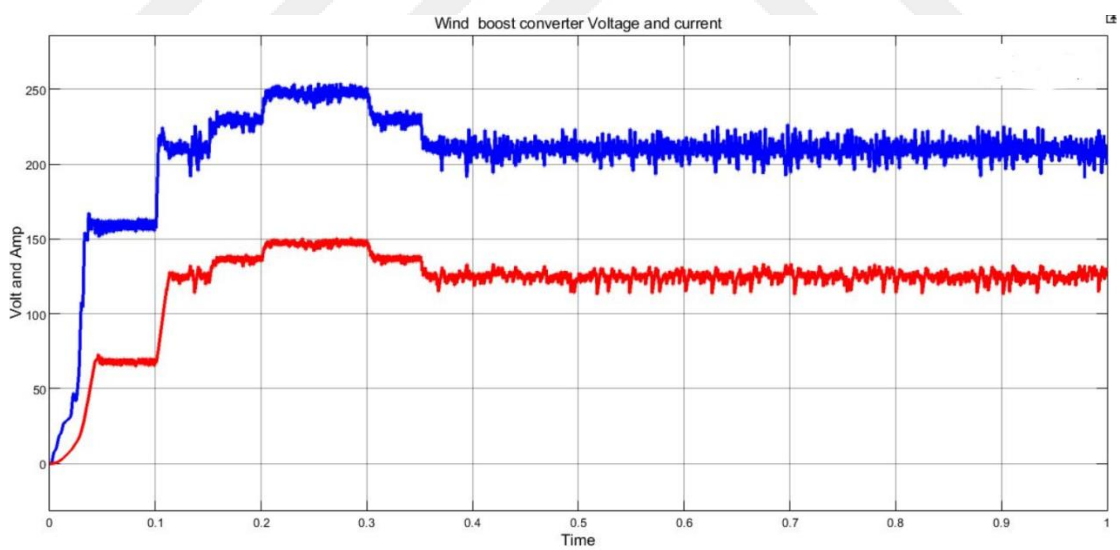

Figure4.18: Simulation results for DNN-Wind MPPT converter current and voltage (different wind speeds)

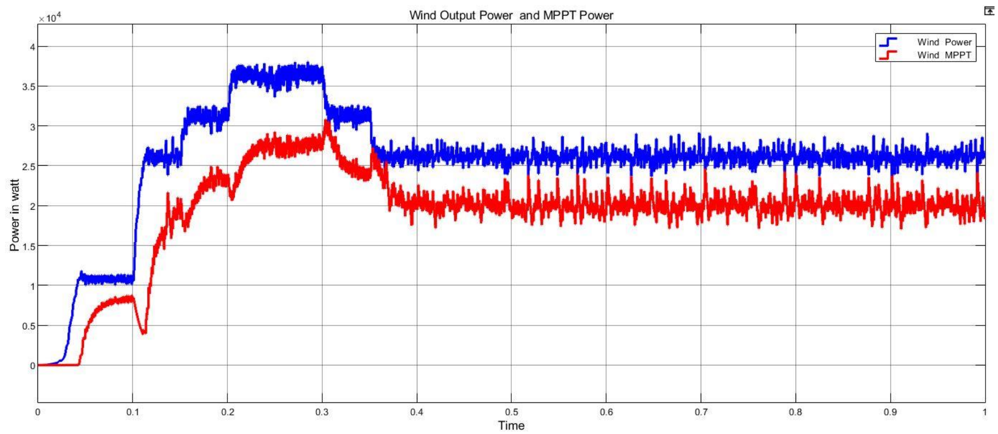

Figure4.19: Comparative analysis with and without Wind MPPT power (for different wind speeds)

The NN-based MPPT algorithm was proposed, developed, and then applied using a 30kW wind energy system and then, it was simulated and analyzed keeping in view several possible wind speeds. Figure 4.17 shows the wind energy systemindicatingpower outputsatdifferent wind speeds. The current waveform and the boost converter's output areFigure 4.18 shows. The outputs of awind-based system with/without a DNN-based MPPT controller are provided in Figure 4.19.

II. Microgrid integration with a hybrid PV / wind power system

Now, we will explain how a microgrid is integrated with awind-based system/hybrid PV, which is controlled with a DNN-based MPPT algorithm[95]. Figure 4.20 shows the details of the simulation when a 50kW hybrid PV was used. The power microgrid is integrated with the wind power system by means of a smart inverter, anda DNN-based voltage source controller controls it[96][97]. This controller is equipped with three sub-controllers, including a current regulator, a voltage regulator, and a phase-lock loop, asFigure 4.21 shows. At last, the generation of PWM signals takes place through a current regulator, which synchronizesthe microgrid system and a 50kW hybrid PV/wind-based generator.

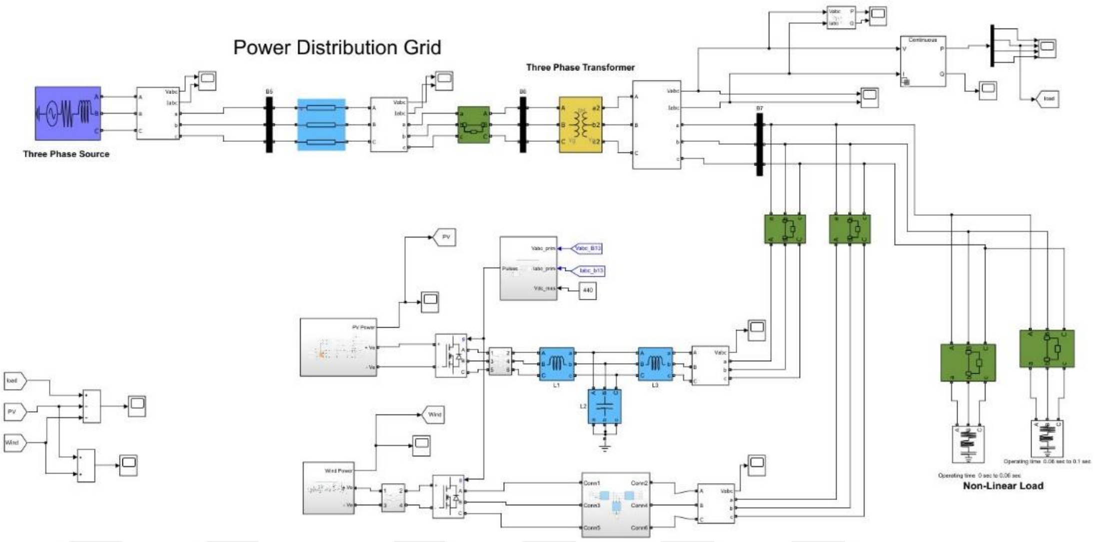

Figure4.20: Simulation model of the proposed DNN controller-based microgridintegrated with a hybrid PV/wind energy system

III. Deep Neural Network (DNN)Controller based Grid-integrated Smart Inverter

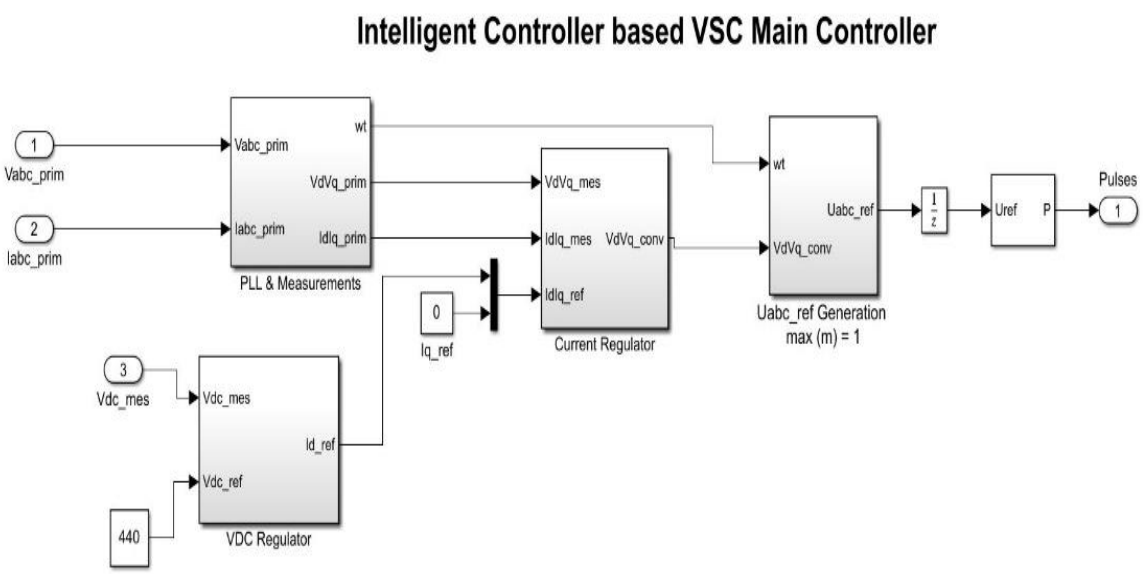

Figure4.21: Voltage source controller (DNN controller-based) for smart inverters

For developinga suitable current regulating controller to meet the needs ofa hybrid wind energy system and grid-connected PV, a DNN controller is used. We have mentioned before that the DNN learning algorithm uses 60,000 data items to develop a current regulating algorithm. The proposed smart inverter needs a simulation model, for which, we used MATLAB (see Figure 4.22).

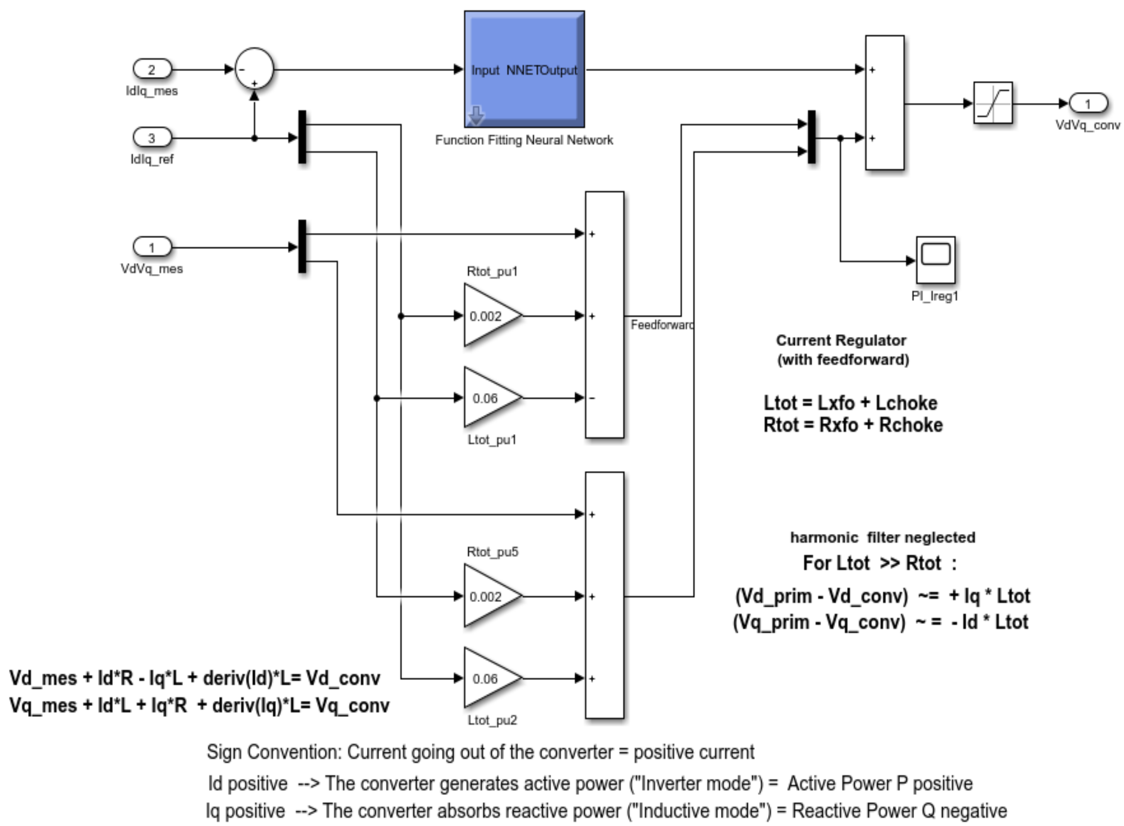

Figure4.22: DNN based current regulator for smart inverter

Figures 4.23a and b showa specific DNN layer, which hasan output neuron, 2000 hidden-layer neurons and two input neurons. This type of DNN layer is used to train a current regulator network, with the help of the following:The output of a smart inverter comprises PWM signals while the input is shown by direct and quadrant axis.

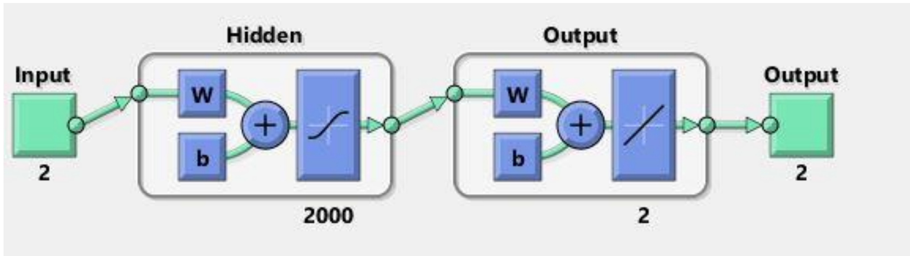

(a)

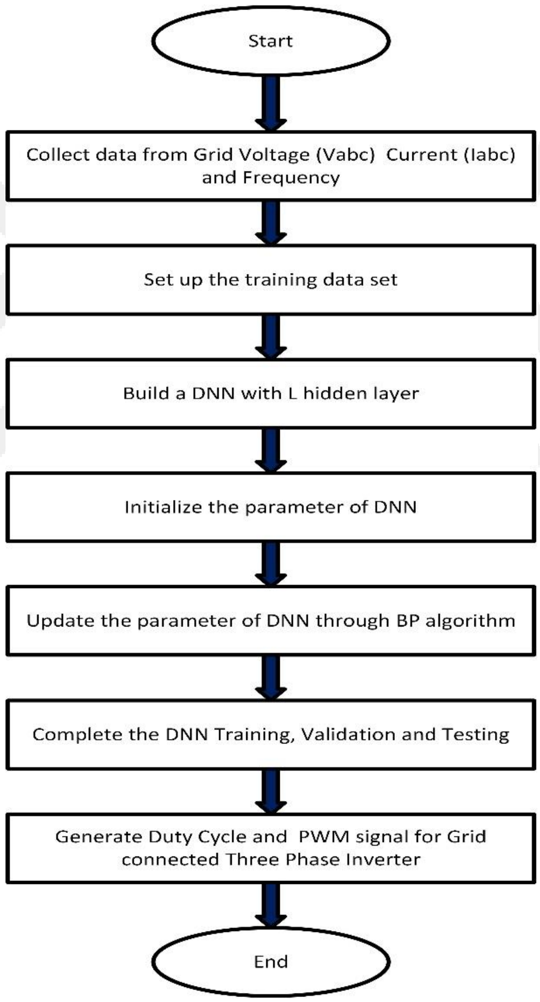

(b)

Figure4.23:a) A DNN current regulator model for smart inverters, b) Flow chart of the DNN model

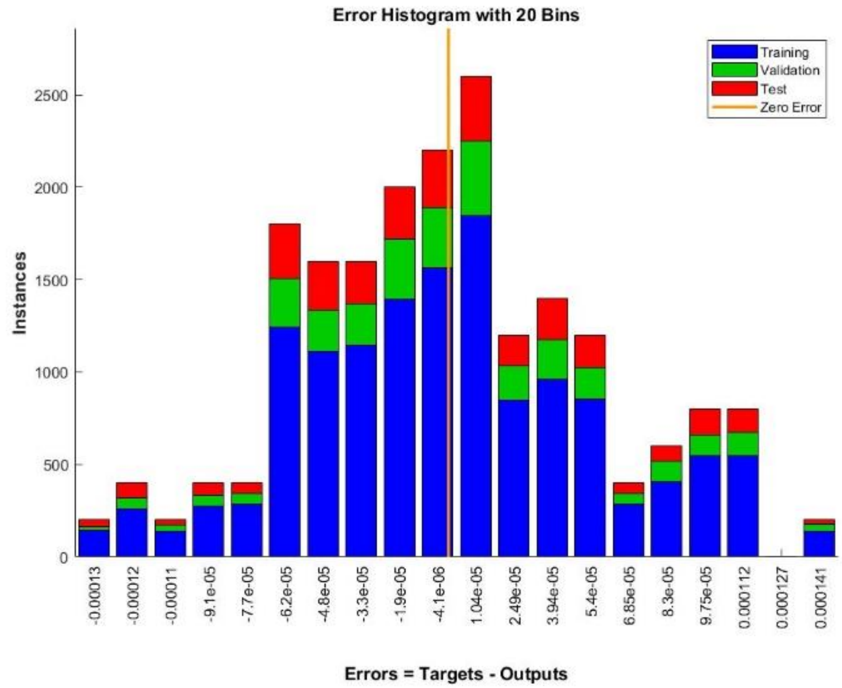

Figure4.24: Histogram of the DNNcurrent regulator error

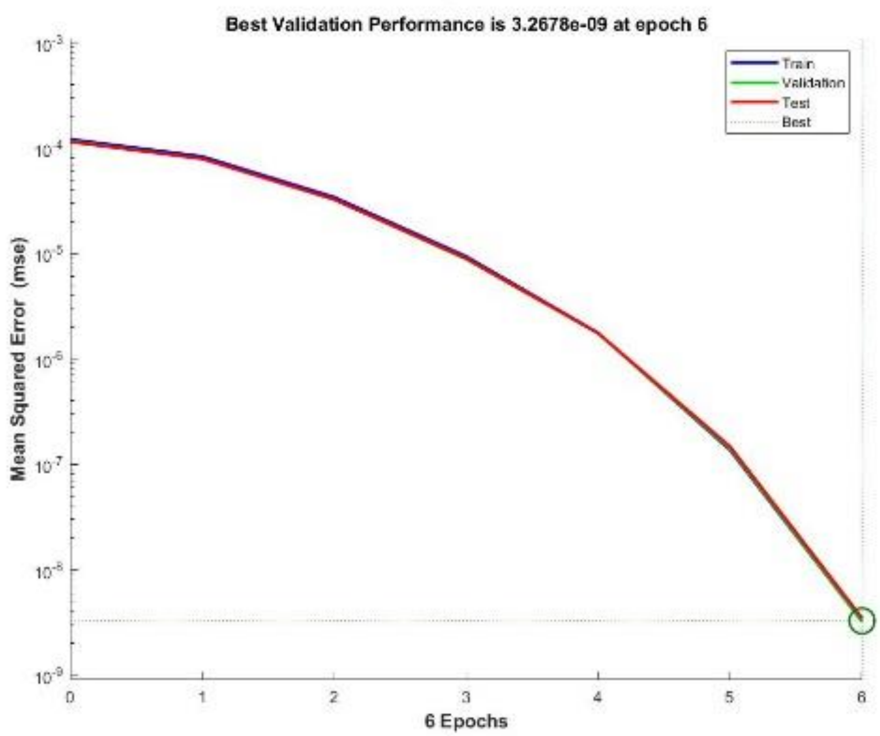

Figure4.25: Best validation performance of a DNN-current regulator

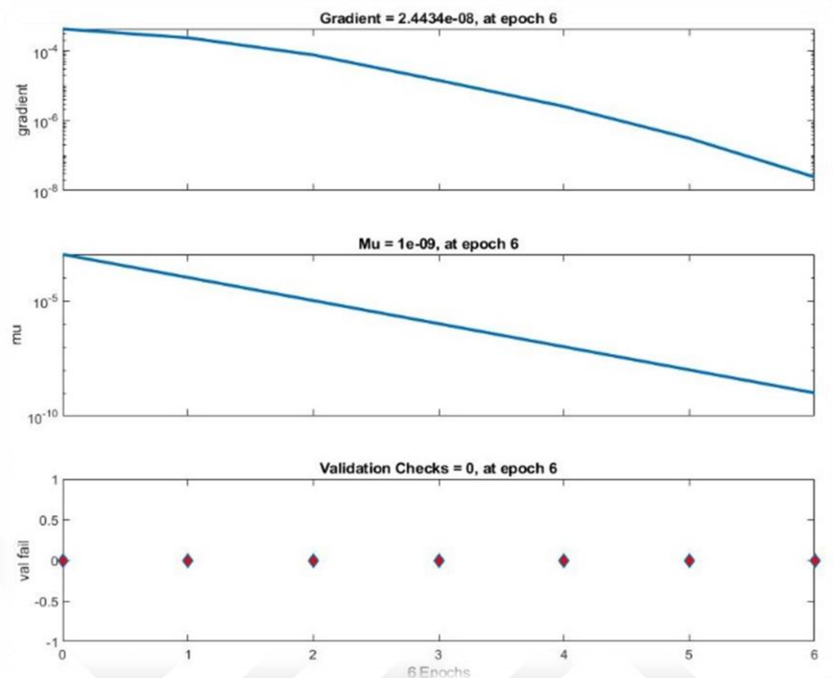

Figure4.26: Data for the DNN-current regulator training

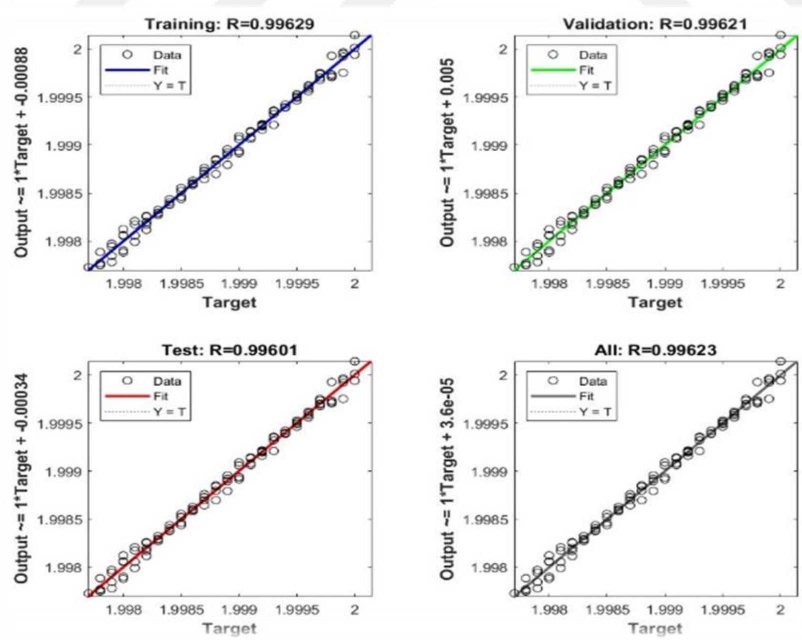

Figure4.27: Training, testing and validation of a DNN-current regulator

Table4.3: DNN data of the grid system controller

DNNgrid	**Values**
Best Validation	3.2678 e-9
Mu	1.0 e-9
Gradient	2.4434 e-8
Training	0.99629
Validation	0.99621
Test	0.99601
Overall regression	0.99623

The DNN controller training was accomplished using the above system and Figure 4.25 presents the best validation. Figure 4.24 presents DNN controller error data through a histogram. Figure 4.26 shows the validation and gradient of the DNN-trained network. Later, the proposed algorithm was developed and presented that showedthe best regression for testing, training, performance, and validation data, asFigure 4.27 shows. An output variable (PWM) is predicted through ANNregression and it is an input function (DC and quadrant axis current). Table 4.3 presents the overall DNN data.

4.2 DISCUSSION

First, we developed our proposed system, which was later simulated in MATLABconsidering different operationalconditions. Both simulation data and results were monitored and noted. Figure 4.28 shows the real power consumption of a consumer, whose load is 170kW. In Figure 4.29, it is shown that 220kVRreactive power was transmitted from a microgrid to the consumer. A hybrid PV/wind energy system's power generation is given in Figure 4.30. For maintainingboth voltage and current in a microgrid without oscillations, we analyzed the power flow. The voltage and current in a microgridand the current waveform are linked to the mentioned hybrid system througha non-linear source of grid-integratedpower generation. In power generating stations, power management is important, but it mainly depends onconsumer demand. Our proposed model generated almost 40kW power. The power supply is shown in Figure 4.32, which was supplied through the microgrid. The current research is conducted to decreasethe THD value at the common coupling point for improving the quality of power. We analyzedthe THD valuesforall the generating sources and the microgrid. THD values for current are shown in Figure 4.33 while THD values for voltage are shown in Figure 4.34. For a wind energy system, Figures4.35shows THD values for current, and Figure 4.36shows the same for voltage. Finally, we analyzed the THD values for the microgrid current and load voltage, which are exhibited in Figures4.37 and 4.38, respectively, andTable 4.4 also mentions the THD values.

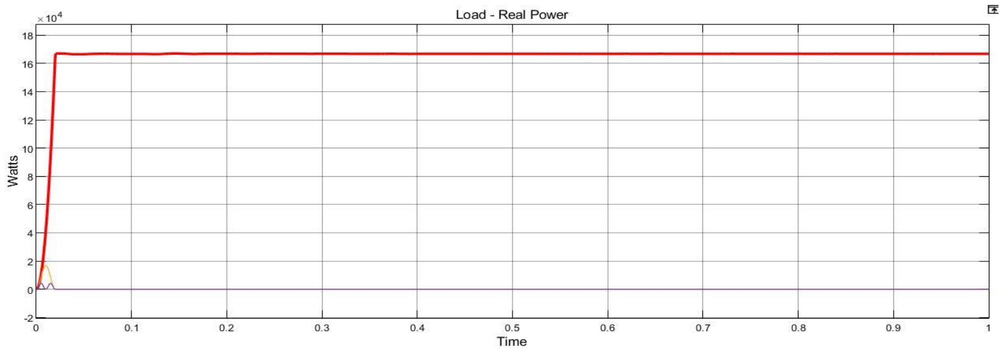

Figure4. 28: Real power consumed by the load

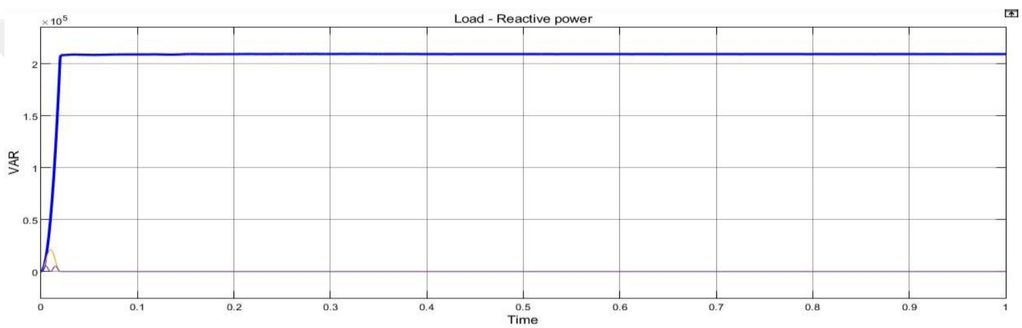

Figure4. 29: Reactive power consumed by the laod

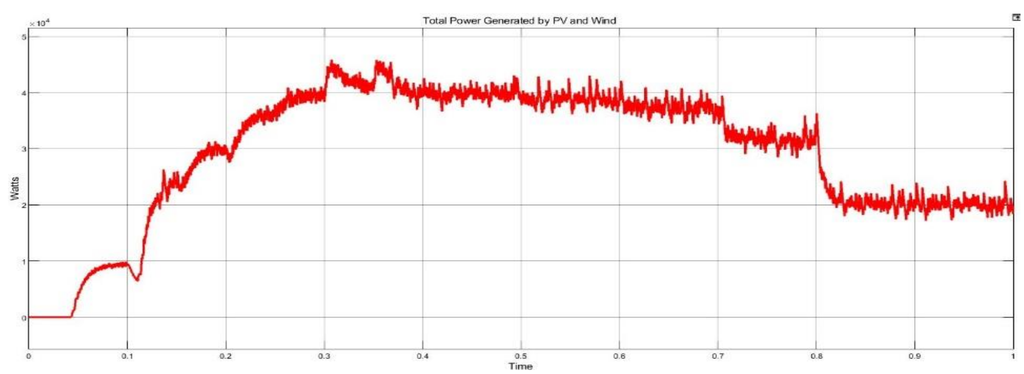

Figure4.30: Total power generated by the hybrid PV / wind energy system

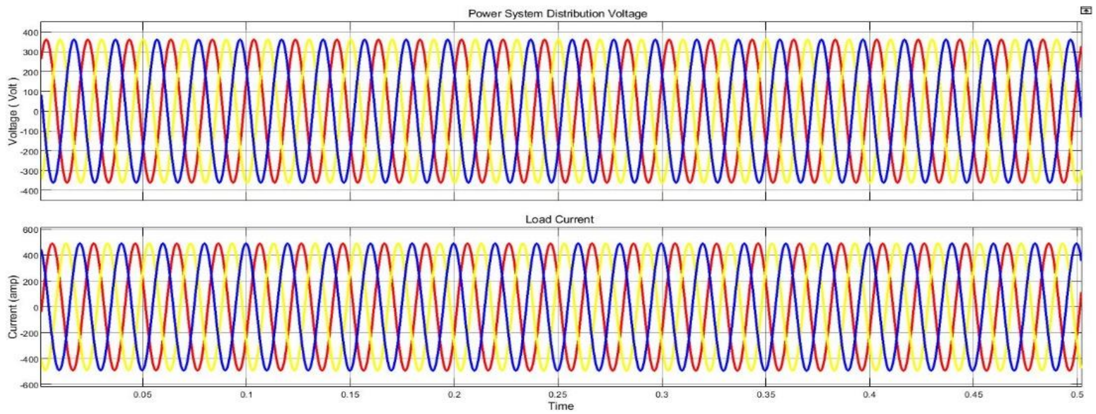

Figure4.31: Current waveform and microgrid voltage

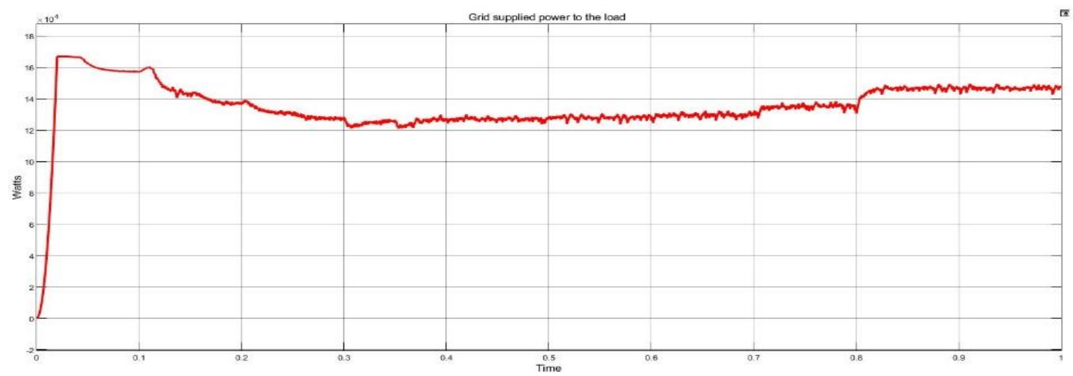

Figure4.32: Grid-power supplied to the load

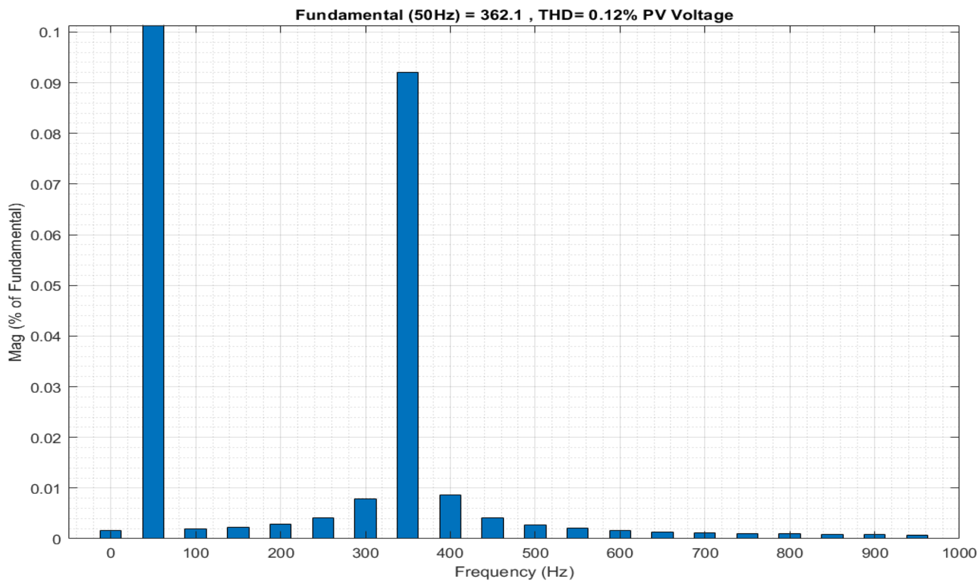

Figure4.33: THD values of PV system voltage

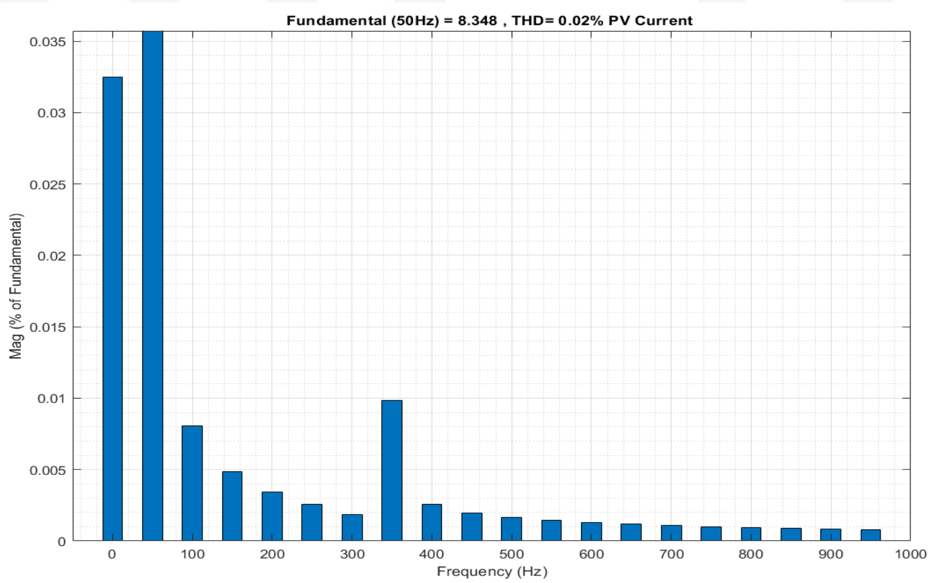

Figure4.34: THD values of PV system current

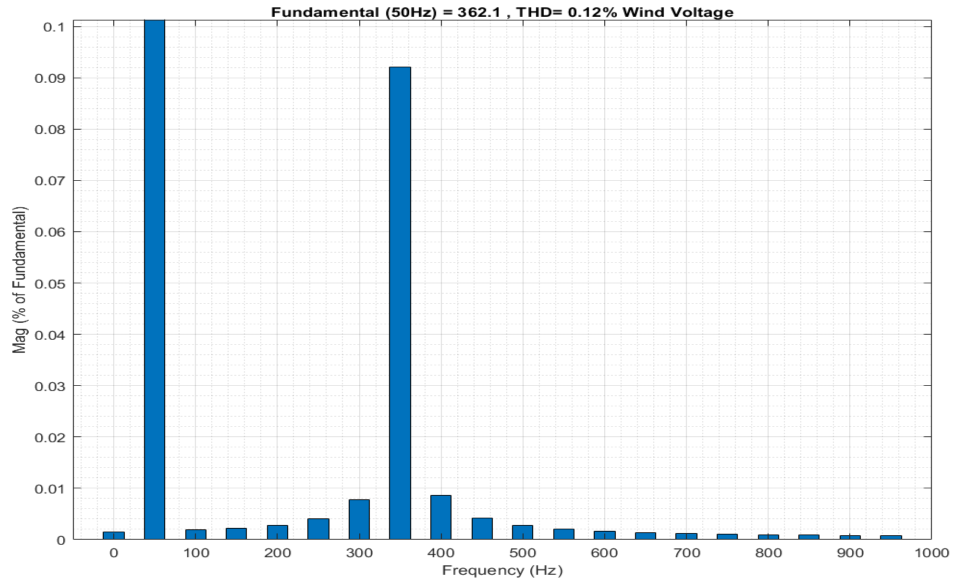

Figure4.35: THD values of wind voltage

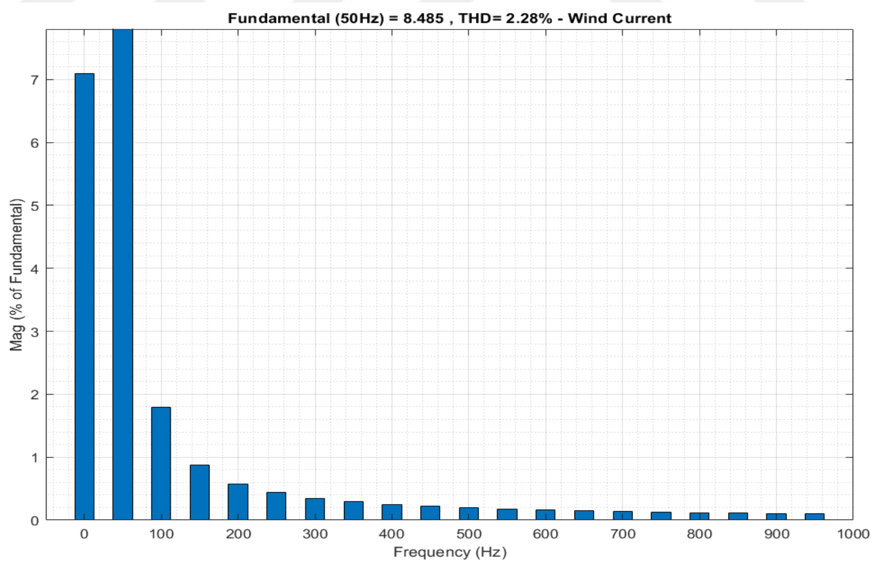

Figure4.36: THD values of wind current

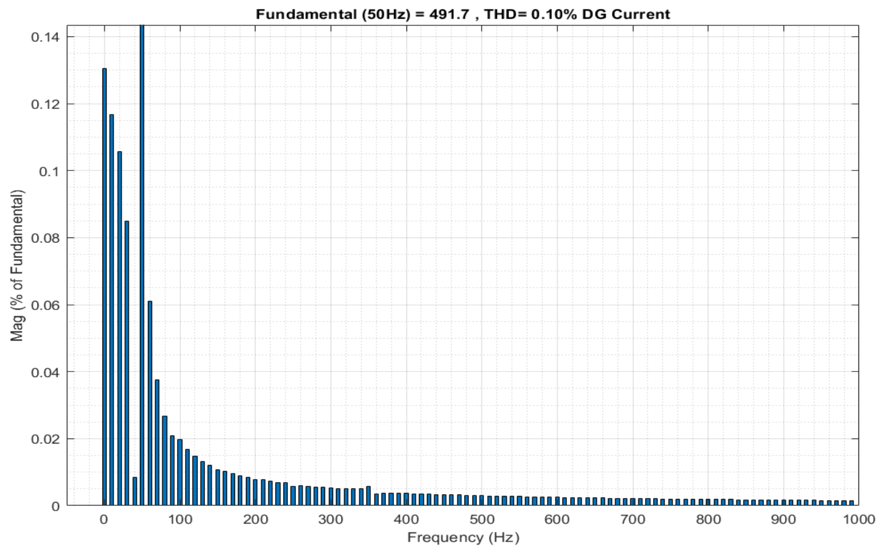

Figure4.37: THD values of Microgrid load current

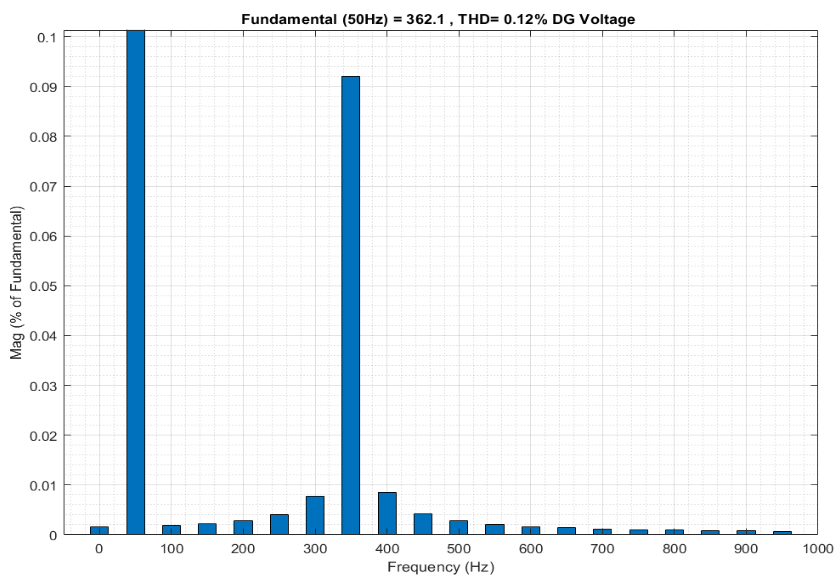

Figure4.38: THD values of Microgrid load voltage

Table4.4: Comparative Analyses of THD values, grid, wind and PV

Profile	**Voltage – THD**	**Current - THD**	**Voltage – THD**	**Current - THD**
	DNN Controller		PI Controller	
Grid	0.12 %	0.10 %	0.17%	3.62%
Wind	0.12 %	2.28 %	0.17%	29.9%
PV	0.12%	0.02 %	0.17 %	0.35%

5. CONCLUSION AND FUTURE WORK

5.1 CONCLUSION

Amodel of wind energy conversion system and thephotovoltaic system has been discussed in this thesis. We simulated both wind energy and PVbefore analyzingtheir performancesin different weathers and conditions. After evaluating the proposed DNN-based MPPT controller, we analyzedthe MPPT algorithm both fora PV and a wind energy system. We compared the simulated results with a fuzzy logic controller, which is based on the MPPT controller. Comparative analysesshow that the proposed DNN-based MPPT controller is effective.A hybrid PV/wind energy conversion system wassimulated using MATLAB after multiple analyses and careful evaluations. In this thesis, we have successfully modeled an algorithm and demonstrated it for a DNN-based MPPT controller, which operates as a part of a hybrid wind/PV energy system. After that, we analyzed the simulations under changing weather conditions for comprehensive effectiveness tests of the proposed controller. As mentioned earlier, we used MATLAB for simulating the proposed system, andlinkedit with a microgrid. We also developed a simulation model foran inverter-based smart microgrid in the proposed researchtask. The proposed system was integratedwith a DNN algorithm and a hybrid PV/wind generation system was testedusing MATLAB. After simulations, the proposed system was analyzed in multiple operationalsituations and the results are presented in this thesis. This research has a primary aim to findthe THD values forwind,distributed grid voltage, current profiles, and PV. The values show that the power quality actually improvedwhen renewable energy resource is linked to a microgrid. Since theproposed system's THD values arebelow 5%, it is right according to therequired standard (IEEE 1547); therefore, the proposed system is effective.

5.2 FUTURE WORK

- For future studies, a hybrid system with other renewable sources such as biomass, water, etc. for remote areas should be planned and built.
- Improve accessibility and reliability while guaranteeing quality assurance
- A fascinating problem to build is the future ancillary service furniture, the microgrid may be an important way of participating not only in the management of the voltage plan but also in the frequency plan. Other possibilities may also be discussed, such as improving power efficiency.
- The study can be further enhanced and the system economy can be more accurately calculated if more related data such as the minute load curve, land price, variable interest rate, and environmental hazard effects are taken into account.

.

REFERENCES

[1] M. Nurunnabi, N. K. Roy, E. Hossain, and H. R. Pota, “Size Optimization and Sensitivity Analysis of Hybrid Wind/PV Micro-Grids-A Case Study for Bangladesh,” *IEEE Access*, vol. 7, pp. 150120–150140, 2019.

[2] R. Singh, R. C. Bansal, A. R. Singh, and R. Naidoo, “Multi-objective optimization of hybrid renewable energy system using reformed electric system cascade analysis for islanding and grid connected modes of operation,” *IEEE Access*, vol. 6, pp. 47332–47354, 2018.

[3] J. Ke and X. Liu, “Empirical analysis of optimal hidden neurons in neural network modeling for stock prediction,” in *2008 IEEE Pacific-Asia Workshop on Computational Intelligence and Industrial Application*, 2008, vol. 2, pp. 828–832.

[4] M. Xu, L. Wu, H. Liu, and X. Wang, “Multi-objective optimal scheduling strategy for wind power, PV and pumped storage plant in VSC-HVDC grid,” *J. Eng.*, vol. 2019, no. 16, pp. 3017–3021, 2019.

[5] A. Elgammal and M. El-Naggar, “Energy management in smart grids for the integration of hybrid wind–PV–FC–battery renewable energy resources using multi-objective particle swarm optimisation (MOPSO),” *J. Eng.*, vol. 2018, no. 11, pp. 1806–1816, 2018.

[6] X. Li, D. Hui, and X. Lai, “Battery energy storage station (BESS)-based smoothing control of photovoltaic (PV) and wind power generation fluctuations,” *IEEE Trans. Sustain. energy*, vol. 4, no. 2, pp. 464–473, 2013.

[7] U. Akram, M. Khalid, and S. Shafiq, "An innovative hybrid wind-solar and battery-supercapacitor microgrid system—Development and optimization," *IEEE access*, vol. 5, pp. 25897–25912, 2017.

[8] A. Benali, M. Khiat, T. Allaoui, and M. Denai, "Power quality improvement and low voltage ride through capability in hybrid wind-PV farms grid-connected using dynamic voltage restorer," *IEEE Access*, vol. 6, pp. 68634–68648, 2018.

[9] Z. Ullah, S. Wang, J. Radosavljević, and J. Lai, "A solution to the optimal power flow problem considering WT and PV generation," *IEEE Access*, vol. 7, pp. 46763–46772, 2019.

[10] A. Sujil, R. Kumar, and R. C. Bansal, "FCM Clustering-ANFIS-based PV and wind generation forecasting agent for energy management in a smart microgrid," *J. Eng.*, vol. 2019, no. 18, pp. 4852–4857, 2019.

[11] A. A. Z. Diab, H. M. Sultan, I. S. Mohamed, O. N. Kuznetsov, and T. D. Do, "Application of different optimization algorithms for optimal sizing of PV/wind/diesel/battery storage stand-alone hybrid microgrid," *IEEE Access*, vol. 7, pp. 119223–119245, 2019.

[12] T. Adefarati, R. C. Bansal, and J. J. Justo, "Techno-economic analysis of a PV–wind–battery–diesel standalone power system in a remote area," *J. Eng.*, vol. 2017, no. 13, pp. 740–744, 2017.

[13] N. T. Mbungu, R. C. Bansal, and R. Naidoo, "Smart energy coordination of a hybrid wind/PV with battery storage connected to grid," *J. Eng.*, vol. 2019, no. 18, pp. 5109–

5113, 2019.

[14] D. H. Tungadio, R. C. Bansal, M. W. Siti, and N. T. Mbungu, "Predictive active power control of two interconnected microgrids," *Technol. Econ. Smart Grids Sustain. Energy*, vol. 3, no. 1, p. 3, 2018.

[15] M. W. Siti, D. H. Tungadio, Y. Sun, N. T. Mbungu, and R. Tiako, "Optimal frequency deviations control in microgrid interconnected systems," *IET Renew. Power Gener.*, vol. 13, no. 13, pp. 2376–2382, 2019.

[16] N. T. Mbungu, R. M. Naidoo, R. C. Bansal, M. W. Siti, and D. H. Tungadio, "An overview of renewable energy resources and grid integration for commercial building applications," *J. Energy Storage*, vol. 29, p. 101385, 2020.

[17] N. T. Mbungu, R. Naidoo, R. C. Bansal, and M. Bipath, "Optimisation of grid connected hybrid photovoltaic–wind–battery system using model predictive control design," *IET Renew. Power Gener.*, vol. 11, no. 14, pp. 1760–1768, 2017.

[18] A. Krenker, J. Bester, and A. Kos, "Introduction to the artificial neural networks," in *Artificial neural networks-methodological advances and biomedical applications*, IntechOpen, 2011.

[19] Y. Ru, J. Kleissl, and S. Martinez, "Storage size determination for grid-connected photovoltaic systems," *IEEE Trans. Sustain. energy*, vol. 4, no. 1, pp. 68–81, 2012.

[20] B. Belvedere, M. Bianchi, A. Borghetti, C. A. Nucci, M. Paolone, and A. Peretto, "A microcontroller-based power management system for standalone microgrids with hybrid

power supply," *IEEE Trans. Sustain. Energy*, vol. 3, no. 3, pp. 422–431, 2012.

[21] K. T. Tan, P. L. So, Y. C. Chu, and M. Z. Q. Chen, "Coordinated control and energy management of distributed generation inverters in a microgrid," *IEEE Trans. power Deliv.*, vol. 28, no. 2, pp. 704–713, 2013.

[22] X. Wang, Y. Pi, W. Mao, and H. Huang, "Network coordinated power point tracking for grid-connected photovoltaic systems," *IEEE J. Sel. Areas Commun.*, vol. 32, no. 7, pp. 1425–1440, 2014.

[23] P. García, C. A. García, L. M. Fernández, F. Llorens, and F. Jurado, "ANFIS-based control of a grid-connected hybrid system integrating renewable energies, hydrogen and batteries," *IEEE Trans. Ind. informatics*, vol. 10, no. 2, pp. 1107–1117, 2013.

[24] L. G. Meegahapola, D. Robinson, A. P. Agalgaonkar, S. Perera, and P. Ciufo, "Microgrids of commercial buildings: Strategies to manage mode transfer from grid connected to islanded mode," *IEEE Trans. Sustain. Energy*, vol. 5, no. 4, pp. 1337–1347, 2014.

[25] G. Wang, M. Ciobotaru, and V. G. Agelidis, "Power smoothing of large solar PV plant using hybrid energy storage," *IEEE Trans. Sustain. Energy*, vol. 5, no. 3, pp. 834–842, 2014.

[26] K. Y. Khouzam, "Technical and economic assessment of utility interactive PV systems for domestic applications in South East Queensland," *IEEE Trans. Energy Convers.*, vol. 14, no. 4, pp. 1544–1550, 1999.

[27] F. Giraud and Z. M. Salameh, "Steady-state performance of a grid-connected rooftop

hybrid wind-photovoltaic power system with battery storage," *IEEE Trans. energy Convers.*, vol. 16, no. 1, pp. 1–7, 2001.

[28] E. Serban and H. Serban, "A control strategy for a distributed power generation microgrid application with voltage-and current-controlled source converter," *IEEE Trans. Power Electron.*, vol. 25, no. 12, pp. 2981–2992, 2010.

[29] S.-K. Kim, J.-H. Jeon, C.-H. Cho, J.-B. Ahn, and S.-H. Kwon, "Dynamic modeling and control of a grid-connected hybrid generation system with versatile power transfer," *IEEE Trans. Ind. Electron.*, vol. 55, no. 4, pp. 1677–1688, 2008.

[30] A. Khorsandi, M. Ashourloo, and H. Mokhtari, "A decentralized control method for a low-voltage DC microgrid," *IEEE Trans. Energy Convers.*, vol. 29, no. 4, pp. 793–801, 2014.

[31] H. Zhou, T. Bhattacharya, D. Tran, T. S. T. Siew, and A. M. Khambadkone, "Composite energy storage system involving battery and ultracapacitor with dynamic energy management in microgrid applications," *IEEE Trans. power Electron.*, vol. 26, no. 3, pp. 923–930, 2010.

[32] G. R. Walker and P. C. Sernia, "Cascaded DC-DC converter connection of photovoltaic modules," *IEEE Trans. power Electron.*, vol. 19, no. 4, pp. 1130–1139, 2004.

[33] D. D.-C. Lu and V. G. Agelidis, "Photovoltaic-battery-powered DC bus system for common portable electronic devices," *IEEE Trans. Power Electron.*, vol. 24, no. 3, pp. 849–855, 2009.

[34] S. Vighetti, J.-P. Ferrieux, and Y. Lembeye, “Optimization and design of a cascaded DC/DC converter devoted to grid-connected photovoltaic systems,” *IEEE Trans. Power Electron.*, vol. 27, no. 4, pp. 2018–2027, 2011.

[35] H. Mahmood, D. Michaelson, and J. Jiang, “A power management strategy for PV/battery hybrid systems in islanded microgrids,” *IEEE J. Emerg. Sel. Top. Power Electron.*, vol. 2, no. 4, pp. 870–882, 2014.

[36] R. G. Wandhare and V. Agarwal, “Novel integration of a PV-wind energy system with enhanced efficiency,” *IEEE Trans. power Electron.*, vol. 30, no. 7, pp. 3638–3649, 2014.

[37] M. M. R. Singaravel and S. A. Daniel, “MPPT with single DC–DC converter and inverter for grid-connected hybrid wind-driven PMSG–PV system,” *IEEE Trans. Ind. Electron.*, vol. 62, no. 8, pp. 4849–4857, 2015.

[38] Y. Hu, C. Gan, W. Cao, Y. Fang, S. J. Finney, and J. Wu, “Solar PV-powered SRM drive for EVs with flexible energy control functions,” *IEEE Trans. Ind. Appl.*, vol. 52, no. 4, pp. 3357–3366, 2016.

[39] T. A. Nguyen, M. L. Crow, and A. C. Elmore, “Optimal sizing of a vanadium redox battery system for microgrid systems,” *IEEE Trans. Sustain. energy*, vol. 6, no. 3, pp. 729–737, 2015.

[40] B. Lu and M. Shahidehpour, “Short-term scheduling of battery in a grid-connected PV/battery system,” *IEEE Trans. Power Syst.*, vol. 20, no. 2, pp. 1053–1061, 2005.

[41] A. V Savkin, M. Khalid, and V. G. Agelidis, “A constrained monotonic

charging/discharging strategy for optimal capacity of battery energy storage supporting wind farms," *IEEE Trans. Sustain. Energy*, vol. 7, no. 3, pp. 1224–1231, 2016.

[42] E. Romero-Cadaval, B. Francois, M. Malinowski, and Q.-C. Zhong, "Grid-connected photovoltaic plants: An alternative energy source, replacing conventional sources," *IEEE Ind. Electron. Mag.*, vol. 9, no. 1, pp. 18–32, 2015.

[43] H. Fakham, P. Degobert, and B. François, "Control system and power management for a PV based generation unit including batteries," in *2007 International Aegean Conference on Electrical Machines and Power Electronics*, 2007, pp. 141–146.

[44] H. Fakham, D. Lu, and B. Francois, "Power control design of a battery charger in a hybrid active PV generator for load-following applications," *IEEE Trans. Ind. Electron.*, vol. 58, no. 1, pp. 85–94, 2010.

[45] M. Falahi, H.-M. Chou, M. Ehsani, L. Xie, and K. L. Butler-Purry, "Potential power quality benefits of electric vehicles," *IEEE Trans. Sustain. energy*, vol. 4, no. 4, pp. 1016–1023, 2013.

[46] Y.-X. Wang, F.-F. Qin, and Y.-B. Kim, "Bidirectional DC-DC converter design and implementation for lithium-ion battery application," in *2014 IEEE PES Asia-Pacific Power and Energy Engineering Conference (APPEEC)*, 2014, pp. 1–5.

[47] Z. Rasin and M. F. Rahman, "Design and simulation of quasi-Z source grid-connected PV inverter with battery storage," in *2012 IEEE International Conference on Power and Energy (PECon)*, 2012, pp. 303–308.

[48] T. Ma, B. Serrano, and O. Mohammed, "Distributed control of hybrid AC-DC microgrid with solar energy, energy storage and critical load," in *2014 Clemson University Power Systems Conference*, 2014, pp. 1–6.

[49] B. Mariappan, B. G. Fernandes, and M. Ramamoorty, "A novel single-stage solar inverter using hybrid active filter with power quality improvement," in *IECON 2014-40th Annual Conference of the IEEE Industrial Electronics Society*, 2014, pp. 5443–5449.

[50] S. S. Nag and S. Mishra, "Current-fed DC/DC topology based inverter," in *2013 IEEE Energy Conversion Congress and Exposition*, 2013, pp. 2751–2756.

[51] R. Carbone and A. Tomaselli, "Recent advances on AC PV-modules for grid-connected photovoltaic plants," in *2011 International Conference on Clean Electrical Power (ICCEP)*, 2011, pp. 124–129.

[52] L. Zhang, K. Sun, Y. Xing, and J. Zhao, "Parallel operation of modular single-phase transformerless grid-tied PV inverters with common DC bus and AC bus," *IEEE J. Emerg. Sel. Top. Power Electron.*, vol. 3, no. 4, pp. 858–869, 2015.

[53] Q. Mo, M. Chen, Z. Zhang, M. Gao, and Z. Qian, "Research on a non-complementary active clamp flyback converter with unfolding DC-AC inverter for decentralized grid-connected PV systems," in *2011 IEEE Energy Conversion Congress and Exposition*, 2011, pp. 2481–2487.

[54] K. M. Shafeeque, "PV fed flyback DC-AC inverter with MPPT control," in *2014 Annual International Conference on Emerging Research Areas: Magnetics, Machines and Drives*

(AICERA/iCMMD), 2014, pp. 1–6.

[55] B. Zhang, J. Zhu, M. He, R. Zheng, and W. Chen, “A Novel Dual-Boost DC-AC Circuit for PV Inverter,” in *2011 Second International Conference on Digital Manufacturing & Automation*, 2011, pp. 85–88.

[56] S. Razali, Q. Meng, and S.-H. Yang, “A refined immune systems inspired model for multi-robot shepherding,” in *2010 Second World Congress on Nature and Biologically Inspired Computing (NaBIC)*, 2010, pp. 473–478.

[57] V. Blasko and V. Kaura, “A novel control to actively damp resonance in input LC filter of a three-phase voltage source converter,” *IEEE Trans. Ind. Appl.*, vol. 33, no. 2, pp. 542–550, 1997.

[58] G. Shen, D. Xu, L. Cao, and X. Zhu, “An improved control strategy for grid-connected voltage source inverters with an LCL filter,” *IEEE Trans. Power Electron.*, vol. 23, no. 4, pp. 1899–1906, 2008.

[59] A. Yazdani and R. Iravani, *Voltage-sourced converters in power systems: modeling, control, and applications*. John Wiley & Sons, 2010.

[60] B. Wacker, J. V Seebaß, and J. C. Schlüter, “A modular framework for estimating annual averaged power output generation of wind turbines,” *Energy Convers. Manag.*, vol. 221, p. 113149, 2020.

[61] R. A. Campos, L. R. do Nascimento, and R. Rüther, “The complementary nature between wind and photovoltaic generation in Brazil and the role of energy storage in utility-scale

hybrid power plants," *Energy Convers. Manag.*, vol. 221, p. 113160, 2020.

[62] D. H. Wollz, S. A. O. da Silva, and L. P. Sampaio, "Real-time monitoring of an electronic wind turbine emulator based on the dynamic PMSG model using a graphical interface," *Renew. Energy*, 2020.

[63] J. Zhang, M. Zhang, Y. Li, J. Qin, K. Wei, and L. Song, "Analysis of wind characteristics and wind energy potential in complex mountainous region in southwest China," *J. Clean. Prod.*, vol. 274, p. 123036, 2020.

[64] P. E. Battaiotto, R. J. Mantz, and P. F. Puleston, "A wind turbine emulator based on a dual DSP processor system," *Control Eng. Pract.*, vol. 4, no. 9, pp. 1261–1266, 1996.

[65] M. Chinchilla, S. Arnaltes, and J. L. Rodriguez-Amenedo, "Laboratory set-up for wind turbine emulation," in *2004 IEEE International Conference on Industrial Technology, 2004. IEEE ICIT'04.*, 2004, vol. 1, pp. 553–557.

[66] M. Arifujjaman, M. T. Iqbal, and J. E. Quaicoe, "An isolated small wind turbine emulator," in *2006 Canadian Conference on Electrical and Computer Engineering*, 2006, pp. 1854–1857.

[67] W. Li, D. Xu, W. Zhang, and H. Ma, "Research on wind turbine emulation based on DC motor," in *2007 2nd IEEE Conference on Industrial Electronics and Applications*, 2007, pp. 2589–2593.

[68] R. Patel, C. V Patki, and V. Agarwal, "Armature and field controlled DC motor based wind turbine emulation for wind energy conversion systems operating over a wide range

of wind velocity," in *Sustainability in Energy and Buildings*, Springer, 2009, pp. 117–125.

[69] A. Mahdy, S. M. El-Hakim, and H. H. Hanafy, "Small wind turbine emulator with separately excited DC motor using analog electronic circuit," 2011.

[70] A. S. Satpathy and N. C. Sahoo, "Development of control scheme for a stand-alone wind system: Wind turbine emulated using DC motor," in *2012 IEEE Students' Conference on Electrical, Electronics and Computer Science*, 2012, pp. 1–4.

[71] S. Kouadria, S. Belfedhal, E. M. Berkouk, and Y. Meslem, "Development of real time wind turbine emulator based on DC motor controlled by PI regulator," in *2013 Eighth International Conference and Exhibition on Ecological Vehicles and Renewable Energies (EVER)*, 2013, pp. 1–5.

[72] F. Martinez, L. C. Herrero, and S. de Pablo, "Open loop wind turbine emulator," *Renew. Energy*, vol. 63, pp. 212–221, 2014.

[73] A. K. Yadav, M. Singh, and D. C. Meena, "Modelling and simulation of wind turbine emulator using DC motor," in *2016 IEEE 7th Power India International Conference (PIICON)*, 2016, pp. 1–5.

[74] M. P. K. Bailapudi and N. Sinha, "Fuzzy logic controlled wind turbine emulator (WTE)," in *2016 International Conference on Information Communication and Embedded Systems (ICICES)*, 2016, pp. 1–8.

[75] L. Benaaouinate, M. Khafallah, A. Mesbahi, and A. Martinez, "Development of a useful wind turbine emulator based on permanent magnet DC motor," in *2017 14th International*

Multi-Conference on Systems, Signals & Devices (SSD), 2017, pp. 44–48.

[76] Y. Sirouni, S. El Hani, N. Naseri, A. Aghmadi, and K. El Harouri, "Design and Control of a Small Scale Wind Turbine Emulator with a DC Motor," in *2018 6th International Renewable and Sustainable Energy Conference (IRSEC)*, 2018, pp. 1–6.

[77] I. Moussa, A. Bouallegue, and A. Khedher, "New wind turbine emulator based on DC machine: Hardware implementation using FPGA board for an open-loop operation," *IET Circuits, Devices Syst.*, vol. 13, no. 6, pp. 896–902, 2019.

[78] P. Satish Kumar, R. P. S. Chandrasena, and K. Victor Sam Moses Babu, "Design and implementation of wind turbine emulator using FPGA for stand-alone applications," *Int. J. Ambient Energy*, pp. 1–13, 2020.

[79] M. E. Emna, K. Adel, and M. F. Mimouni, "The wind energy conversion system using PMSG controlled by vector control and SMC strategies," *Int. J. Renew. Energy Res.*, vol. 3, no. 1, pp. 41–50, 2013.

[80] I. I. Artyukhov, S. F. Stepanov, S. V Molot, G. N. Tulepova, E. T. Erbaev, and K. K. Tulegenov, "Autonomous power supply system based on a diesel generator and renewable energy sources for remote rural areas," in *2018 19th International Scientific Conference on Electric Power Engineering (EPE)*, 2018, pp. 1–4.

[81] K. Premkumar and B. V Manikandan, "Fuzzy PID supervised online ANFIS based speed controller for brushless dc motor," *Neurocomputing*, vol. 157, pp. 76–90, 2015.

[82] K. Premkumar and B. V Manikandan, "Bat algorithm optimized fuzzy PD based speed

controller for brushless direct current motor," *Eng. Sci. Technol. an Int. J.*, vol. 19, no. 2, pp. 818–840, 2016.

[83] K. Premkumar and B. V Manikandan, "Stability and performance analysis of ANFIS tuned PID based speed controller for brushless DC motor," *Curr. Signal Transduct. Ther.*, vol. 13, no. 1, pp. 19–30, 2018.

[84] K. Premkumar and B. V Manikandan, "Online Fuzzy Supervised Learning of Radial Basis Function Neural Network Based Speed Controller for Brushless DC Motor," in *Power Electronics and Renewable Energy Systems*, Springer, 2015, pp. 1397–1405.

[85] K. Premkumar and B. V Manikandan, "GA-PSO optimized online ANFIS based speed controller for Brushless DC motor," *J. Intell. Fuzzy Syst.*, vol. 28, no. 6, pp. 2839–2850, 2015.

[86] K. Prem Kumar, T. Thamizhselvan, M. V. Priya, S. B. R. Carter, and L. P. Sivakumar, "Fuzzy anti-windup PID controlled induction motor," *Int J Eng Adv Technol*, vol. 9, no. 1, pp. 184–189, 2019.

[87] T. Thamizhselvan, R. Seyezhai, and K. Premkumar, "Maximum power point tracking algorithm for photovoltaic system using supervised online coactive neuro fuzzy inference system," *J. Electr. Eng.*, vol. 17, no. 1, pp. 270–286, 2017.

[88] A. A. Hepzibah and K. Premkumar, "ANFIS current–voltage controlled MPPT algorithm for solar powered brushless DC motor based water pump," *Electr. Eng.*, vol. 102, no. 1, pp. 421–435, 2020.

[89] D. Shyam, K. Premkumar, T. Thamizhselvan, A. Nazar Ali, and M. Vishnu Priya, "Symmetrically modified laddered H-bridge multilevel inverter with reduced configurational parameters," *Int. J. Eng. Adv. Technol.*, vol. 9, no. 1, pp. 5525–5532, 2019.

[90] M. J. Prabu, P. Poongodi, and K. Premkumar, "Genetic algorithm tuned PID controller for rotor position control of BLDC motor," *World Appl. Sci. J.*, vol. 35, no. 2, pp. 199–207, 2017.

[91] S. Yushu, Z. Zhenxing, Y. Min, J. Dongqiang, P. Wei, and X. Bin, "Research overview of energy storage in renewable energy power fluctuation mitigation," *CSEE J. Power Energy Syst.*, 2019.

[92] R. Indumathi, M. Venkateshkumar, and R. Raghavan, "Integration of D-Statcom based photovoltaic cell power in low voltage power distribution grid," in *IEEE-International Conference on Advances in Engineering, Science and Management (ICAESM-2012)*, 2012, pp. 460–465.

[93] C. S. Chin, J. Xiao, A. M. Y. M. Ghias, M. Venkateshkumar, and D. U. Sauer, "Customizable Battery Power System for Marine and Offshore Applications: Trends, Configurations, and Challenges," *IEEE Electrif. Mag.*, vol. 7, no. 4, pp. 46–55, 2019.

[94] B. Xu *et al.*, "Modeling a pumped storage hydropower integrated to a hybrid power system with solar-wind power and its stability analysis," *Appl. Energy*, vol. 248, pp. 446–462, 2019.

[95] I. Mahendravarman, S. A. Elankurisil, M. Venkateshkumar, A. Ragavendiran, and N. Chin, “Artificial intelligent controller-based power quality improvement for microgrid integration of photovoltaic system using new cascade multilevel inverter,” *Soft Comput.*, pp. 1–18, 2020.

[96] M. Venkateshkumar, R. Raghavan, and N. Kumarappan, “Design of a new multilevel inverter standalone hybrid PV/FC power system,” *Fuel Cells*, vol. 15, no. 6, pp. 862–875, 2015.

[97] T. Hemanand, N. P. Subramaniam, and M. Venkateshkumar, “Comparative analysis of intelligent controller based microgrid integration of hybrid PV/wind power system,” *J. Ambient Intell. Humaniz. Comput.*, pp. 1–20, 2018.

APPENDIX

PrposedPv code programming

```
clear all, clc,closeall
Tr1 = 40; % Reference temperature in degree fahrenheit

Tr=((Tr1-32)*5/9  )+273;  %  Reference  temperature  in
kelvin
T = 28+273;
S  =  [1000,800,600,400,200];  %  Solar  radiation  in
mW/sq.cm
%S=70;
ki = 0.00023; % in A/K
Iscr = 3.7500; % SC Current at ref. temp. in A
Irr = 2.1000e-05; % in A
k = 1.3806e-23; % Boltzmann constant
q = 1.6022e-19; % charge of an electron
A = 2.1500;
Eg0=1.1666;
alpha=0.4730
beta = 636;
Eg  = Eg0-(alpha*T*T)/(T+beta)*q; % band gap energy of
semiconductor used
Eq=1,1666;
Np = 4;
Ns = 60;
V0 = [0:1:300];

for i = 1:length(S)
Iph=(Iscr+ki*(T-Tr))*((S(i))/1000);
Irs=Irr*((T/Tr)^3)*exp(q*Eg/(k*A)*((1/Tr)-(1/T)));
I0(i,:)=Np*Iph-Np*Irs*(exp(q/(k*T*A)*V0./Ns)-1);
P0(i,:)=V0.*I0(i,:);
figure(1)
H1=plot(V0,I0(i,:));
if i==1
```

```
set(H1, 'Color', 'b','LineWidth',2 ) % 'Marker', 'o'
elseifi==2
set(H1, 'Color', 'r', 'LineWidth',2) % 'Marker', 'o'
elseifi==3
set(H1, 'Color', 'g', 'LineWidth',2) % 'Marker', 'o'
elseifi==4
set(H1, 'Color', 'm', 'LineWidth',2) % 'Marker', 'o'
elseifi==5
set(H1, 'Color', 'k', 'LineWidth',2) % 'Marker', 'o'
end
axis([0,50,0,20]);
xlabel('Voltage in volt');
ylabel('Current in amp'); grid on;
hold on;
figure(2)
H2=plot(V0,P0(i,:)); axis([0,50,0,400]);
xlabel('Voltage in volt');
ylabel('Power in watt'); grid on;
hold on;
if i==1
set(H2, 'Color', 'b','LineWidth',2 ) % 'Marker', 'o'
elseifi==2
set(H2, 'Color', 'r', 'LineWidth',2) % 'Marker', 'o'
elseifi==3
set(H2, 'Color', 'g', 'LineWidth',2) % 'Marker', 'o'
elseifi==4
set(H2, 'Color', 'm', 'LineWidth',2) % 'Marker', 'o'
elseifi==5
set(H2, 'Color', 'k', 'LineWidth',2) % 'Marker', 'o'
end

figure(3)
H3=plot(I0(i,:),P0(i,:));
axis([0,20,0,400]);
xlabel('Current in amp');
ylabel('Power in watt');
hold on; grid on;
if i==1
set(H3, 'Color', 'b','LineWidth',2 ) % 'Marker', 'o'
```

```
elseifi==2
set(H3, 'Color', 'r', 'LineWidth',2) % 'Marker', 'o'
elseifi==3
set(H3, 'Color', 'g', 'LineWidth',2) % 'Marker', 'o'
elseifi==4
set(H3, 'Color', 'm', 'LineWidth',2) % 'Marker', 'o'
elseifi==5
set(H3, 'Color', 'k', 'LineWidth',2) % 'Marker', 'o'
end
end
figure(1)
legend('S=100     mW/cm^2     ','S=80     mW/cm^2','S=60
mW/cm^2','S=40 mW/cm^2','S=20 mW/cm^2')
figure(2)
legend('S=100     mW/cm^2     ','S=80     mW/cm^2','S=60
mW/cm^2','S=40 mW/cm^2','S=20 mW/cm^2')
figure(3)
legend('S=100     mW/cm^2     ','S=80     mW/cm^2','S=60
mW/cm^2','S=40                        mW/cm^2','S=20
mW/cm^2','Location','northwest')
```

SPICIFICTION OF THE PV Array System

Parameters	Values
Number of Solar cells per module	60
Number of series connected modules per string	6
Number of parallel strings	20
Solar irradiance(input)	1000W/m 2 specified temperture
Output Voltage (v)	72
Maximum Power (w)	213.15
Operating Temperature	
Open Circuit Voltage (Voc)	36.3
(Short-Circuit Current (Isc)	7.84

Vmp (Voltage at Maximum Power Point)	29
Imp (Current at Maximum Power Point)	7.35
PV Data Module	1Soltech 1STH-215-P

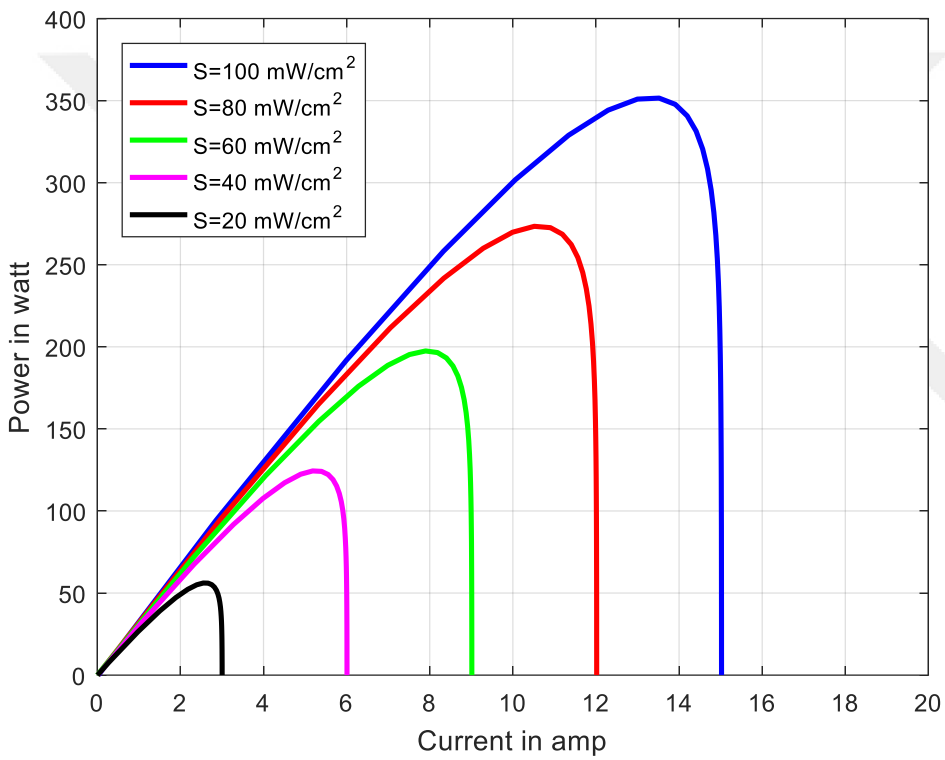

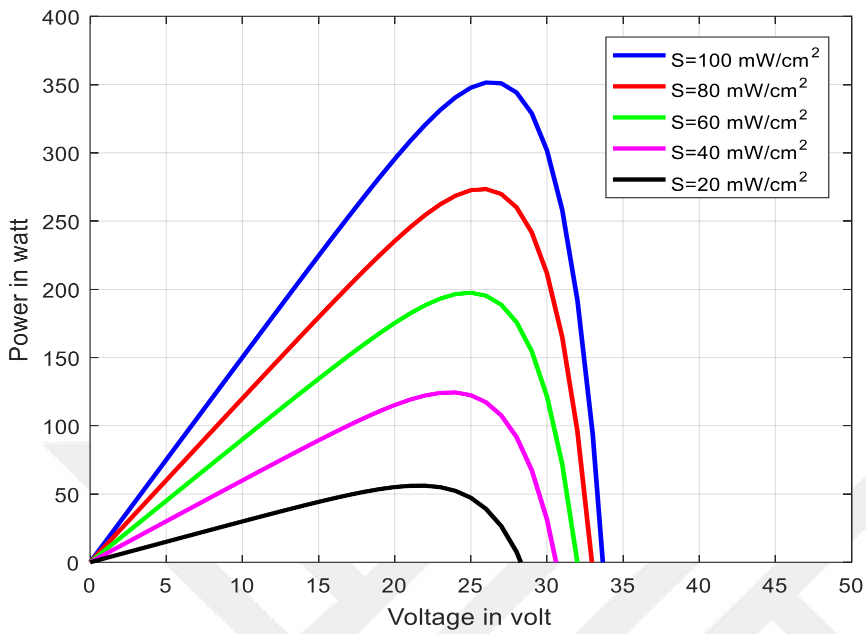
Power in watt
Voltage in volt
S=100 mW/cm2
S=80 mW/cm2
S=60 mW/cm2
S=40 mW/cm2
S=20 mW/cm2

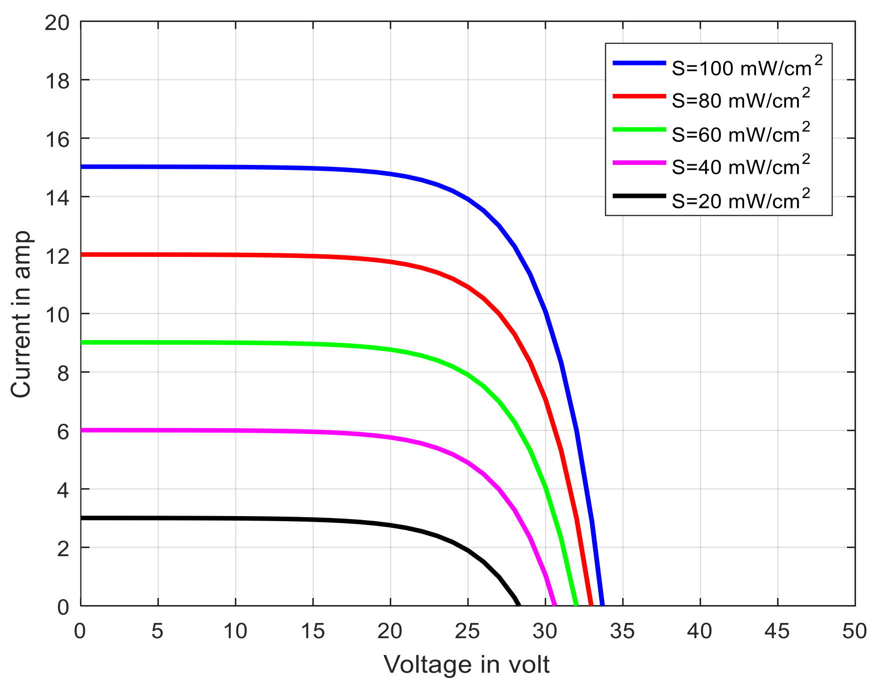
Current in amp
Voltage in volt
S=100 mW/cm2
S=80 mW/cm2
S=60 mW/cm2
S=40 mW/cm2
S=20 mW/cm2

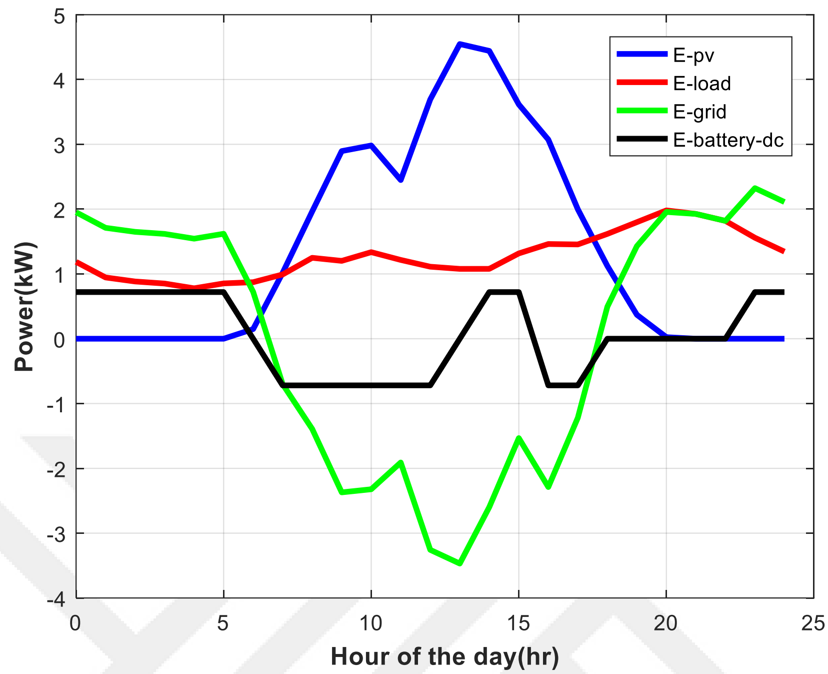
E-pv
E-load
E-grid
E-battery-dc
Power(kW)
Hour of the day(hr)

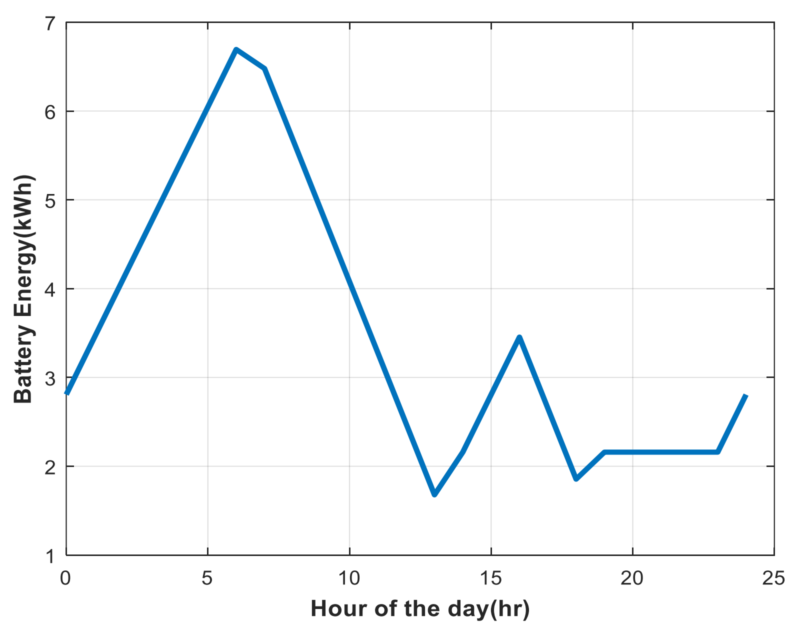
Battery Energy(kWh)
Hour of the day(hr)

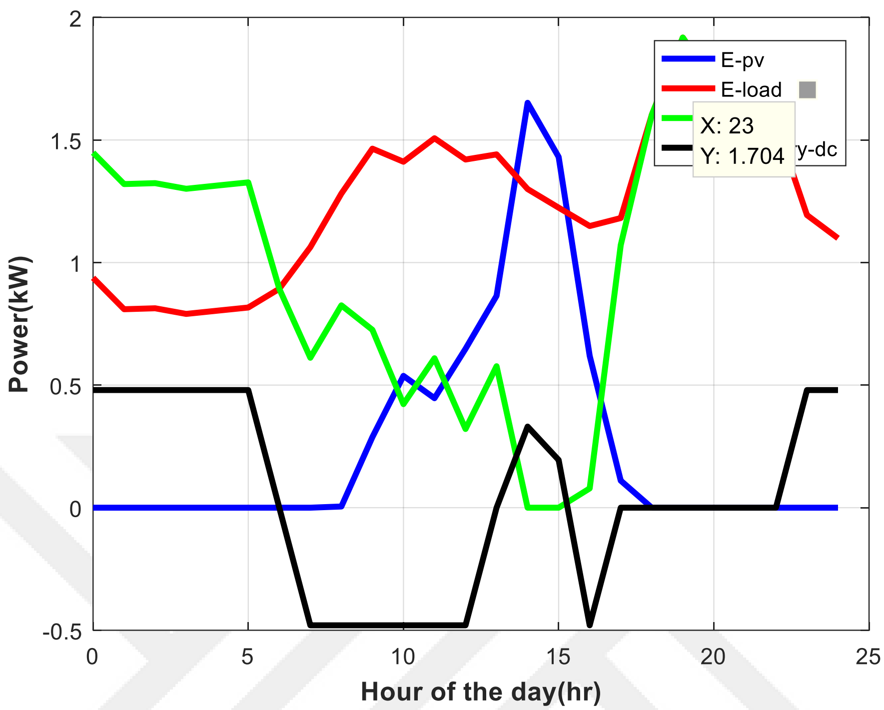
E-pv
E-load
X: 23
Y: 1.704
Power(kW)
Hour of the day(hr)

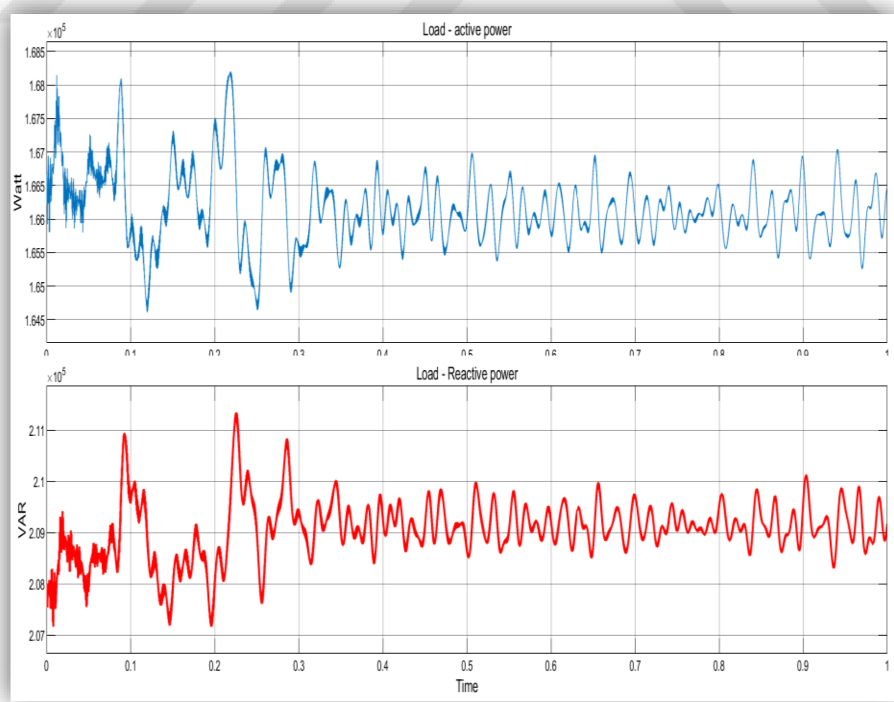
Load - active power
Watt
Load - Reactive power
VAR
Time

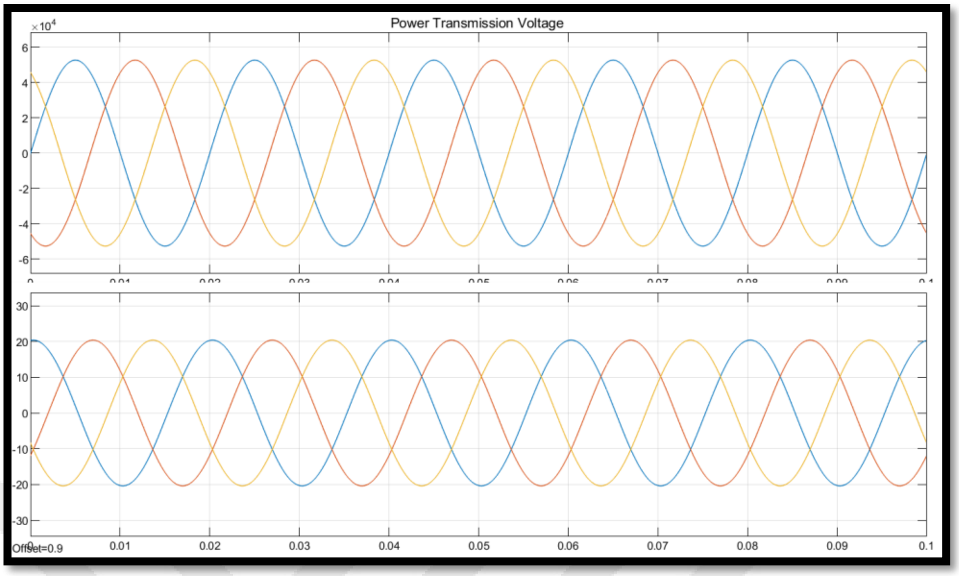
Power Transmission Voltage
×10^4
Offset=0.9

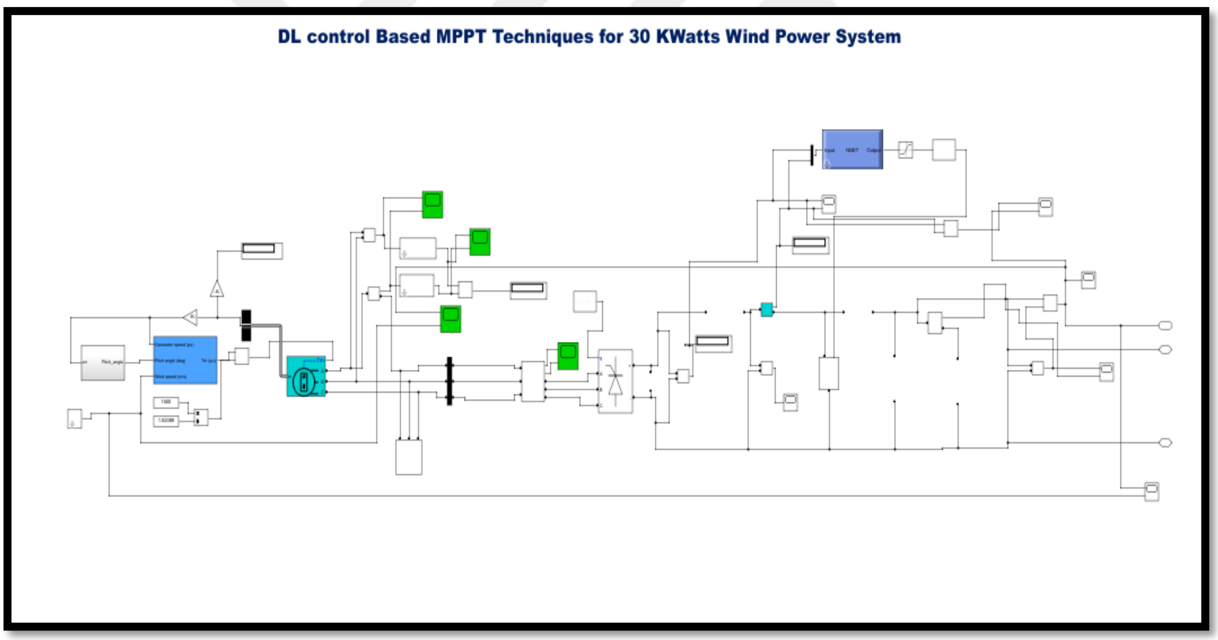
DL control Based MPPT Techniques for 30 KWatts Wind Power System

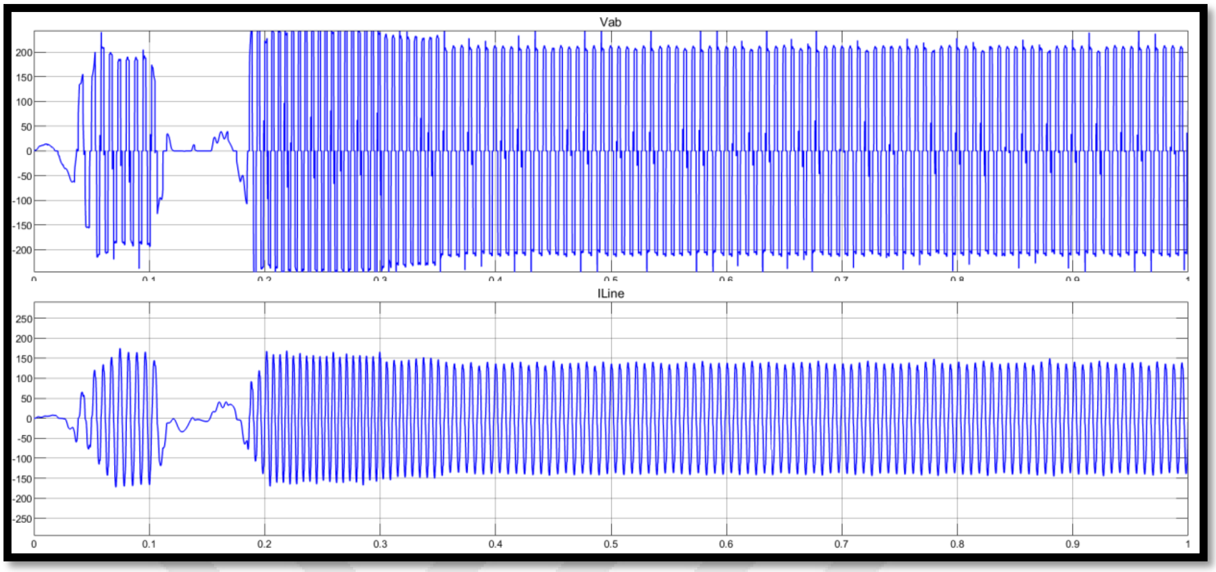
Vab
ILine

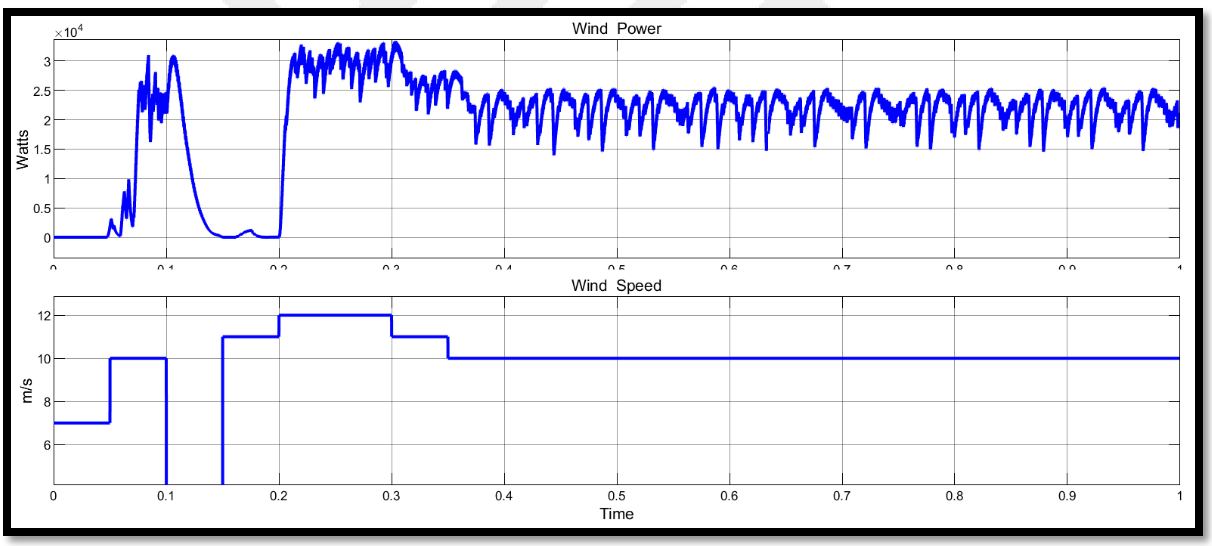
Wind Power
Watts
Wind Speed
m/s
Time

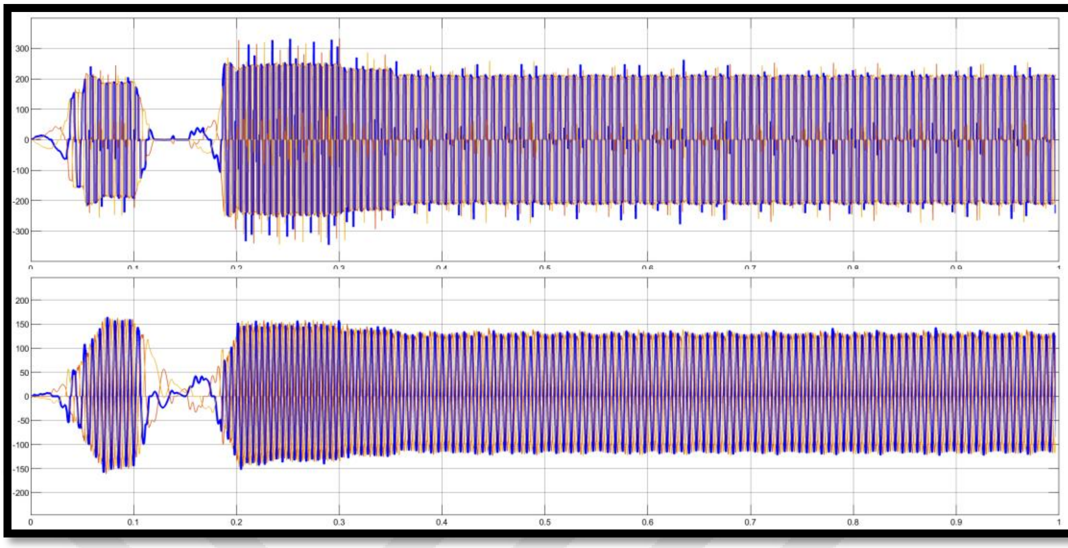

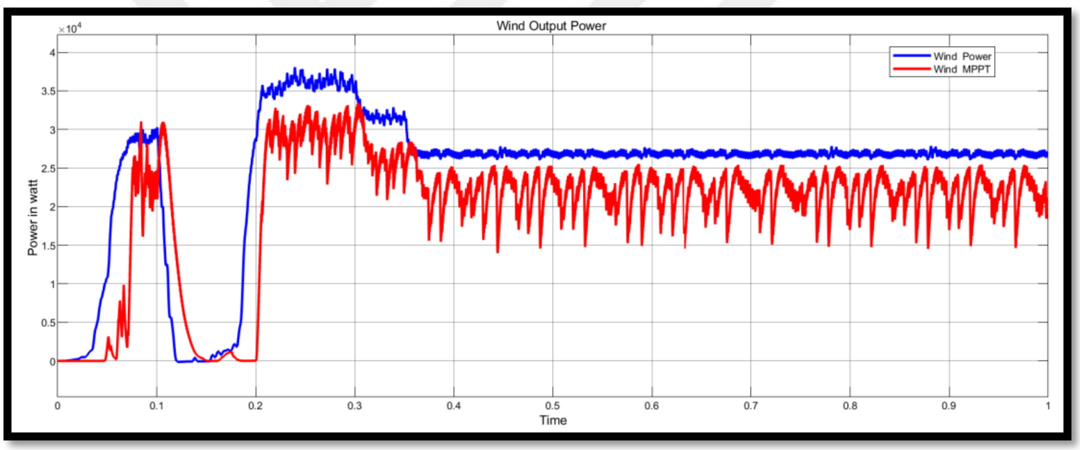
Wind Output Power
Wind Power
Wind MPPT
Power in watt
Time

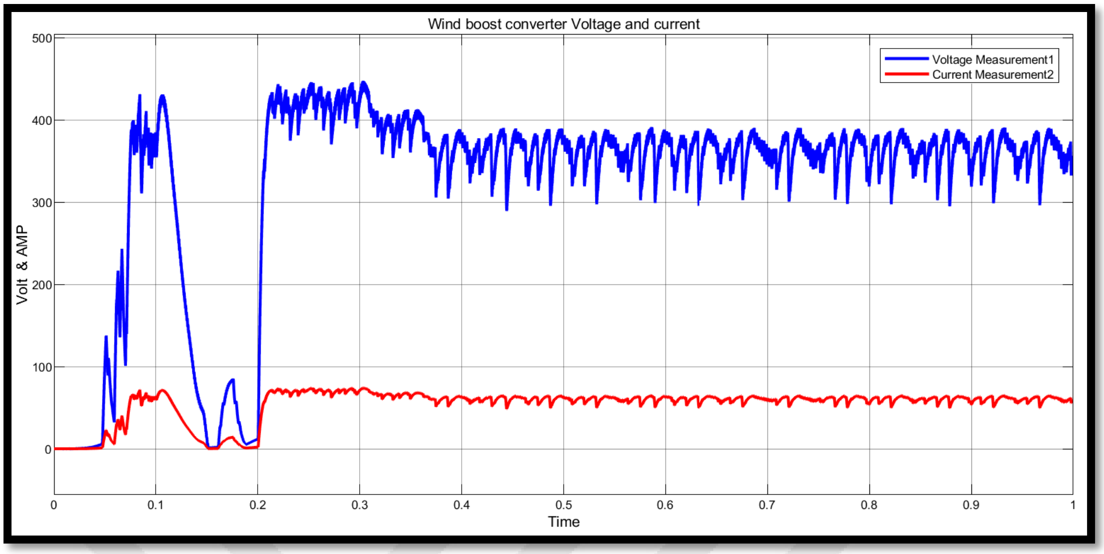

Wind boost converter Voltage and current
Voltage Measurement1
Current Measurement2
Volt & AMP
Time

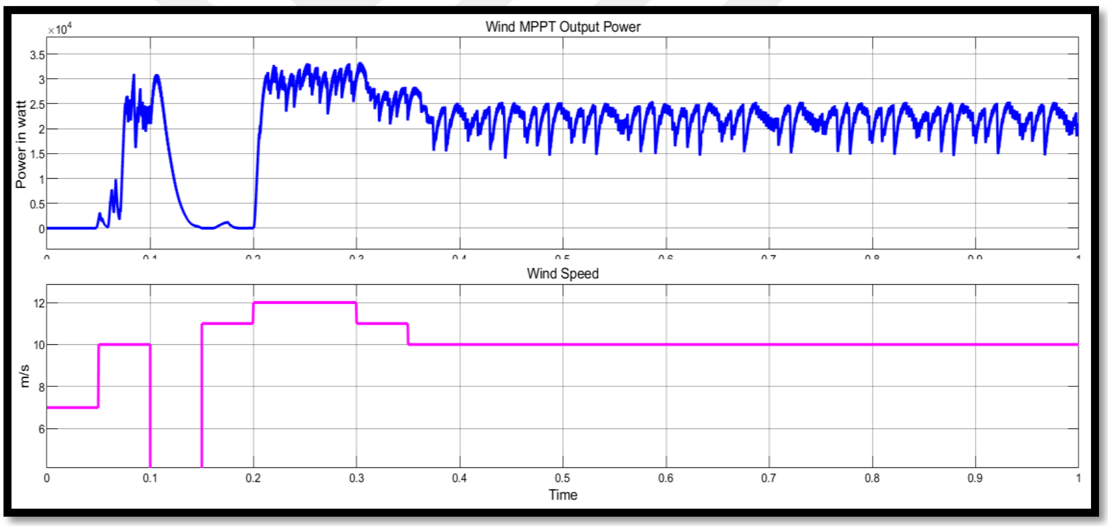

Wind MPPT Output Power
Power in watt
Wind Speed
m/s
Time

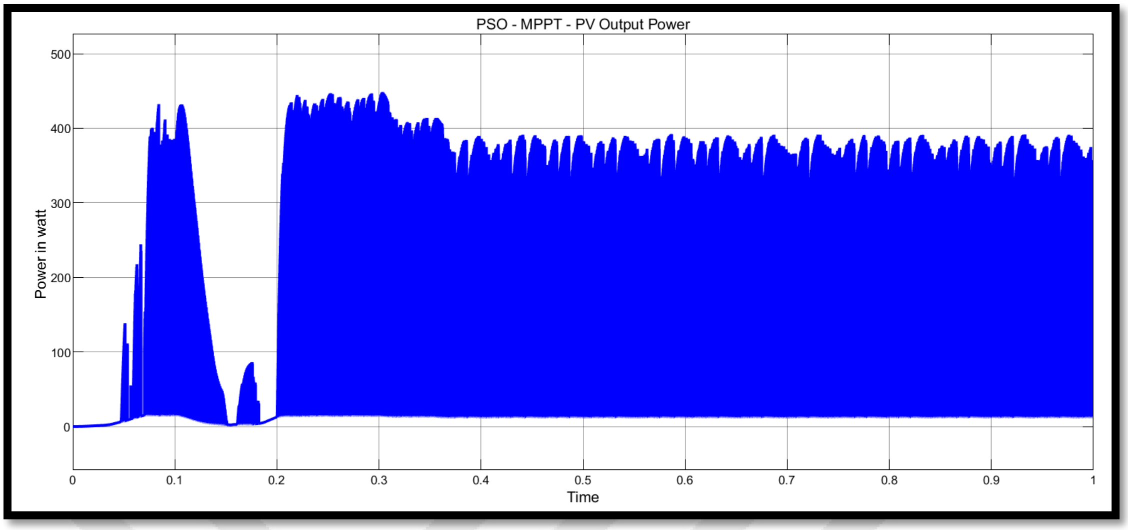
PSO - MPPT - PV Output Power
Power in watt
Time
500
400
300
200
100
0
0
0.1
0.2
0.3
0.4
0.5
0.6
0.7
0.8
0.9
1

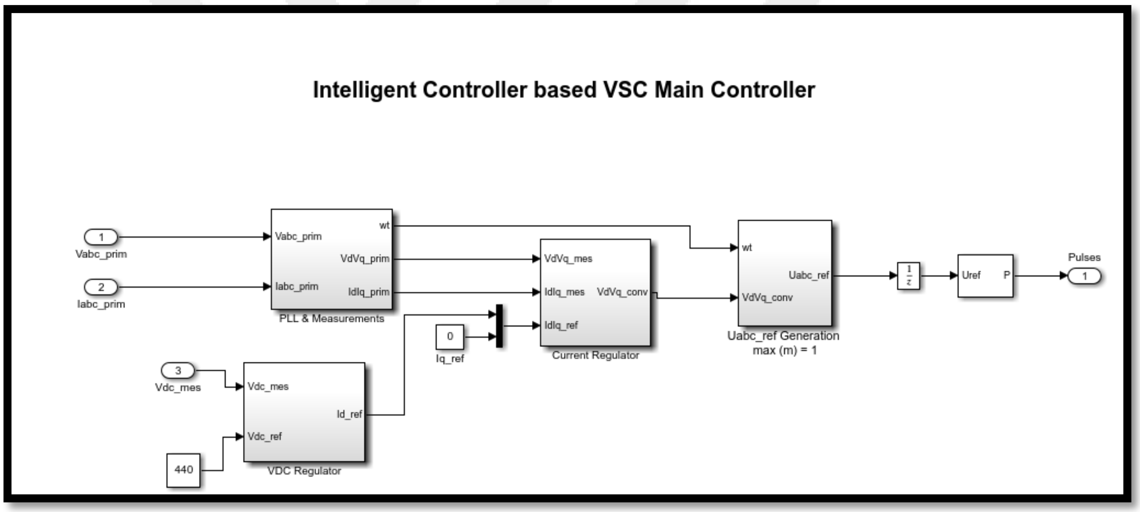
Intelligent Controller based VSC Main Controller
Vabc_prim
Iabc_prim
Vdc_mes
440
PLL & Measurements
wt
VdVq_prim
IdIq_prim
VdVq_mes
IdIq_mes
IdIq_ref
VdVq_conv
Current Regulator
Iq_ref
Vdc_ref
Id_ref
VDC Regulator
Uabc_ref
Uabc_ref Generation
max (m) = 1
Uref
P
Pulses